Aus dem Institut für Molekulare Immunologie

Leiterin：Prof. Dolores Schendel

HMGU-München

Functional characterization of FMNL1
as potential target for novel anti-tumor therapies

Dissertation

Zum Erwerb des Doktorgrades der Humanbiologie

an der Medizinischen Fakultät der

Ludwig-Maximilians-Universität München

vorgelegt   von

Yanyan Han

aus Nanjing, China

2010

Mit Genehmigung der Medizinischen Fakultät

Der Universität München

Berichterstatter: Prof. Dr. Reinhard Zeidler

Mittberichterstatter: Prof. Dr. Christiane J. Bruns

Priv. Doz. Dr. Marion Subklewe

Mitbetreuung durch die

Promovierte Mitarbeiterin: Dr. med. Angela Krackhardt

Dekan: Prof. Dr. med, Dr. h.c. M.Reiser, FACR, FRCR

Tag der mündlichen Prüfung: 10.03.2010

Contents

5   Results 58

11 **Appendix**:

Yanyan Han, Elfriede Eppinger, Ingrid G. Schuster, Luise U. Weigand, Xiaoling Liang, Elisabeth Kremmer, Christian Peschel and Angela M. Krackhardt

Formin-like 1 (FMNL1) is regulated by N-terminal myristoylation and induces polarized membrane blebbing.

The Journal of biological chemistry; 2009; 284(48): 33409–33417

1   Abstract

Formins represent a protein family indispensable for many fundamental actin-dependent polarized processes including migration, vesicle trafficking, morphogenesis and cytokinesis (Faix and Grosse 2006). The hematopoietic lineage-restricted formin protein formin-like 1 (FMNL1) has been previously demonstrated to be overexpressed in chronic lymphocytic leukemia (CLL), other leukemias and lymphomas and in cell lines derived from solid tumors. In healthy tissue, it is almost exclusively expressed in hematopoietic cells. This restricted expression suggests FMNL1 to be an attractive target for novel immunotherapies in malignant and inflammatory diseases (Krackhardt, Witzens et al. 2002; Schuster, Busch et al. 2007). An allorestricted T-cell clone expressing a single defined T cell receptor recognizing a peptide derived from FMNL1 has been identified and showed potent antitumor activity against lymphoma and renal cell carcinoma cell lines, Epstein-Barr virus (EBV)-transformed B cells and primary tumor samples derived from patients with CLL (Schuster, Busch et al. 2007). However, the function and regulation of FMNL1 is recently not well understood which might be necessary for antigen validation. Previous work has shown involvement of FMNL1 in the reorientation of the microtubule organizing center (MTOC) towards the immunological synapse and cytotoxicity of T cells (Gomez, Kumar et al. 2007). In addition, the murine homologue FRL, which has 85% homology to the human counterpart, has been shown to be involved in cell adhesion and motility of macrophages as well as Fc receptor-mediated phagocytosis (Yayoshi-Yamamoto, Taniuchi et al. 2000; Seth, Otomo et al. 2006).

The aim of this project is to investigate functional characteristics of FMNL1 for further validation of this protein as potential target for novel anti-tumor therapies. Moreover, we have identified a novel splice variant (FMNL1γ) containing an intron retention at the C-terminal end affecting the DAD and exhibiting a distinct membranous and cortical localization in diverse cell lines compared to the cytoplasma localization of other FMNL1 splice variants. Similar localization of FMNL1 was observed for a mutant lacking the DAD domain (FMNL1ΔDAD) indicating that deregulation of autoinhibition is effective in FMNL1γ which therefore represents a constitutively active form of FMNL1 potentially playing a role in cellular transformation. Both expression of FMNL1γ and FMNL1ΔDAD could induce polarized non-apoptotic blebbing which is dependent on myosin, actin and tubulin integrity but independent of Src and ROCK activity. We have additionally confirmed FMNL1 as a myristoylated protein and identified the N-terminal myristoylation as an important regulatory tool for FMNL1 enabling fast and reversible membrane localization.

Moreover, FMNL1γ located at the contractile ring and cortex of FMNL1γ

transfected mitotic cells and induced slightly accelerated cell proliferation. We have also observed colocalization of human endogenous FMNL1 with α-tublin at the cortex and mitotic spindles of dividing T cells linking its role to mitosis and cell growth. FMNL1 could induce higher intracellular free calcium concentration suggesting its involvement in the calcium signaling pathway.

Thus our results provide novel insights into the regulation and function of FMNL1 and point to its involvement in diverse polarized processes. The identification of interaction partners of FMNL1 in diverse hematopoietic-derived cells as well as the further characterization of splice variants will be highly interesting to identify key molecules regulating different FMNL1 functions potentially revealing possibilities for specific therapeutic interaction in malignant and inflammatory diseases.

1 Zusammenfassung

Formine spielen eine wichtige Bedeutung bei der Regulierung polarisierter Aktin-gesteuerter Prozesse. Dies betrifft beispielsweise die Zellmigration, den Vesikeltransport, die Morphogenese und die Zytokinese (Faix und Grosse 2006). In früheren Arbeiten konnte nachgewiesen werden, dass das Protein Formin-like 1 (FMNL1) in Zellen von Patienten mit chronischer lymphatischer Leukämie (CLL), anderen Leukämien und Lymphomen und in Zelllinien, die von soliden Tumoren stammen, überexprimiert wird. Im gesunden Gewebe wird es fast ausschließlich in hämatopoetischen Zellen exprimiert. Diese selektive Expression macht FMNL1 zu einem attraktiven Ziel für neuartige Immuntherapien bei malignen und entzündlichen Erkrankungen (Krackhardt, Witzens et al. 2002; Schuster, Busch et al. 2007). In Vorarbeiten der Gruppe wurde ein allorestringierter T-Zellklon mit einem definierten T-Zellrezeptor identifiziert, der ein Peptid von FMNL1 erkennt und eine starke Antitumor-Aktivität gegen Lymphom- und Nierenzellkarzinom-Zelllinien, Epstein-Barr-Virus (EBV)-transformierte B-Zellen und von CLL-Zellen zeigt (Schuster, Busch et al. 2007). Allerdings sind die Funktion und Regulation von FMNL1 – beide wichtig für die Validierung dieses Proteins als Antigen – noch nicht gut untersucht. Frühere Arbeiten haben eine Beteiligung von FMNL1 bei der Neuausrichtung des MTOC (Mikrotubulin-organisierendes Zentrum) in Richtung der immunologischen Synapse und zusätzlich bei der Zytotoxizität von T-Zellen beschrieben (Gomez, Kumar et al gezeigt. 2007). Darüber hinaus wurde gezeigt, dass das murine FRL, das zu 85% homolog zum menschlichen FMNL1 ist, an der Zelladhäsion und Motilität von Makrophagen sowie an der Fc-Rezeptor-vermittelten Phagozytose beteiligt ist (Yayoshi-Yamamoto, et al Taniuchi hat. 2000; Seth, Otomo et al. 2006).

Das Ziel dieses Projekts war es, die Funktion von FMNL1 für die weitere Validierung dieses Proteins als mögliche Zielscheibe für neue Anti-Tumor-Therapien zu untersuchen. Wir haben eine neue Spleißvariante (FMNL1γ) identifiziert, die am C-terminalen Ende ein residuelles Intron aufweist, welches einen Einfluss auf die Diaphanous-autoinhibierende-Domäne (DAD) hat. Im Gegensatz zu anderen FMNL1-Spleißvarianten, die eine zytoplasmatischen Lokalisierung aufweisen, zeigt diese Speißvariante eine kortikale und membranständige Lokalisation in verschiedenen Zelllinien. Eine FMNL1 Mutante, bei der die DAD-Domäne fehlt (FMNL1ΔDAD), weist eine ähnliche Lokalisierung auf. Das weist darauf hin, dass es bei FMNL1γ zu einer Deregulierung der Autoinhibition kommt, die zu einer konstitutiv aktiven Form von FMNL1 führt, die möglicherweise bei der zellulären Transformation eine Rolle spielen könnte. FMNL1γ und FMNL1ΔDAD können eine polarisierte, nicht mit einer Apoptose-assoziierten Blasenbildung an der Membran hervorrufen, die von Myosin, Aktin und

Tubulin abhängig ist, aber unabhängig von Src und ROCK zu sein scheint. Wir haben außerdem nachgewiesen, dass FMNL1 als myristoyliertes Protein vorliegt und konnten zeigen, dass die N-terminale Myristoylierung wichtig für die Regulierung der Funktion von FMNL1 ist, indem sie eine schnelle und reversible Membran-Lokalisierung ermöglicht.

Des Weiteren haben wir gezeigt, dass FMNL1γ, das auch am kontraktilen Ring und Kortex von FMNL1γ-transfizierten mitotischen Zellen lokalisiert ist, die Zellproliferation moderat verstärkt. Eine gemeinsame Lokalisierung von menschlichem endogenem FMNL1 und α-Tubulin am Kortex und den mitotischenden Spindeln von sich teilenden T-Zellen weist ebenfalls auf eine Rolle von FMNL1 in der Mitose und dem Zellwachstum hin. Überexpression von FMNL1 konnte eine höhere Konzentration von intrazellulärem freiem Calcium nach Zell-Stimulation induzieren, was auf eine Beteiligung von FMNL1 am Calcium-Signalweg deutet.

Unsere Ergebnisse eröffnen neue Einblicke in die Regulation und Funktion von FMNL1 und zeigen dessen Beteiligung an unterschiedlichen Polarisierungsprozessen. Die Identifizierung von Interaktionspartnern von FMNL1 in verschiedenen hämatopoetischen Zellen sowie die weitere funktionelle Charakterisierung der Spleißvarianten wird von besonderer Bedeutung sein, und möglicherweise zur Entwicklung einer spezifischen therapeutischen Beeinflussung maligner und entzündlicher Erkrankungen beitragen.

2   Introduction

2.1   Tumor antigens

2.1.1   Identification of tumor antigens

The immune system can respond to cancer cells by T cells recognizing tumor antigens (TA) on the cancer cells (Finn 2008). However, this mechanism remained in doubt until the development of methods for identifying and isolating tumor antigens. The first experimental evidence for the existence of human tumor antigens was obtained in the late 1960s, when it was found that lymphocytes from urinary bladder carcinomas patients other than from unrelated tumours patients or various normal tissues were cytotoxic for bladder carcinoma cells in vitro, and that serum of some patients contained antibodies specific to this tumor antigen (Bubenik, Perlmann et al. 1970). From then on, identifying potential tumor antigens has been essential in the progress towards the development of successful cancer immunotherapy (Graziano and Finn 2005).

Monoclonal antibodies derived from mice immunized with human tumors were used to detect potential human tumor antigens (Hellstrom, Hellstrom et al. 1982). However, it was not clear that if the human immune system could also recognize these tumor antigens identified by mice monoclonal antibodies (Finn 2008).

Identification of tumor antigens by tumor-infiltrating lymphocytes (TILs) based methods

A melanoma-specific antigen, MAGE-1, was the first human tumour antigen identified by being recognized in vitro by cytotoxic T cells derived from the tumor-bearing patient (van der Bruggen, Traversari et al. 1991), which proved that the human immune system could respond to tumor antigens. Furthermore, to identify the tumor antigens recognized by tumor-infiltrating lymphocytes (TILs), cDNA libraries prepared from tumor cells were transfected into target cells that expressed the appropriate major histocompatibility complex (MHC) molecule. These transfectants were then tested for their specific anti-tumor reactivity by using cytokine release or lysis by human T cells (Rosenberg 1996; Rosenberg 1999). Using this strategy, a number of tumor antigens from melanoma were successfully identified, such as MART-1, gp100, Tyrosinase, Tyrosinase-associated protein 1 (TRP1), p15 and Beta-Catenin (Rosenberg 1996; Graziano and Finn 2005).

Identification of tumor antigens by biochemical methods

By biochemical methods, peptides were eluted and fractionated from tumor cells or from MHC molecules purified from tumor cells and loaded onto antigen-presenting cells (APCs) to prime the tumor-reactive T cells. Fractions capable of inducing a T cell response are further analyzed using mass spectrometry (MS) analysis to identify the peptide sequence (Cox, Skipper et al. 1994). An alternative biochemical approach was performed without using known tumor-reactive T cells. After elution, peptides were analyzed by MS and tested for their ability to bind to MHC molecules. Peptides are identified depending on their natural processing and presentation on tumor cells, without known immunogenicity (Schirle, Keilholz et al. 2000). Although this approach allows for the rapid screening of large numbers of tumor genes, it is limited by the need of highly specialized equipment and the requirement of sufficient amounts of peptides present on the tumor cell surface (Rosenberg 1999; Graziano and Finn 2005).

Identification of tumor antigens by dendritic cells (DCs) based method

Tumor antigen proteins are broken down into small peptides by the proteasomes of normal and neoplastic cells. APCs could then present these peptides on the cell surface to cytotoxic CD8 T cells by MHC class I molecules. Dendritic cells (DC) are considered the most potent APCs, expressing high level of MHC molecules and costimulatory molecules, essential for capturing and presenting antigens to naive T cells (Banchereau, Briere et al. 2000).The biggest advantage of this approach is to load peptides extracted from tumors onto in vitro-generated DCs and prime naive T cells from healthy donors instead of T cell lines or clones from cancer patients. Peptides which successfully prime tumor-specific T cells have been sequenced in search for tumor-specific antigens. This approach has led to the identification of the tumor antigen cyclin B1 (Kao, Amoscato et al. 2001). Beside peptides derived from tumors, DCs could also be loaded with proteins or even whole tumor cells and prime T cells, mimicking what occurs in vivo (Finn 2008). This approach of identifying new tumor antigens is different from others which relied on the availability of T cell lines or clones from cancer patients.

Identification of tumor antigens by serological analysis of recombinant cDNA expression libraries (SEREX)

Another technique for the identification of tumor antigens which also does not dependent on the prior availability of antitumor T cells is based on the humoral immune response to an antigen. This approach is used by serological analysis of recombinant cDNA expression libraries, or SEREX. In this approach, a cDNA library is constructed from a fresh tumor specimen, packaged into a lambda-phage vector and expressed in *E. coli*. The recombinant proteins are transferred onto nitrocellulose membranes and screened for recognition by high-titer IgG antibodies present in the patient's serum. Any positive clones are

subcloned further to monoclonality, and the sequence of the inserted cDNA is determined (Sahin, Tureci et al. 1997). Proteins recognized by antibodies in serum samples from patients with a particular tumor, and not from healthy controls, were tagged as candidate tumor antigens. This approach is based on the assumption that antibody production implies that a helper T cell reaction exists against the detected antigen (Rosenberg 1999). Several new tumor antigens were identified by SEREX, among which NY-ESO-1 is one of the most actively studied tumor antigens (Chen, Stockert et al. 1996). NY-ESO-1 belongs to a family of cancer–testis antigens that are expressed by a variety of human tumors but not by any normal cells or tissues, except for the testis.

2.1.2 Characterization of tumor antigens

To date a number of tumor antigens have been identified through the previously described approaches. Among several criteria for selecting particular ones for clinical development, safety is of primary concern. It means the immune responses against tumor antigens would only destroy tumor cells but no normal cells (Finn 2008). Beside, the expression of tumor antigens should be present at the very earliest stages of tumorigenesis, or even during a pre-malignant stage. In addition to the primary tumor, a specific tumor antigen should be expressed on metastatic lesions in able to prevent metastatic growth and recurrence of the tumor after removing the primary tumor surgically (Graziano and Finn 2005). However, one important issue at least reagarding adoptive T cell therapies is the question if antigen expression correlates with peptide ligand presentation which seems not always to be the case (Weinzierl, Lemmel et al. 2007).

Perfect target tumor antigens would be unique mutant antigens which are expressed in the malignant but not the normal cell type. An additional important feature of unique antigens is that the mutated protein may be crucial to the oncogenic process and indispensable for maintaining the neoplastic state or required for tumor cell survival. This kind of antigen would overcome the immunoselection, either by further mutation or loss of expression (Ho, Blattman et al. 2003; Parmiani, De Filippo et al. 2007). Moreover, since the majority of human tumor antigens described so far are self-proteins, mutant proteins which differ from normal self proteins have the advantage to potentially overcome peripheral tolerance (Theobald, Biggs et al. 1997). The first description of such a unique antigen was a human melanoma antigen, resulting from a point mutation of cyclin-dependent kinase (CDK4) in 1995 (Wolfel, Hauer et al. 1995). After that, a series of tumor-specific mutant proteins have be identified which are encoded by oncogenes or suppressor genes that have undergone structural mutations resulting from point mutations (e.g: p21/ras mutations found in multiple malignancies), chromosomal translocations (e.g: BCR/ABL translocation in chronic myelogenous leukemia), internal deletions (e.g: the epidermal growth factor receptor gene deletion in

human primary brain tumor) and viral insertional mutagenesis (e.g: HPV proteins in cervical cancer and EBV proteins in Hodgkin's disease and nasopharyngeal carcinoma) (Urban and Schreiber 1992).

However, most tumor antigens are nonmutated proteins which are over-expressed or aberrantly expressed by the tumor. These antigens are named tumor-associated antigens (TAA). Compared to tumor unique antigens, a large number of peptides from tumor associated antigens which are also produced from normal cells are much more successfully presented on the cell surface. That is the reason that the majority of tumor antigens identified as cytotoxic T-lymphocyte (CTL) targets in cancer patients are tumor associated antigen (Morris, Bendle et al. 2003).

The tumor-associated antigens which are important for maintaining the malignant phenotype are considered as the second choice beside the unique tumor antigens. Because higher expression of such proteins in malignant cells than in normal tissues may make it possible for immune system to recognize and eliminate tumors while ignoring the low levels of antigen expressed by normal tissues. Overexpressed protein antigens associated with tumorigenicity include the WT1 (Wilms' tumor) gene in leukemias and various solid tumors as well as HER-2/neu in breast and ovarian cancer (Ho, Blattman et al. 2003). The cancer testis antigens, such as NY-ESO-1, which have unknown functions are expressed by a variety of human tumors such as ovarian cancer and melanoma but not by any normal tissues, except for the testis (Chen, Stockert et al. 1996). The melanoma antigen MAGE-1 also belongs to this category. The family of cancer testis antigens provides nearly unique potential target antigens.

Many tumor-associated antigens are derived from malignant melanomas and have been found not only on melanomas but also on other tumor types. These normal, non-mutated genes are differentiation antigens which are limited to melanomas as well as melanocytes, the cell of origin of this tumor, and pigment-producing cells in retina (Rosenberg 1999). In this category, MART-1/MelanA antigen which have an unknown function are targets of tumor-reactive T cells in melanoma patients (Coulie, Brichard et al. 1994). gp100 antigen encodes an enzyme involved in melatonin synthesis (Kawakami, Eliyahu et al. 1994) and tyrosinase is an enzyme critical for the synthesis of melatonin (Brichard, Van Pel et al. 1993).

In conclusion, the classification of tumor antigens was reviewed by Daniel F. Graziano and Olivera J. Finn as follows:

1. Cancer testis antigens: These antigens are expressed only in tumors and germ cells of the testes. This group includes a large number of MAGE antigens,

GAGE and the more recently discovered NY-ESO-1.

2. Melanocyte differentiation antigens: This group of antigens is expressed during melanocyte differentiation, in normal melanocytes and in melanomas. Included in this group are MART-1/MelanA, tyrosinase and gp100.

3. Tumor-specific mutated gene products: This group includes antigens that are products of mutated normal genes. These mutations are usually responsible for oncogenic properties of the tumor cell. CDK-4, β-catenin, MUM-1, mutated p53 and ras (H- and K-ras) all belong to this group.

4. Overexpressed or widely expressed self-antigens: This class of TA is encoded by genes that are widely expressed in normal tissues but are also selectively expressed on tumor cells. This group includes PRAME, SART-1, P15, wild type p53, MUC1, cyclin B1, Her2-neu and CEA.

5. Viral antigens. Examples are the products of the E6 and E7 genes of the human papillomavirus and EBNA-1, the Epstein–Barr virus nuclear antigen.

2.1.3   Cancer immunotherapies based on tumor antigens

To date, continuous efforts have been made to improve the conventional cancer therapy such as chemotherapy and radiotherapy to obtain a long-term eradication of tumour cells without any side effects. However, the conventional approaches are limited by both their lack of specificity and toxicity (Morris, Bendle et al. 2003). The development of immunotherapies based on the identification of tumor antigens has supplied a promise option of cancer therapy (Rosenberg 1995). Cancer immunotherapies can be categorized as passive and active approaches. In passive immunotherapy, immune cells or monoclonal antibodies with anti-tumor abilities are generated and adoptively transferred to the patients. In active immunizations, patients are directly immunized the with the therapeutic cancer vaccines which could induce endogenous immune responses against tumors (Rosenberg 1996).

Passive immunotherapy:

After the development of monoclonal antibodies in 1975, monoclonal antibodies against cancer cells have been investigated as an immunotherapy (Chapman 2004). The infusion of manufactured monoclonal antibodies can generate an immediate immune response which is independent of MHC molecules restriction bypassing many of the limitations that impede endogenous immunity. However, the lack of monoclonal antibodies to penetrate tissues and the extracellular matrix to reach their target cells limits the efficiency of the treatment, especially for solid tumors which are characterized by heterogeneous and tortuous vasculature, high interstitial fluid pressure and high viscosity of the tumour blood supply. (Chames, Van Regenmortel et al. 2009). Therefore, although melanoma antigens were the first targets chosen by investigators, most successfully developed immunotherapeutic monoclonal antibodies are against haematological antigens and surface antigens or tumor mediator of other types of tumors. For

example, alemtuzumab anti-CD52 for CLL, gemtuzumab anti-CD33 for AML, rituximab anti-CD20 for B-cell lymphoma, More recently, antibodies are more successful also in solid tumors as trastuzumab anti-HER2/*neu* for breast cancer, cetuximab anti-epidermal growth factor receptor for colon cancer and bevacizumab anti-vascular endothelial growth factor for colon cancer (Adams and Weiner 2005).

Another passive cancer immunotherapy is based on the tumor-specific T-cell responses which have several advantages over monoclonal antibody therapy. Specific T cells can penetrate the tissue barriers and home in to antigen-expressing tumors despite of their location. In addition, T cells can continue to proliferate in response to tumor antigens until all the tumour cells are eradicated. Moreover, memorial T cells with specificity for tumor antigens can be generated in able to eliminate antigen-bearing tumors when they relapse (Disis, Bernhard et al. 2009). However, there are also some drawbacks of T-cell immunotherapy such as the restriction of MHC molecules and undesirable toxicity induced by unspecific reaction. Furthermore, the majority of T cell-recognized tumour antigens in humans are encoded by genes that are also present in normal tissues. Low levels of gene expression in normal cells can lead to the inactivation of high avidity T cells by immunological tolerance mechanisms.

Recently, a number of novel approaches have been developed to circumvent the tolerance mechanisms to generate high-avidity cytotoxic T cells or monoclonal antibodies specific for tumour-associated antigens (Figure 2.1).
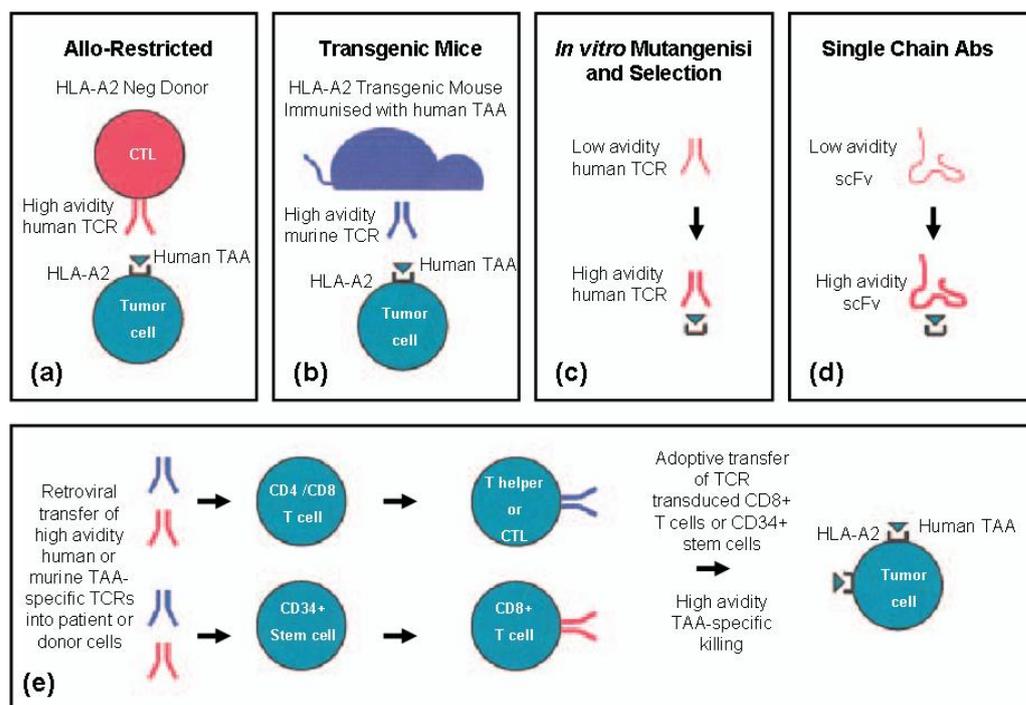
Figure 2.1 Novel approaches for the generation of high-avidity CTL specific for tumor-associated antigens. (a) and (b) take advantage of the TCR repertoire of healthy individuals or transgenic mice that are not tolerant to A2-presented peptide epitopes of tumor-associated antigens. (c) and (d) take advantage of *in vitro* mutagenesis and selection of high affinity TCRs (c) or high-affinity single chain antibodies specific for the peptide/HLA combination. (e) Strategies to transfer high avidity HLA-restricted receptors into patient T cells or stem cells to produce tumor-reactive T cells. (Morris, Bendle et al. 2003)

A tumor associated antigen, p53, has been reported to be an attractive immunotherapy target, because it is only expressed in normal tissues of low amounts. However, p53 turns may be not suitable to be targeted by immunotherapeutic approaches since the low expression of p53 in normal cells could still sufficiently stimulate T cells activation (Theoret, Cohen et al. 2008). Therefore, the functional characterizations of tumor antigens which are selected as targets are critical for the development of cancer immunotherapy.

Active immunotherapy:

The active immunotherapy refers to cancer therapeutic vaccines which could elicit or boost similar tumor antibodies and T cells in the patients other than infusion of antibodies or T cells (Finn 2008). These strategies are usually directed against tumor associated antigens, or against an unidentified number of antigens such as whole tumour cells, cell lysates or heat shock proteins and RNA isolated from tumour cells. Although vaccines based on multiple unidentified antigens have shown promise in the experimental setting, it is difficult to monitor vaccine-induced immune responses without knowing the specific target antigens (Morris, Bendle et al. 2003). The progressive improvement of vaccines is more probable with defined antigens, including immunodominant peptides, peptides modified to increase immunogenicity, proteins, "naked" DNA encoding cancer antigens, antigen-presenting cells expressing the antigen or recombinant viruses or bacteria containing the genes encoding tumor antigens (Rosenberg 1996; Morris, Bendle et al. 2003). Some examples are vaccines against breast cancer (the HER2 antigen), B-cell lymphoma (the tumor immunoglobulin idiotype), lung cancer (the MUC1 antigen), melanoma (dendritic cells loaded with tumor peptides or killed tumor cells), pancreatic cancer (telomerase peptides), and prostate cancer (dendritic cells loaded with prostatic acid phosphatase).

A predominant limiting factor of therapeutic vaccines is the immunosuppressive microenvironment both during the induction of immunity and in the effector phase of the response. One approach to improve the induction phase is by using antibodies against a negative regulator of the activation of effector T cells named cytotoxic T-lymphocyte–associated antigen 4 (CTLA-4) (Korman, Peggs et al. 2006; Ribas, Hanson et al. 2007).

Unfortunately, the enhancing tumor immunity induced by anti-CTLA 4 antibody is accompanied by serious autoimmunity. Combination of therapeutic vaccine with chemotherapy could also induce the synergistic action of immunotherapy probably because of the elimination of regulatory T cells by chemotherapy (Emens and Jaffee 2005).

2.2 FMNL1 as a tumor associated antigens

2.2.1 Identification of FMNL1

The formin-like 1 (FMNL1) protein is a lymphoma-associated antigen identified by using the SEREX approach in patients with chronic lymphocytic leukemia (CLL) (Krackhardt, Witzens et al. 2002). It belongs to the formin protein family indispensable for many fundamental actin-dependent processes including migration, endocytosis, vesicle trafficking, morphogenesis and cytokinesis (Faix and Grosse 2006). FMNL1 is restrictedly expressed in hematopoietic-lineage derived cells and overexpressed in malignant cells of different origins (Figure 2.2). Detailed expression analysis was performed on mRNA level. FMNL1 is most highly expressed in peripheral blood leukocytes (PBL) and seldom expressed in normal tissues with the exception of bone marrow, thymus and lung where hematopoietic cells accumulate. Moreover, FMNL1 expression is up-regulated in PBLs derived from patient with CLL and acute leukemia. This restricted expression suggests FMNL1 to be an attractive target for novel immunotherapies in malignant and inflammatory diseases (Krackhardt, Witzens et al. 2002; Schuster, Busch et al. 2007).

However, function and regulation of FMNL1 is less well characterized. Previous work has shown involvement of FMNL1 in the reorientation of the microtubule organizing center (MTOC) towards the immunological synapse and cytotoxicity of T cells (Gomez, Kumar et al. 2007). It demonstrated a fringe-like localization of FMNL1 at the leading edge of the lamellipod in spreading T cells. This FMNL1 accumulation was also apparent at the edge of F-actin structures, which formed during APC recognition, along with a distinct, ''ring-like'' localization of FMNL1 around the centrosome within the T cell. Moreover, this FMNL1 ring reoriented along with the MTOC to face stimulating APCs and regulate centrosome polarization in T cell as the absence of FMNL1 negatively effects MTOC polarization and cytotoxic T cell function. Additionally, the murine homologue FRL, which has 85% homology to the human counterpart, has been shown to be involved in cell adhesion and motility of macrophages as well as Fc receptor-mediated phagocytosis (Yayoshi-Yamamoto, Taniuchi et al. 2000; Seth, Otomo et al. 2006).
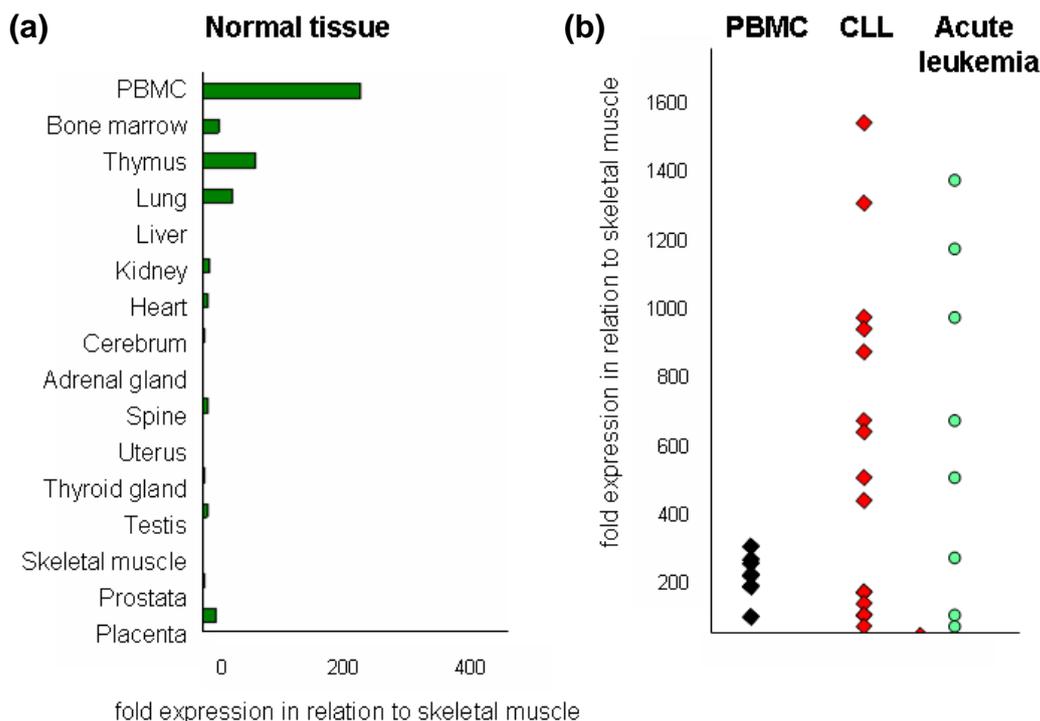
Figure 2.2 Expression of FMNL1 in normal and malignant tissue. (a) Relative quantitative mRNA expression of FMNL1 in different tissues pooled from different healthy donors was measured using quantitative real-time PCR. The relative quantitative expression compared to skeletal muscle was calculated using the delta-delta Ct method. (b) Relative quantitative mRNA expression of FMNL1 in CLL samples and tumor cells derived from patients with acute B- and T-ALL as well as AML is shown in comparison to normal PBMC.

2.2.2   Formin protein family

Formin proteins are a widely expressed family of proteins, generally more than 1000 amino acids in size, and contain a series of domains and functional motifs which associate with a variety of other cellular proteins. Formins are defined by a unique and highly conserved C-terminal formin homology (FH) 2 domain containing around 400 amino residues that mediates the actin assembly (Higgs 2005; Faix and Grosse 2006; Goode and Eck 2007). Bioinformatics studies show that eukaryotic species have multiple formin genes, including *S. cerevisiae* (2 formins), *S. pombe* (3 formins), *Drosophila melangastor* (6 formins), *Caenorhabditis elegans* (6 formins), *Dictyostelium discoideum* (10 formins), and mammals (15 formins) (Higgs and Peterson 2005; Rivero, Muramoto et al. 2005). Phylogenetic analyses of the FH2 domain have led to the classification of the 15 mammalian formin genes into seven group (Higgs and Peterson 2005):

1. the Diaphanous formins (Dia1);
2. the formin-related proteins identified in leucocytes (FRL1);

3. the disheveled-associated activators of morphogenesis (DAAM1);

4. Delphilin (Delphilin);

5. the "inverted" formins (INF1);

6. the formin homology domain containing proteins (FHOD);

7. the original "namesake" formins (FMN).

Most eukaryotes have multiple formin isoforms, suggesting diverse cellular roles. The FH2 core domain and the intervening linker region between the FH1 and FH2 domains are necessary and sufficient to nucleate actin polymerization from G-actin in vitro (Pruyne, Evangelista et al. 2002; Kovar, Kuhn et al. 2003). Before FH2 domain is a proline-rich FH1 domain which binds with low micromolar affinity to profilin (Evangelista, Blundell et al. 1997; Watanabe, Madaule et al. 1997).
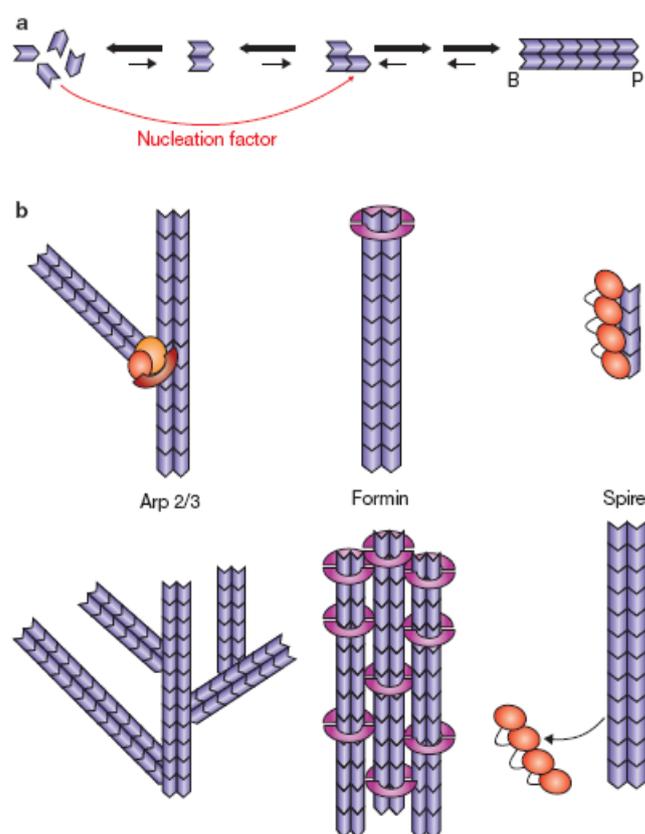
Figure 2.3 Filament polymerization by actin assembly factors. (a) Actin filaments are polar structures, with the barbed end (B) being the only site of elongation in non-muscle cells. (b) The Arp2/3 complex (multi-coloured) nucleates a new filament from the side of an existing filament. The Arp2/3 complex remains at the branch point between the pointed end of the new filament and the side of the existing filament. Repeated branching results in the assembly of a dendritic network. The formin FH2 domain (semi-circles) nucleates a filament, and then moves processively with the barbed end as it elongates. Some formins can also bundle filaments. Spire (circles with black connectors) nucleates a filament by stabilizing a longitudinal tetramer and dissociates from filaments soon after nucleation. (Chhabra and Higgs 2007)

14

Eukaryotic cells nucleate actin filaments from a large pool of monomeric actin bound to profilin in order to elicit temporal and spatial remodeling of the actin cytoskeleton. This process underlies several cellular functions such as the establishment of cell shape, cytokinesis, or cell motility (Faix and Grosse 2006). The actin filament is a polar structure with a 'barbed' and a 'pointed' end, since all the actin subunits face the same direction. Monomers can add to or depolymerize from either end, but both processes are much more efficient at the barbed end (Goode and Eck 2007). The step to assemble dimeric and trimeric actin complexes limits the rate of actin filament nucleation. So far, three major classes of actin nucleators are known to nucleate actin filaments in vivo: the Arp2/3 complex, Spire, and the formin-homology proteins with different mechanisms to accomplish their tasks (Figure 2.3).

The first identified actin nucleator was the Arp2/3 complex, which binds to the side of pre-existing actin filaments, and nucleates a branched filament structure with an angle of 70° between the filaments. The Arp2/3 complex remains at the branch point between two filaments. Repeated branching leads to a 'dendritic network'. Therefore, the Arp2/3 complex functions not only as a nucleation factor, but also provides structure to the network. Spire nucleates the assembly of unbranched actin filaments and, like the Arp2/3 complex, remains bound to the pointed ends of the nucleated filaments. Pointed-end nucleators, such as Arp2/3 and Spire, will experience only limited growth before being capped at their barbed ends by capping proteins (Faix and Grosse 2006; Chhabra and Higgs 2007).

Formins were identified more recently as an additional family of actin assembly factors. All formins studied to date are dimeric because of their FH2 domain, which initiates actin filament assembly and remains persistently associated with the fast-growing barbed end, enabling rapid insertion of actin subunits while protecting the end from capping proteins (Higgs 2005). Central function of FH2 domain is to nucleate new actin filaments through binding tightly to the barbed end of the filaments with low nanomolar affinity (Moseley, Sagot et al. 2004). Meanwhile, the FH2 domain moves processively with this elongating actin filament barbed end. It means, the FH2 domain remains contacting with actin filaments barbed ends when adding new actin monomers without dissociation and reassociation. Related to processive barbed-end movement, FH2 domains antagonize the effects of barbed-end capping proteins which could completely block monomer addition to barbed ends. Therefore, the barbed ends of actin filaments retain the ability to elongate even in the presence of capping protein (Higgs 2005). Formin-mediated elongation is further enhanced by the association of profilin with the FH1 domain of formin. The adjacent FH1 domain recruits profilin-actin complexes and accelerates filament elongation. The profilin–actin complex participates in actin assembly at the barbed end as fast as free actin monomers do, whereas profilin

interferes with actin nucleation. Normally, free actin monomers exist only at a submicromolar concentration in cells, and thus profilin prevents spontaneous actin nucleation while it allows fast actin elongation (Watanabe and Higashida 2004).

Vavylonis *et al.* suggested a model of formin-associated actin filament elongation. They assumed that FH1 domains capture profilin-actin complex from the bulk solution and transfer the captured subunit to the barbed end of the filament (Figure 2.4a). The FH1 domains vary in the length and number of proline-rich stretches, separated by proline-poor "linker" stretches. Both of them serve as the profilin binding sites but differ in affinity. If the profilin binding sites were immobile at fixed locations relative to the barbed end, an actin unit would be released and to diffuse to the barbed end. Otomo *et al.* proposed that the FH2 dimer exists in equilibrium between two states (Figure 2.4b): the closed (or blocked) configuration that prevents polymerization and the open (or accessible) state that allows actin subunit addition. The transition from the closed to the open state involves movement of the FH2 dimer toward the barbed end (Otomo, Tomchick et al. 2005; Vavylonis, Kovar et al. 2006).
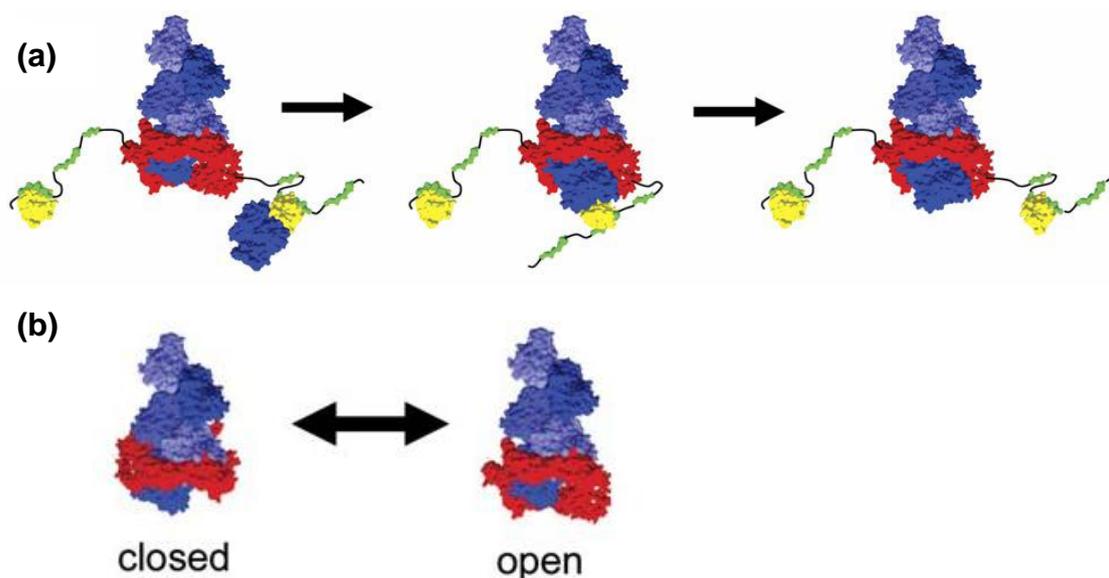
Figure 2.4 Model of actin filament growth mediated by formin dimer. FH2 domains (red) are shown as a dimer encircling the barbed end of the filament (blue). The FH1 domain (black, green) is shown unstructured with three profilin binding sites (green). (a) FH1-mediated polymerization: (1) assembly of profilin-actin to FH1; (2) transfer of actin from FH1 to the barbed end; (3) detachment of profilin. (b) Mechanism of FH2 processivity: FH2 in states preventing or allowing actin subunit incorporation. (Otomo, Tomchick et al. 2005)

2.2.3 Diaphanous-related formins (DRFs)
In a conserved and widely expressed subfamily of formins known as

Diaphanous-related formins (DRFs), the FH1 and FH2 domains are flanked by an array of regulatory domains at the N-terminus and by a single C-terminal Diaphanous autoregulatory domain (DAD) (Alberts 2001). The large N-terminal regulatory region includes the GTPase binding domain (GBD) followed by an adjacent Diaphanous-inhibitory domain (DID) and a dimerization domain (DD) (Rose, Weyand et al. 2005; Faix and Grosse 2006; Nezami, Poy et al. 2006) (Figure 2.5a). In the basal state, DRFs exist as autoinhibited proteins via intramolecular interactions between DID and DAD (Figure 2.5b) (Alberts, 2001; Li and Higgs, 2003; Watanabe et al., 1999). As revealed by the mDia1 crystal structure, the DID domain is composed of five armadillo repeats, a structural motif of three helices arrayed in a superhelical coil. The DAD polypeptide binds along the entire length of the domain, roughly perpendicular to the B helices, and establishes an extensive interface through numerous mainly hydrophobic contacts (Figure 2.5c) (Otomo, Otomo et al. 2005; Rose, Weyand et al. 2005; Nezami, Poy et al. 2006).
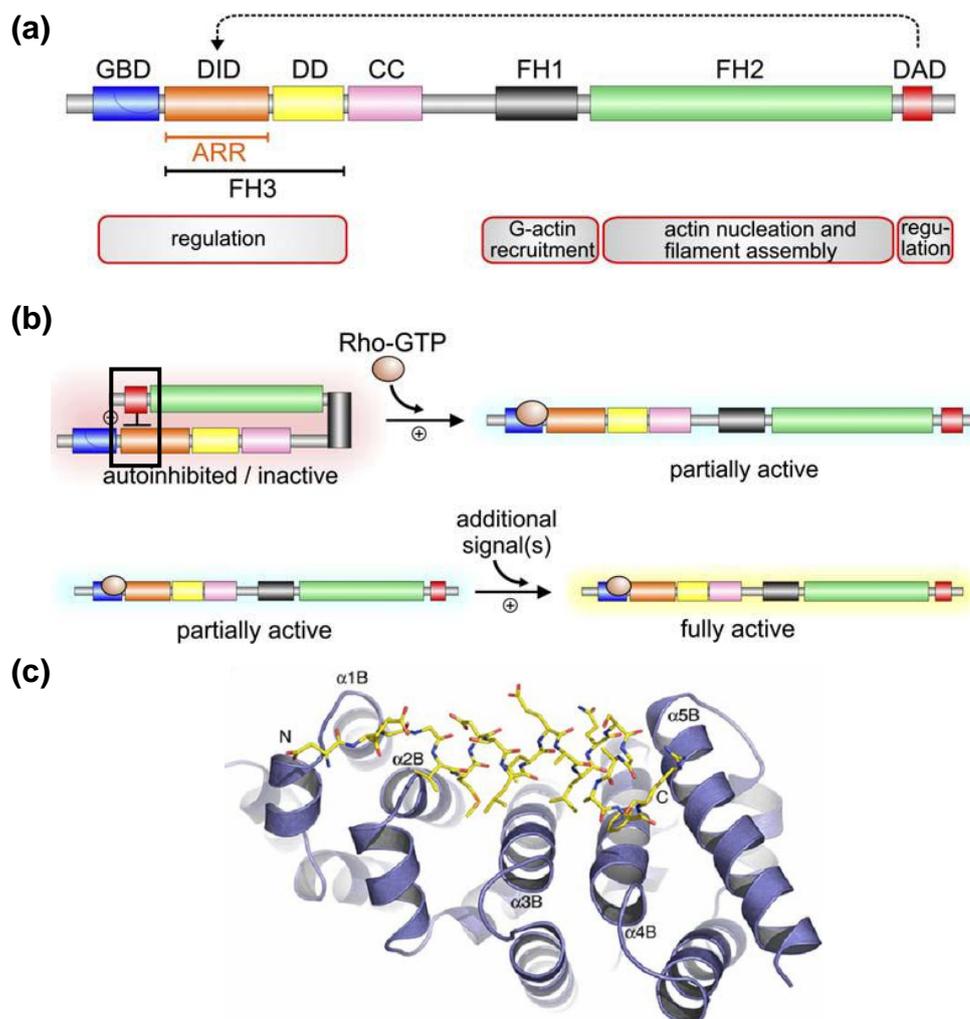
Figure 2.5 Domain organization and molecular regulation of diaphanous-related formins. (a) Schematic representation of the domain organization of a representative DRF. GBD: GTPase binding domain; DID: Diaphanous-inhibitory

domain; DD: dimerization domain; CC: coiled coil; FH1: formin homology 1 domain; FH2: formin homology 2 domain; FH3: formin homology 3 domain; ARR: armadillo-repeat region. Based on its structure, DID is also referred to as ARR. (b) Autoinhibition of DRFs caused by the interaction of DAD with DID is relieved by binding a Rho GTPase to GBD, which releases DAD and lead to a partial activation of the DRF. An unknown additional signal(s) is required to fully activate the DRF. (c) Ribbon diagram showing the overall structure of the DID/DAD complex. The DID domain is shown in blue, and the DAD domain is shown in yellow. The B helices of armadillo repeats 1–5 are labeled from left to right, and the N and C termini of the DAD domain are indicated. (Faix and Grosse 2006; Nezami, Poy et al. 2006)

This autoinhibition is relieved after binding of an active Rho GTPase to the GBD domain. The binding induces displacement of the DAD, because the GTPase binds to the GBD/DID fragment more tightly than does the DAD segment (Faix and Grosse 2006; Nezami, Poy et al. 2006). The mammalian diaphanous 1 (Dia1) as well as the macrophage-enriched murine Formin-like protein 1 (FRL) are both regulated by autoinhibition in a DAD-dependent manner (Yayoshi-Yamamoto, Taniuchi et al. 2000; Li and Higgs 2003; Harris, Li et al. 2004; Seth, Otomo et al. 2006).

In addition to the domain specific functions, formin proteins seem to be intensively regulated by splicing. Splicing at the N-terminus of human Dia2 has been demonstrated to be involved in a novel signal transduction pathway, in which hDia2C and c-Src are sequentially activated by RhoD to regulate the motility of early endosomes through interactions with the actin cytoskeleton (Gasman, Kalaidzidis et al. 2003). The DAD domain is also a hotspot of splicing. Within this area, two splice variants have been characterized for FRL although functional differences have not been observed (Harris, Li et al. 2004). In contrast, abrogation of autoinhibition in mutants lacking the C-terminal end in Dia1 and FRL specifically induces peripheral and plasma membrane localization (Seth, Otomo et al. 2006; Copeland, Green et al. 2007). The exact mechanism how DRFs locate to the plasma membrane is, however, currently unknown.

2.3   Non-Hodgkin's lymphoma (NHL)

FMNL1 has been reported as a tumor-associated antigen in chronic lymphocytic leukemia and overexpressed in various lymphomas (Krackhardt et al, 2002b, Schuster et al, 2007). Malignant lymphoma is a group of malignant neoplasms characterized by accumulation of cells native to the lymphoid tissues, such as lymphocytes, histiocytes, and their precursors and derivatives. The group is divided into two major categories: Hodgkin disease (HD) and non-Hodgkin lymphoma (NHL), with subtypes, classified according to predominant cell type and degree of differentiation. Hodgkin's disease was

named after Thomas Hodgkin, who first described abnormalities in the lymph system in 1832. It has a histological feature of the Reed-Sternberg giant cells, which emerge from the so-called Hodgkin cells. Non-Hodgkin's lymphomas are defined by the absence of these giant cells of Hodgkin's lymphoma. The NHL is a group of malignant clonal neoplasms, originating from the B-(80 to 85% of cases) or T-lymphocytes (15 to 20% of cases). They arise from different lymphoid components of the immune system (Kuppers 2009). One widely used classification is based on two criteria: cytologic characteristics of the constituent cells and type of cell growth pattern (defined as either follicular or diffuse). Another system of classification is based on the cell type of origin: T- or B-lymphocytes or histiocytes. FMNL1 has been demonstrated to be expressed in all these subtypes of NHL as follicular NHL, diffuse large B cell NHL and T cell NHL, and most highly expressed in T cell NHL (Favaro, Traina et al. 2006) although partially at low levels. The most recent lymphoma classifications, the 1994 Revised European-American Lymphoma (REAL) classification and the 2001 WHO classification, abandoned the HD vs. NHL grouping. Instead, 43 different forms of lymphoma are listed and discussed separately.

2.3.1   Chronic lymphocytic leukemia (CLL)

Chronic lymphocytic leukemia is the most frequent leukemia in adults in western countries, accounting for 25% of all leukemias, but fewer than 5% of the cases in the eastern hemisphere (Kalil and Cheson 1999). It is characterized by the clonal proliferation and accumulation of neoplastic B lymphocytes in the blood, bone marrow, lymph nodes, and spleen. The normal counterpart of CLL cells is a subpopulation of mature CD5+ B lymphocytes (also known as B-1 cells) present in the mantle zone of lymph nodes and also in small numbers in blood. These CD5+ B cells are increased in diseases with an autoimmune basis, such as rheumatoid arthritis, systemic lupus erythematosus, and Sjoeren's syndrome (Rozman and Montserrat 1995). The median age of patients at diagnosis is 65 years, with only 10 to 15 percent under 50 years of age. In most series, more men than women are affected. The course of the disease is variable. Whereas some patients with CLL have a normal life span, others die within five years after diagnosis. The etiology of CLL is unknown. Several lines of evidence suggest a genetic component, such as the increased prevalence of CLL among first-degree relatives. Environmental factors, such as ionizing radiation, chemicals, and drugs have shown no apparent relationship (Rozman and Montserrat 1995; Kalil and Cheson 1999; Montserrat and Moreno 2008).

Patients with CLL have progressive immunodeficiency, which chiefly manifests as hypogammaglobulinaemia (up to 60% of CLL patients), but involves all elements of the immune system. Compared with normal peripheral blood B cells, CLL B cells express relatively low levels of surface-membrane

immunoglobulin, mostly IgM and IgD with a single light chain (kappa or lambda) (Rozman and Montserrat 1995). Only 15% of patients with CLL have completely normal serum immunoglobulins. The extent of hypogamma-globulinaemia depends on the stage and duration of the disease and lead to bacterial infections of the respiratory tract, skin or urinary tract. They are the major causes of death in between a quarter and a half of patients with CLL (Hamblin and Hamblin 2008). The mechanisms of immune defects in CLL have not been completely elucidated, although several explanations have been proposed, including abnormalities in T regulatory cells and non-neoplastic B cells (Montserrat and Moreno 2008). One critical step for the immune response to antigen is the expression of the CD40 ligand on the surface of activated T cells. Downregulation of this ligand induced by CLL lymphocytes results in severe immunodeficiency states. Gene transfer of CD40 ligand into B cells of CLL patients has been reported to induce cytotoxic T lymphocytes against autologous leukemic cells (Cantwell, Hua et al. 1997; Kato, Cantwell et al. 1998). B-CLL cells are resistant to most currently available gene transfer systems. Several virus vectors such as replication defective adenovirus vector and recombinant adeno-associated virus (rAAV) vector have been used to enable efficient transduction of CD40 ligand to primary B-CLL cells and already entered the clinical trial (Wendtner, Kofler et al. 2004). However, the specificity and safety need to be further confirmed.

2.3.2 Therapies for CLL

CLL is generally considered not curable. The former standard treatment, chlorambucil only leads to a very low level of complete response (10%). The more effective agent fludarabine results in a much higher complete response rate (20–40%) and a longer disease-free interval, however, survival is not prolonged (Montserrat and Moreno 2008). The target therapy using monoclonal antibodies rituximab (anti-CD20) and alemtuzumab (anti-CD52) has brought great improvement in the treatment of CLL. It has dramatically improved complete response rates and progression-free survival in patients with both newly-diagnosed and relapsed CLL when incorporating of these monoclonal antibodies with chemoimmunotherapy, however, the overall survival has not been changed (Quintas-Cardama and O'Brien 2009). Stem cell transplants have been performed in an increasing number of subjects with CLL. Autologous stem cell transplants do not cure CLL but could prolong survival in extremely selected patients (Dreger, Stilgenbauer et al. 2004). However, the necessary condition for the success of an autologous transplant is to achieve complete remission before the procedure, which is rare in patients failed in chemo or chemo-immunotherapy (Dreger and Montserrat 2002). An additional problem with autotransplant is the risk of secondary myelodysplasia/acute myeloid leukaemia, particularly in patients having performed with total body irradiation. In contrast, allogeneic transplants can cure about 40% of the patients, but leads to a high toxicity and mortality

(Moreno, Villamor et al. 2005; Dreger, Corradini et al. 2007).

Since the beneficial effects of allogeneic stem cell transplantation partly depend on the graft-versus-leukaemia effects, one promising strategy consists of the genetic manipulation of effector T lymphocytes with tumor specific T-cell receptors or chimeric antigen receptors on the surface directed against surface antigens on the CLL cells. This strategy may produce therapeutic benefits without the adverse effects of more generalized allo-reactivity (Foster, Brenner et al. 2008). A number of tumour-associated antigens overexpressed on CLL cells can be selected as the target of specific CTL responses, including fibromodulin, MDM2 (murine double minute 2), survivin, oncofetal antigen-immature laminin receptor protein (OFAiLRP), FMNL1, preferentially expressed antigen of melanoma (PRAME) and receptor for hyaluronic-acid mediated motility (RHAMM/CD168) (Giannopoulos and Schmitt 2006). Moreover, the idiotypic determinants of the unique monoclonal immunoglobulin on CLL cells may serve as tumour-specific antigens (Trojan, Schultze et al. 2000). It has been already reported that an allorestricted T-cell clone, SK22, expressing a single defined T cell receptor recognizing a peptide derived from FMNL1 shows potent antitumor activity against lymphoma and renal cell carcinoma cell lines, Epstein-Barr virus (EBV)-transformed B cells and primary tumor samples derived from patients with CLL. SK22 recognizes preferentially malignant cells and has only limited reaction against normal hematopoietic cells. (Schuster, Busch et al. 2007). This suggests FMNL1 to be a highly attractive target antigen in CLL patients and gene-modified TCR-transgenic T cells might be suitable therapeutic tools in the autologous setting. However, functional investigation of FMNL1 might be highly important in order to identify FMNL1-dependent processes of diverse hematopoietic-lineage derived cells which may be associated with enhanced FMNL1 ligand presentation and therefore affected by FMNL1-specific immunotherapeutic approaches.

2.4   Aim of the project

The aim of this project is to investigate functional role of FMNL1 in order to evaluate and validate FMNL1 as potential target antigen for novel immunotherapies：
1. Testing of novel FMNL1-specific antibodies for potential application in immunofluorescence analysis and investigation of the localization of native FMNL1 in diverse hematopoietic-lineage derived cells, especially focusing on the function-associated localization with the help of confocal microscopy.
2. Functional analysis of different splice variants of FMNL1 using diverse cell biochemical and biological assays.
3. Investigation of functional aspects of FMNL1, associated with the newly identified interaction partners.

3   Materials

3.1   Equipments and supplies

- Cell culture bottles, Becton Dickinson, Heidelbuerg
- Centrifuge, Hettich, Kirchlengern, Germany
- Centrifuge 4K15, Sigma Laborzentrifugen GmbH, Osterode an Herz, Germany
- Centrifuge 5417R , Eppendorf-Netheler-Hinz-GmbH, Hamburg, Germany
- Counting chamber, Brand GmbH & Co., Wertheim, Germany
- Confocal microscopy, LEICA TCS SP2/405, Leica Microsystems GmbH, Wetzlar, Germany
- Coverslip 10 mm X 10 mm, Josef Peske, Aindling, Germany
- FACS Calibur cell sorter, Becton Dickinson, Heidelbuerg
- Fluorescence Microscope, Leica Microsystems GmbH, Wetzlar, Germany
- Gloves latex, Rösner-Mautby Meditrade GmbH, Kiefersfelden, Germany
- Gloves nitrile, Kimberly-Clark Corporation, Neenah, USA
- Hyperfilm MP, Amersham Bioscience, Freiburg, Germany
- Incubator, Heraeus Holding GmbH, Hanau, Germany
- Incubator for bacteria, Bachofer, Reutlingen, Germany
- Incubator shaker, INFORS AG, Bottmingen, Switzerland
- InGenius gel documentation (gel doc) system, Synoptics Ltd, Cambridge, England
- Irradiation facility Gammacell 40, Atomic Energy of Canada Limited, Ottawa, Canada
- Microplate reader ELISA Reader, SLT Labinstruments, Crailsheim, Germany
- Microscope, Zeiss AG, Jena, Germany
- Midi Electrophoresis chamber, Harnischmacher, Labor- und Kuststofftechnick, Kassel, Germany
- MilliQ System, Millipore GmbH, Schwalbach, Germany
- *MoFlow*TM, Dako, Hamburg, Germany
- Multichannel pipets, Eppendorf-Netheler-Hinz-GmbH, Hamburg, Germany
- PCR thermocycler, Biometra Biomedizinische Analytik GmbH, Göttingen, Germany
- PH-meter 766, Knick Elektronische Messgeräte GmbH & CO. KG, Berlin, Germany
- Pipets, Stripette 5 ml, 10 ml, 25 ml, Corning, New York, USA
- Pipet boy, Integra Biosciences, Fernwald, Germany
- Pipets, Eppendorf-Netheler-Hinz-GmbH, Hamburg, Germany
- Polystyrene round bottom FACS tubes, Becton Dickinson, Heidelbuerg
- Power supply, Pharmacia GmbH, Erlangen, Germany
- Pursep-A Xpress disinfection agent, Metz Consumer Care GmbH, Frankfurt,

Germany
- Slides, Glaswarenfabrik Karl Hecht KG, Sondheim, Germany
- Sterile bench, BDK, Sonnenbühl-Genkingen, Germany
- Sterile polypropylene round bottom FACS tubes with cap, Becton Dickinson, Heidelbuerg
- Sterile filters, Techno Plastic Products AG, Trasadingen, Switzerland
- Syringes 10ml, 50 ml, BD Perfusion, Becton Dickinson, Heidelbuerg
- Thermomixer, Eppendorf-Netheler-Hinz-GmbH, Hamburg, Germany
- Tips 1–10 µl, 10–200 µl, 100–1000 µl, Greiner Bio-One International AG, Kremsmünster, Austria
- Ultraspec 1100 pro UV/ vis Spectrophotometer, Biochrom Ltd, Cambridge, England
- Vortexer, Bender & Hobei AG, Switzerland
- Water bath, Memmert, Schwab Bach
- XCell *SureLock*^{TM} Mini-Cell, Invitrogen Cooperation, Karlsruhe
- XCell II^{TM} Blot Module, Invitrogen Cooperation, Karlsruhe
- X-ray film, valmex, Augsburg, Germany
- 12-, 24- well tissue culture plates, Becton Dickinson, Heidelbuerg
- 96 well U-bottom tissue culture plates, Becton Dickinson, Heidelbuerg
- 96 well flat-bottom tissue culture plates, Becton Dickinson, Heidelbuerg
- 50 ml, 15ml Falcons, Becton Dickinson, Heidelbuerg
- 1.5 ml, 0.5 ml tubes, Eppendorf-Netheler-Hinz-GmbH, Hamburg, Germany

3.2   Chemicals, enzymes and cytokines

- Ampicillin sodium salt, Sigma-Aldrich Chemie GmbH, Taufkirchen, Germany
- A23187, Sigma-Aldrich Chemie GmbH, Taufkirchen, Germany
- Agarose, Bio & Sell Nürnberg, Germany
- $CaCl_2$, Merck KGaA, Darmstadt, Germany
- CD40 ligand, Peprotech, London, UK
- Chloroform (1 Bromo-3-choloro-prapan), Sigma Aldrich Chemie GmbH, Taufkirchen, Germany
- Chloroform: Isoamyl alcohol (CIA) 24:1, Sigma Aldrich Chemie GmbH, Taufkirchen, Germany
- Ciprofloxacin, Sigma-Aldrich Chemie GmbH, Taufkirchen, Germany
- Cyclosporin A, Sigma-Aldrich Chemie GmbH, Taufkirchen, Germany
- Complete (25 X), Roche, Basel, Switzerland
- 4`,6-Diamidino-2-phenylindole dihydrochloride (DAPI), Sigma-Aldrich Chemie GmbH, Taufkirchen, Germany
- Diethylpyrocarbonat (DEPC) H_2O, Invitrogen Corporation, Karlsruhe, Germany
- Dulbecco's modified Eagle's medium (DMEM), Gibco, Invitrogen Corporation, Karlsruhe, Germany

- Dimethyl Sulfoxide (DMSO), Merck KGaA, Darmstadt, Germany
- Desoxinucleosidtriphosphate (dNTP) (2mM/10mM), Fermentas GmbH, St.Leon-Rot, Germany
- Dithiothreitol (DTT), 0.1M, Fermentas GmbH, St.Leon-Rot, Germany
- EcoR I enzyme, Fermentas GmbH, St.Leon-Rot, Germany
- Ethanol, Merck KGaA, Darmstadt, Germany
- Ethidium Bromide, Invitrogen Corporation, Karlsruhe, Germany
- Fetal calf serum (FCS), PAA Laboratories GmbH, Pasching, Austria
- Ficoll, Biochrom, Berlin, Germany
- First strand buffer (5×), Fermentas GmbH, St.Leon-Rot, Germany
- G418, PAA Laboratories GmbH, Pasching, Austria
- Glucose, Merck KGaA, Darmstadt, Germany
- Granulocyte Macrophage Colony Stimulating Factory (GM-CSF)，Peprotech, London, UK
- [3H]-myristic acid, PerkinElmer, Boston, U.S.A
- HEPES (1M), Gibco, Invitrogen Corporation, Karlsruhe, Germany
- HEPES (powder), Biochrom KG, Berlin, Germany
- HPLC H_2O, Fisher Scientific Corporation, UK
- Human serum, Helmholtz Zentrum Munich, healthy male donors
- HyperLadder I, Bioline GmbH, Luckenwalde, Germany
- IL-1β, Peprotech, London, UK
- IL-2, Chiron Vaccines International, Marburg, Germany
- IL-4, Peprotech, London, UK
- IL-6, Peprotech, London, UK
- Iscove's Modified Dulbecco's Medium (IMDM), Gibco, Invitrogen Corporation, Karlsruhe, Germany
- Indo-1 AM, Sigma-Aldrich Chemie GmbH, Taufkirchen, Germany
- Ionomycine, Sigma-Aldrich Chemie GmbH, Taufkirchen, Germany
- Isopropyl alcohol, Sigma-Aldrich Chemie GmbH, Taufkirchen, Germany
- Kanamycin, Sigma-Aldrich Chemie GmbH, Taufkirchen, Germany
- KCl, Merck KGaA, Darmstadt, Germany
- Kpn I enzyme, New England BioLabs GmbH, Frankfurt am Main, Germany
- 100bp ladder, New England BioLabs Incorporation
- Lusogeny broth (LB) agar, Sigma-Aldrich Chemie GmbH, Taufkirchen, Germany
- L-Glutamine, Gibco, Invitrogen Corporation, Karlsruhe, Germany
- Lipopolysoccharide (LPS), Sigma Aldrich Chemie GmbH, Taufkirchen, Germany
- 6× loading Dye Solution, Fermentas GmbH, St.Leon-Rot, Germany
- LURIA Broth Base, Sigma-Aldrich Chemie GmbH, Taufkirchen, Germany
- Methanol, Merck KGaA, Darmstadt, Germany
- Mfe I enzyme, New England BioLabs GmbH, Frankfurt am Main, Germany
- Milk powder, Frema, Lueneburg, Germany
- Mounting medium, Vector Laboratories, Burlingame, U.S.A

- 3-(4,5)-dimethylthiahiazo (-z-y1)-3,5-di- phenytetrazoliumromide (MTT), Sigma-Aldrich Chemie GmbH, Taufkirchen, Germany
- Na-Acetate, Merck KGaA, Darmstadt, Germany
- $Na_2HPO_4 \cdot 2H_2O$, Merck KGaA, Darmstadt, Germany
- NaN_3, Merck KGaA, Darmstadt, Germany
- NEB buffer, New England BioLabs GmbH, Frankfurt am Main, Germany
- Nhe I enzyme, New England BioLabs GmbH, Frankfurt am Main, Germany
- Non Essential Amino Acids, Gibco, Invitrogen Corporation, Karlsruhe, Germany
- NP-40, Sigma-Aldrich Chemie GmbH, Taufkirchen, Germany
- Okt-3, kindly provided by Elisabeth Kremmer
- Olig(dt)15 Primer, Promega Corporation Madison, USA
- Penicilline Streptomycin, Gibco, Invitrogen Corporation, Karlsruhe, Germany
- Paraformaldehyd (PFA), Sigma-Aldrich Chemie GmbH, Taufkirchen, Germany
- Phenol, Carl Roth GmbH, Karlsruhe, Germany
- Pluronic, Peprotech, Sigma-Aldrich Chemie GmbH, Taufkirchen, Germany
- Phorbol 12-myristate 13-acetate (PMA) , Sigma-Aldrich Chemie GmbH, Taufkirchen, Germany
- Prostaglandin (PG) E-2, Sigma-Aldrich Chemie GmbH, Taufkirchen, Germany
- Pheylmethanesulfonyl (PMSF), Sigma-Aldrich Chemie GmbH, Taufkirchen, Germany
- Poly-L-lysin, Sigma-Aldrich Chemie GmbH, Taufkirchen, Germany
- Ponceau, Sigma-Aldrich Chemie GmbH, Taufkirchen, Germany
- Prodium Iodide (PI), Sigma-Aldrich Chemie GmbH, Taufkirchen, Germany
- RNaseOUT Recombinant Ribonuclease Inhibitor, Invitrogen Corporation, Karlsruhe, Germany
- RPMI 1640 (-L-Glutamin), Gibco, Invitrogen Corporation, Karlsruhe, Germany
- Seminaphtorhodafluor-1 carboxylic acid, acetate and succinimidyl ester (SNARF-1), Invitrogen Corporation, Karlsruhe, Germany
- Sbf I enzyme, New England BioLabs GmbH, Frankfurt am Main, Germany
- Sodium Carbonate, Sigma Aldrich Chemie GmbH, Taufkirchen, Germany
- Sodium Pyruvate, Gibco, Invitrogen Corporation, Karlsruhe, Germany
- Sodium Chloride, Sigma Aldrich Chemie GmbH, Taufkirchen, Germany
- SuperScript II Reverse Transcriptase, Invitrogen Corporation, Karlsruhe, Germany
- T4 DNA ligase (10× ligation buffer), Fermentas GmbH, St.Leon-Rot, Germany
- TAE buffer (10×), Invitrogen Corporation, Karlsruhe, Germany
- Tumor necrosis factor α (TNF α), Peprotech, London, UK
- Trypsin EDTA 0,5 %, Gibco, Invitrogen Corporation, Karlsruhe, Germany

- Trypan blue, Gibco, Invitrogen Corporation, Karlsruhe, Germany
- Tri Reagent, Sigma Aldrich Chemie GmbH, Taufkirchen, Germany
- Tween 20, Sigma Aldrich Chemie GmbH, Taufkirchen, Germany
- Western Lighting[TM] Plus-ECL, Amersham Bioscience, Freiburg, Germany
- Xba I enzyme, New England BioLabs GmbH, Frankfurt am Main, Germany
- Xho I enzyme, Fermentas GmbH, St.Leon-Rot, Germany
- ß2-Microglobulin, EMD Biosciences, Darmstadt, Germany

3.3 Kits

- BCA[TM] Protein Assay kit, Pierce, Rockfold, U.S.A
- B cell negative isolation kit, Dynal, Invitrogen Corporation, Karlsruhe, Germany
- BrdU flow kit, Becton Dickinson, Heidelbuerg, Germany
- KOD Hot Start DNA Polymerase kit, Novagen, EMD Biosciences, Darmstadt, Germany
- LightCycler[®] - FastStart DNA Master[PLUS] SYBR Green I kit, Roche, Basel, Schweiz
- Venor[®]*GeM*-Mykoplasmen Detektions Kit, MinervaBiolabs, Berlin, Germany
- NucleoSpin® Extract II kit for PCR gel extraction, Macherey-Nagel Corporation, Düren, Germany
- Jetstar 2.0 kit for plasmid purification, Genomed GmbH, Löhne, Germany

3.4 Buffers and Solutions

- Dulbecco's Phosphate-Buffered Saline (DPBS), Gibco, Invitrogen Corporation, Karlsruhe, Germany
- Phosphate buffered saline (PBS), Dulbecco's Biochrom AG, Berlin, Germany
- Binding Buffer (10 X), Becton Dickinson, Heidelbuerg, Germany
- MOPS buffer (20 X), Invitrogen Corporation, Karlsruhe, Germany
- NuPAGE[®] Transfer Buffer (20 X), Invitrogen Corporation, Karlsruhe, Germany
- NuPAGE[®] LDS Sample Buffer (4 X), Invitrogen Corporation, Karlsruhe, Germany
- Protein G–Sepharose 4 Fast Flow, Amersham Bioscience, Freiburg, Germany
- Amplify[TM] Fluorographic Reagent, Amersham Bioscience, Freiburg, Germany
- FACS buffer
  - o PBS
  - o 1 % Δ FCS
- Ripa Buffer (stock solution):

- o 10 mM Tris-Cl
- o 10 mM NaCl
- o 1 % SDS
- o 0.5 % Deoxycholic
- o 1 % NP-40
- Ripa Buffer (working solution):
  - o Ripa Buffer (stock solution)
  - o 1 mM PMSF
  - o 1 X complete
- Lysate Buffer for immunoprecipitation (stock solution):
  - o 20 mM Tris-Cl
  - o 150 mM NaCl
  - o pH 7.4
- Lysate Buffer for immunoprecipitation (working solution):
  - o Lysate Buffer (stock solution)
  - o 150 mM Chaps
  - o 1 mM Na_3VO_4
  - o 1 mM NaF
  - o 1 mM PMSF
  - o 1 X complete
- Fixation buffer for SDS/PAGE gel:
  - o 25% volume isoproponal
  - o 65% volume water
  - o 10% volume acetic acid
- Tris buffered saline (TBS) buffer (10 X) pH 8.0:
  - o 10 mM Tris-base
  - o 150 mM NaCl
  - o H_2O
- TBST buffer:
  - o 1 X TBS buffer
  - o 0.05% Tween 20
- Western blot washing buffer:
  - o 1 X TBS buffer
  - o 0.05 % Tween 20
- 5 % or 1 % milk powder in TBST
- Immunofluoresence washing buffer:
  - o PBS
  - o 0.5 % NP-40
  - o 0.01 % NaN_3
- Fixation buffer for Immunofluoresence staining:
  - o PBS
  - o 10 % PFA
- Saline-sodium citrate (SSC) buffer (20 X) pH 7.0:
  - o H_2O

- o   0.3 M Na Citrat 2 H_2O
- o   3 M NaCl
- DAPI solution:
  - o   1 X SSC buffer
  - o   5 µg/ul DAPI
- 2× Hanks Balanced Salt Solution (HBSS) Buffer pH 7.06:
  - o   280 mM NaCl
  - o   10 mM KCl
  - o   12 mM Glucose
  - o   50 mM HEPES
  - o   1.5 mM Na2HPO4·2H20

3.5   Cell culture medium

- Complete DMEM/ RPMI
  - o   DMEM/RPMI1640
  - o   10% Δ FCS
  - o   2 mM L-Glutamine
  - o   Penicillin (100 U/ml)-Streptomycin (100 µg/ml)
  - o   10 mM Non essential amino acid
  - o   1 mM Sodium-Pyruvate
- DMEM hunger medium
  - o   DMEM
  - o   3 % Δ FCS
  - o   2 mM L-Glutamine
  - o   Penicillin (100 U/ml)-Streptomycin (100 µg/ml)
  - o   10 mM Non essential amino acid
  - o   1 mM Sodium-Pyruvate
- T cell medium
  - o   RPMI1640
  - o   10 % Δ human serum
  - o   2 mM L-Glutamine
  - o   Penicillin (100 U/ml)-Streptomycin (100 µg/ml)
  - o   10 mM Non essential amino acid
  - o   1 mM Sodium-Pyruvate
  - o   10 mM HEPES (pH 7.4)
  - o   Gentamycin (16.6 µg/ml)
- B cell medium
  - o   IMDM
  - o   10 % Δ FCS
  - o   2 mM L-Glutamine
  - o   Insulin-Transferrin (50 µg/ml)
  - o   Gentamycin (16.6 µg/ml)
- AIM-V medium

- o   AIM-V Medium
- o   0.1 % Natriumacid
- o   0.1 % BSA
- Medium for CD40-Fibroblasts
  - o   F12 + DMEM medium
  - o   2 mM L-Glutamine
  - o   10 mM Non essential amino acid
  - o   10 mM HEPES (pH 7.4)
  - o   Gentamycin (16.6 µg/ml)
  - o   G418 (400 µg/ml)

3.6   Cell lines and bacteria

Table 3.1: Cell lines and bacteria

Cell lines	Decription	Culture medium	Qwelle/Reference
BJAB	EBV-negative lymphoma cell line	RPMI (10% FCS)	Joseph Mautner, Helmholtz Zentrum Muenchen
DG75	EBV-negative Burkitt lymphoma cell line, (ATCC CRL-2625)	RPMI (10% FCS)	Joseph Mautner, Helmholtz Zentrum Muenchen
T2	TAP-deficient hybrid of T-and B-Lympho-blastoiden cell line, HLA-A2 +, (ATCC CRL-1992)	RPMI (10% FCS)	IMI, Helmholtz Zentrum Muenchen (Salter and Cresswell, 1986)
Namalwa	Burkitt lymphoma B-lymphoblasts, (ATCC CRL-1432)	RPMI (10% FCS)	Helmholtz Zentrum Muenchen
Daudi	Burkitt lymphoma B-lymphoblasts, (ATCC CCL-213)	RPMI (10% FCS)	Helmholtz Zentrum Muenchen
Raji	Burkitt's lymphoma cell line, EBV + (ATCC CCL-86)	RPMI (10% FCS)	Helmholtz Zentrum Muenchen
Ramos	Human Burkitt's lymphoma cell line (ATCC CRL-1596)	RPMI (10% FCS)	Helmholtz Zentrum Muenchen
AK-EBV-B	Epstein-Barr virus-transformed lymphoblastoid cell line	RPMI (10% FCS)	Helmholtz Zentrum Muenchen
G361	Human melanoma cell	RPMI (10% FCS)	Helmholtz Zentrum

	line		Muenchen
RCC26	Human renal cell carcinoma cell line	RPMI (10% FCS)	IMI, Helmholtz Zentrum Muenchen
RCC53	Human renal cell carcinoma cell line	RPMI (10% FCS)	IMI, Helmholtz Zentrum Muenchen
KT195	Human renal cell carcinoma cell line	RPMI (10% FCS)	Helmholtz Zentrum Muenchen
NN26	Human renal cell	RPMI (10% FCS)	Helmholtz Zentrum Muenchen
293T	Human embryonic kidney cell line, (ATCC CRL-1573)	DMEM (10% FCS)	Joseph Mautner, Helmholtz Zentrum Muenchen
293A	Human embryonic kidney cells transformed with sheared human adenovirus type 5 DNA	DMEM (10% FCS)	Invitrogen
Molt4	Human acute lymphoblastic leukemia T lymphoblast. (ATCC CRL-1582)	RPMI (10% FCS)	Helmholtz Zentrum Muenchen
K562	Humane Chronic myeloid leukemia (CML)-cell line, (ATCC CCL-243)	RPMI (10% FCS)	Helmholtz Zentrum Muenchen
MDA-MB 231	Human adenocacinoma epithelial cells (ATCC HTB-26)	DMEM (10% FCS)	Cell Line Service
HT1080	human fibrosarcoma cell line	DMEM (10% FCS)	Helmholtz Zentrum Muenchen
CD40L-fibroblasts	NIH3T3 fibroblasts, expressing CD40L	CD40L-medium with 400 g / ml G418	Boston, USA (Cracking Hardt et al, 2002a)
TOP10	Chemically competent E. coli bacteria	LB-Broth medium	Invitrogen, Karlsruhe

3.7   Antibodies and peptides

Table 3.2: Primary antibodies

Antibodies	Host	Conjugation	Dilution	Manufacturer
anti-FMNL1 6F2	Rat			Elisabeth Kremmer, Helmholtz Zentrum Muenchen
anti-FMNL1 8A8	Rat			Elisabeth Kremmer, Helmholtz Zentrum Muenchen
anti-hCD3	Rabbit		1:50	Dako, Glostrup, Denmark
anti-α tubulin	Mouse		1:100	Santa Cruz Biotechology, Heidelberg
anti-γ tubulin	Mouse		1:100	Sigma, Taufkirchen
anti-ezrin	Rabbit		1:100	Sigma, Taufkirchen
anti-myosin IIa	Rabbit		1:100	Sigma, Taufkirchen
anti-myosin IIb	Rabbit		1:100	Sigma, Taufkirchen
Phalloidine		Alexa Fluor 488	1:100	Invitrogen, Karlsruhe
anti-annexin V		Apc	1:20	Becton,Dickinson, Heidelberg

Table 3.3: Secondary antibodies

Antibosies	Conjugation	Dilution	Manufacturer
anti-Rat	Cy3	1:200	Jackoson, Suffolk, UK
	Cy5	1:100	Jackoson, Suffolk, UK
	Peroxidase	1:2000	Jackoson, Suffolk, UK
anti-Mouse	Alexa Fluor 488	1:100	Invitrogen, Karlsruhe
	Cy5	1:100	Jackoson, Suffolk, UK
	Peroxidase	1:5000	Jackoson, Suffolk, UK
anti-Rabbit	Cy5	1:100	Jackoson, Suffolk, UK

Table 3.4: Peptide

Peptide	Sequence	Description	Manufacturer
FMNL1-PP2	RLPERMTTL	Predict, binding to HLA-A2	BIOSYNTAN GmbH, berlin

3.8 DNA-Material

3.8.1 Vectors

Table 3.5: Vectors

Vector	Description	Resistance	Manufacturer
pcDNA3.1	Vector for high-level expression in mammalian host controlled by	Ampicillin	Invitrogen, Karlsruhe

	CMV promotor		
pACDC entry clone	Entry clone containing GFP for recombination with adenovirus expression clone	Kanamycin	Vigo Heissmeyer, Helmholtz Zentrum Muenchen
pAd/PL-DEST	Adenovirus expression clone	Ampicillin	Invitrogen, Karlsruhe

3.8.2 Primers

5`C5B6 Sbf I:	GAC CTG CAG GCT CTG GGC CTG G
3`C5B6 Xba I:	TAT CTA GAC TAG AGG GGC ATC TCT TC
5`pCD-F-NheI KL2:	ATT GCT AGC CAC CAT GGG CAA CGC GGC CGG CAG CGC CGA GC
3`FMNL1-Ins-Xho I:	TAC TCG AGC AGC ACA TCC AGG CCA CGG TTC TC
5`Adeno-FMNL1-F:	ATG GAT CCC ACC ATG GGC AAC GCG GCC GGC AGC GCC GAG CAG C
3`Adeno-FMNL1-C5B6:	TAG GAT CCC TAG AGG GGC ATC TCT TCT CCC AGG CTG GCC TC
G2TA4T:	AGA TCC CAC CAT GAC CAA CAC GGC CGG CAG CGC
G2TA4T anti:	GCG CTG CCG GCC GTG TTG GTC ATG GTG GGA TCT
5`G2TA4T-Nhe I:	ATT GCT AGC CAC CAT GAC CAA CAC GGC CGG CAG CGC CGA G
3`pCD-F-C-Xba I 2:	ATT CTA GAC TAG CTC TCA TAA ATG AGT GGC TCC TTC TGC TG
5`-G2TA4T-BamH I 2:	ATT GGA TCC CAC CAT GAC CAA CAC GGC CGG CAG CCG CCG A
3`FMNL1-C-BamH I 2:	AAG GAT CCC TAG CTC TCA TAA ATG AGT GGC TCC TTC TGC TG

3.9 Software and website

- Edition of DNA sequence:
    - o Sequencher 4.5
    - o Clone Manager 7
- Analysis of FACS data:
    - o BD CellQuest[TM] Pro
    - o FlowJo
- Analysis of immunofluorescence data: LCS Lite
- Primer synthesis corporations:
    - o MWG-Biotech AG, Ebersberg, Germany
    - o Sigma-Aldrich Chemie GmbH, Steinheim, Germany
- Search restricted enzyme and reaction condition:
    http://www.neb.com/nebecomm/default.asp

4   Methods

4.1   Cell culture method

4.1.1   General cell culture methods

All cells were incubated at 37 °C and in an incubator with 5 to 6% CO_2 and 95% humidity. Cell culture was performed under sterile conditions. Working with adenoviruses or untested blood (testing for HIV, hepatitis B and C) were performed under the genetic conditions of the security level S2 and biological safety conditions L2.

4.1.1.1   Freezing and thawing of cells

Cells were frozen in 1.8ml of 90% FCS and 10% DMSO per tube first at -80 °C for at least 24 h and then in liquid nitrogen for permanent storage.

For thawing, the cells were first briefly incubated at 37 °C in a water bath and immediately transferred into medium, washed and cultured in medium depending on the cell line.

4.1.1.2   Culture of cell lines

Suspension cells were cultured by replacing old medium with fresh medium every 3-4 days. Adherent cells were placed in new bottles and added with fresh medium every 3-4 days. To do this, they were washed once with PBS in the bottle, incubated with trypsin for several minutes and harvested from the bottle within complete medium into 50 ml tubes. After centrifugation (1800 rpm, 5 min), cells were resuspended in fresh medium and transferred 1:2 to 1:40 split to new culture bottles according to cell types.

4.1.1.3   Determination of cell number

To determine cell numbers, the cells were diluted in trypan blue for living-dead distinction. Trypan blue can only penetrate dead cells and dye them blue. Unstained living cells were conducted using a Neubauer-counting chamber and counted in two to four large squares under microscope, the dead cells were excluded. The cell number was determined by the following formula:

c [cells / ml] = number of cells / number of large squares X dilution factor X 10^4

4.1.1.4   Mycoplasma contamination test

Mycoplasma contamination was tested by using Venor$^®$*GeM*- Mykoplasmen

Detektions Kit (Minerva Biolabs). Samples were derived from cell cultures which are at 90-100 % confluence. Cell culture supernatant or cell pellets following DNA extraction were tested for mycoplasma C infection according to the manufacturer. After gel running, the internal control of 191 bp should be seen in every samples and a 265-278 bp band could be seen only in the mycoplasma-contaminated samples.

When culturing mycoplasma-contaminated cells, 6-10µg/ml ciprofioxaxin was added to the cell culture medium.

4.1.2   Isolation of PBL from whole blood

Peripheral blood leukocytes (PBLs) were obtained from donors by ficoll gradient. Blood samples with heparin were firstly diluted 1:1 with RPMI. Each 25-35 ml mixture was then carefully transferred on the top of 15ml pre-warmed ficoll and centrifuged at 2000 rpm for 30 min with slow acceleration and brake. The middle layer buffy coat was carefully taken out and washed with RPMI with centrifugation (1800 rpm, 5 min). Finally, the PBL were resuspended in T-cell medium and counted.

4.1.3   Unspecific stimulation of T cells

For unspecific stimulation, T cells were cultured in T-cell medium with IL2 (50 U/ml) and OKT3 (100 ng/ml) for 3-5 days. In some cases, T cells were also unspecifically stimulated by LPS (1 µg/ml), TNFα (1000 U/ml) or PMA (50 ng/ml) combined with ionomycine (250 ng/ml) for about 16 hours.

4.1.4   Peptide pulsing of T2 cells

T2 cells were washed twice in serum-free RPMI (centrifugation at 1800 rpm 5 min) and then pulsed in AIM-V medium with a concentration of 2 Mio cells/ml containing 5 µg/ml β2-microglobulin and 100 µM peptide. After 2 hours incubation at 37 °C, they were washed once in T-cell medium.

4.1.5   Isolation of B cells from PBL using magnetic beads

B cells were isolated from PBLs of healthy donors using B cell negative isolation kit (Dynal). The cells were incubated with a mixture of monoclonal antibodies against T cells, NK cells, monocytes, granulocytes and erythrothytes to mark all the PBLs with the exception of B cells. Magnetic beads coupled with secondary antibodies binding to the constant part of primary antibodies could separate the B cells with the help of a magnet to all other cells in the PBLs. The magnetic beads were washed twice with PBS

containing 1% FCS. PBLs were incubated with antibodies for 30 min at 4°C under rotation, and washed once. Subsequently, the PBLs were gently mixed and incubated with magnetic beads for another 30 min at 4°C under rotation and placed in the magnet. B cells in supernatants were collected, washed and resuspended in B cell medium. Isolated B cells were investigated using flow cytometry and were about 90% pure.

4.1.6　Unspecific stimulation of B cells and CLL cells

Isolated or thawed B cells or chronic lymphatic leukemia (CLL) cells were added to irradiated (90 Gy) CD40 ligand expressing fibroblasts which were cultured in 6-well plates with the addition of IL-4 (5 ng / ml) and cyclosporin A (0.66 g / ml). After 3-4 days B cells were transferred onto fresh plates containing CD40 ligand expressing fibroblasts. The CD40 ligand-activated CLL cells were tested after 3-7 days. B-cells were tested after approximately 14 days, when the purity of the cells was at least 70%. The purity was determined with an anti-CD19 antibody binding to the surface of B cells.

4.1.7　Isolation and maturation of dendritic cells from PBL

PBLs suspended in B-cell medium (5 Mio/ml) were placed into 6-well plate (3 ml per well). After 2 hours incubation at 37℃, the medium containing non-adherent cells were removed and the adherent immature dendritic cells were stimulated by B-cell medium (3 ml per well) with IL 4 (20 ng/ml) and GM-CSF (100 ng/ml) and incubated at 37℃. Three days later, the immature dendritic cells were restimulated under the same condition. After another 3 days, the immature dendritic cells were matured by either CD40 ligand (1 μg/ml) combined with LPS (1 μg/ml) or a cocktail containing GM-CSF (50 μg/ml), IL-4 (20 ng/ml), IL-1β (10 ng/ml), TNF α (10 ng/ml), PGE-2 (1 μg/ML) and IL-6 (15 ng/ml) for about 7 days.

4.2　Protein biochemical methods

4.2.1　Western blot

4.2.1.1　Cell lysis and protein concentration measurement
The cell pellets of different cell lines were incubated in Ripa lysis buffer for 30 min on ice and vortex 3 times during incubation. The cell lysates were centrifuged (5000rpm, 10min, 4℃) and the supernatants were taken to measure the protein concentration with BCA^TM Protein Assay Kit (Pierce).

4.2.1.2 Electrophoresis and transfer

To prepare loading samples, 65µl protein supernatants were mixed with 25µl 4X NuPAGE® LDS Sample Buffer (Invitrogen) and 10µl 0.5mM DTT. These samples were heated at 95°C for 5 min and loaded equally of the protein concentration into the NuPAGE® Novex Bis-Tris Gel (Invitrogen). The electrophoresis was progressed in XCell SureLock™ Mini-Cell (Invitrogen) using 500 ml MOPS buffer (Invitrogen) under 200V constant for 50 min.

Transfer was performed in the XCell II™ Blot Module (Invitrogen). Briefly, 500 ml of 1X NuPAGE® Transfer Buffer was prepared by adding 25 ml 20X NuPAGE® Transfer Buffer (Invitrogen) and 50 ml methanol to 425 ml deionized water for transferring one gel in one blot module. Two buffer pre-soaked blotting pads were placed into the cathode (-) core of the blot module. A gel/membrane sandwich was prepared by a pre-soaked filter paper, the gel, a pre-soaked nitrocellulose or PVDF membrane and another pre-soaked filter paper. The gel/membrane sandwich was placed on the blotting pads in the correct orientation, so the gel was closest to the cathode core. Finally, enough pre-soaked blotting pads were added to rise to 0.5 cm over rim of cathode core. The anode (+) core was placed on the top of the pads. Transfer was performed under 30V constant for 1 hour.

If two gels need to be transferred in one blot module, 1X NuPAGE® Transfer Buffer was prepared by adding 25 ml 20X NuPAGE® Transfer Buffer (Invitrogen) and 100 ml methanol to 375 ml deionized water. Another pre-soaked blotting pad need to be placed between two gel/membrane sandwiches. Other steps were the same as transferring one gel in one blot module.

4.2.1.3 Blotting

The membrane was stained by ponceau for 1 min and washed by deionized water to analyse the efficiency of protein transfer. The membrane was then blocked in 5% fat-free milk for 1 to 2 hours at room temperature. After washing with TBST buffer, the membrane was incubated with primary antibodies diluted in 1% fat-free milk for 1 hour at room temperature. The membrane was washed with TBST buffer for 3 times (10 min for each time) and incubated with secondary antibodies diluted in 1% fat-free milk for another 1 hour at room temperature. After another 3 washing steps with TBST buffer (10 min for each time), the membrane was incubated with Western Lighting™ Plus-ECL buffer (Amersham) for 1 min and exposed to an X-ray film for half to several minutes. The film was developed using a developing machine.

4.2.2 [^{3}H]- myristic acid uptake assay

293T cells were transfected with FMNL1γ and G2TA4T. 1 day later, the cells were biosynthetically labelled for 16 h with [3H]myristic acid (0.2 mCi/ml) (PerkinElmer) in DMEM supplemented with 5% heat-inactivated FCS.

4.2.2.1   Immunoprecipitation

[3H]myristic acid -labelled cells were washed with PBS and lysed in lysis buffer. Probes were centrifuged at 12000 g for 10 min. 1 ml protein supernatants were cleared by incubation with 50 µl Protein G–Sepharose 4 Fast Flow (Amersham Biosciences) for 1 hour at 4°C. Meanwhile, the Protein G–Sepharose 4 Fast Flow was bound to FMNL1 specific antibody 8A8 and isotype control by coincubation for 1 hour at 4°C. The specific proteins were immunoprecipitated by mixing precleared supernatants and antibodies coupled to Protein G–Sepharose 4 Fast Flow while rotating at 4°C for 3 hours. After that, immunoprecipitated proteins were eluted in LDS buffer through Pall filters (6000 rpm, 2 min, 3 times) and analyzed by western blot.

4.2.2.2   Autoradiography

Immunoprecipitated proteins were resolved by SDS/PAGE. The gel was treated first with fixation solution for 30 min and then with Amplify^{TM} Fluorographic Reagent (Amersham Biosciences) for another 30 min. After drying, the gel was exposed for 12 days to Hyperfilm MP (Amersham Biosciences) at −80°C using an intensifying screen.

4.3   Cell biological assays

4.3.1   Immunofluorescence staining

Adherent cells were settled on sterilized coverslips (1 cm X 1 cm) in 12-well plate overnight (0.2 Mio cells/well). For non-adherent cells, coverslips were treated with poly-L-lysine for 15 min at room temperature, washed with deionized water and then dried in air. Non-adherent cells were then seeded on the coverslips (0.5 Mio cells/well) and incubated for 40 min at room temperature. Cells were fixed by fresh prepared 3% PFA and washed with immunofluoresence washing buffer. After blocking by washing buffer containing 10% FCS, the coverslips were stained with the primary antibody for 1 hour at room temperature. The coverslips were washed by washing buffer containing 10% FCS and incubated with the secondary antibody diluted in washing buffer containing 10% FCS for 30 min at room temperature. After 2 washing steps with immunofluoresence washing buffer, the coverslips were stained with DAPI for 1-2 min and washed again with washing buffer. During fixation, blocking and staining the 12-well plate was kept shaking slowly. The

coverslips were dried and put on the slide prepared with a drop of mounting medium. The edges were sealed with nail polish and stored at -20℃ in dark. Slides were investigated by the Leica TCS SP20/405 confocal microscopy.

4.3.2   Apoptosis assay

K562 cells were adenovirally transduced with FMNL1 isoforms as well as vector control. Meanwhile, K562 cells were incubated with vincristine for 48 hours to induce cell apoptosis as a positive control. The cells were washed twice with cold PBS and resuspended in 1x Binding Buffer (BD) at a concentration of ~1 Mio cells/ml. 100 µl of the solution (~0.1 Mio cells) were transferred to a 5 ml culture tube and then gently mixed with 5 µl APC conjugated annexin V antibody together with 2 µl propidium iodide (PI) and incubated for 15 min at room temperature. After that, 400 µl 1x Binding Buffer was added into the tube and the cells were analyzed by flow cytometry using FACS Calibur (BD) as soon as possible (within 1 hour). The annexin V positive cells represented apoptotic cells.

4.3.3   Proliferation assay

4.3.3.1   SNARF-1 staining
The cells were stained with SNARF-1 at a working concentration of 5 µM for 15 minutes at 37°C. After removing SNARF-1, cells were incubated in medium at 37°C for 30 minutes and then adenovirally transduced with different splice variants of FMNL1 and GFP vector control (Charpter 4.3.2) and cultured for three additional days. Cells were analyzed by flow cytometry using a FACS Calibur (BD).

4.3.3.2   BrdU uptake assay
A BrdU flow kit (BD) was used to determine the cell cycle kinetics by measuring the incorporation of 5`-bromo-2`-deoxyuridine (BrdU) into DNA of proliferating cells and therefore coupling cell cycle and cell proliferation. HT1080 cells were seeded overnight and transduced with different FMNL1 splice variants and GFP vector control on the next day (Chapter 4.3.2). After 24 hours 10 µM BrdU was added. 48 hours later, cells were harvested, fixed and permeabilized followed by DNAse incubation. After washing, APC-conjugated anti-BrdU antibody was added for 20 min at room temperature. Cells were then washed and stained with 7- amino-actinomycin D (7-AAD) followed by flow cytometric analysis using the FACS Calibur (BD).

4.3.4   Analysis of free intracellular Calcium

Cells were harvested and adjusted to 1 Mio/ml in prewarmed RPMI containing 10% FCS in round bottom tubes. Indo-1 AM stain was prepared by adding 40 µl prewarmed 10% pluronic solution (prepared in DMSO) and 1 ml prewarmed RPMI containing 10% FCS to an indo-1 AM stock aliquot (1 µg/ul, 20 ul, dried, store in the dark at -20°C). To stain 1 Mio cells in a round bottom tube, 250 µl indo-1 AM stain was added and the final volume was adjusted to 1 ml with prewarmed RPMI containing 10% FCS. Cells were then incubated for 30 min at 37°C and mixed every 10 min during incubation. Stained cells were diluted to 0.1 Mio/ml and kept in the dark until analysis. The free intracellular calcium was analyzed by flow cytometry at the MoFlow (Dako). The FL7 channel of violet fluorescence (405 nm) represents the calcium-bound dye and the FL8 channel of green fluorescence (530 nm) represents the calscium-free dye. Therefore the ratio FL8/FL7 indicates the free intracellular calcium concentration. Stained cells were measured within 2-3 hours after labeling.

4.4 Protein overexpression

4.4.1 Calcium-phosphate transfection

293T cells or 293A cells were seeded overnight in 6-well plate (5×10^5 per 3ml medium per well). 300 µl 2x HBSS buffer were mixed with 300 µl plasmid mixture containing 200 mM $CaCl_2$, 253.4 µM chloroquine and 6 µg plasmid. The plasmid mixture was dropped into 2x HBSS buffer while generating bubbles with the pipetboy. After 30 min incubation at room temperature, the slightly turbid mixture (300 µl per well) was transferred drop by drop to cells incubated in DMEM hunger medium for about 30-60 min before the transfection. At last, the transfected cells were incubated for another 6 hours at 37°C, washed 1 time with DPBS and finally cultured in complete DMEM.

4.4.2 Adenoviral transduction

4.4.2.1 LR recombination reaction

pAd/PL-DEST^{TM} Gateway$^®$ vector (Invitrogen) was used to induce high-level, transient protein expression in mammalian cells by the ViraPower^{TM} Adenoviral Expression System. 2 µl LR Clonase^{TM} II enzyme (Invitrogen) was added to a mixture containing entry clone (50-150 ng/reaction), pAd/PL-DEST^{TM} Gateway$^®$ vector (300 ng/reaction) and TE buffer (pH 8.0, adjust the total volume to 8µl) and mixed well by pipetting up and down. After incubation at 25°C for 18 hours followed by another incubation with 1 µl of the

Proteinase K solution (Invitrogen) in each reaction for 10 min at 37°C, the reaction mixture transformed into E.*coli* host (Chapter 4.4.1.5) and selected on LB plates containing ampicillin for expression clones.

4.4.2.2   Generation and amplification of adenoviral stocks

The selected pAd/PL-DEST expression clones were digested by Pac I enzyme for 16 hours at 37°C, purified by phenol-chroloform extraction (Chapter 4.4.1.3) and then transfected to 293A cell line (Invitrogen) by calcium-phosphate transfection (Chapter 4.3.1). After around 10-13 days post-transfection during which culture medium were replaced with fresh, complete culture medium every 2-3 days, approximately 80% of cells showed a cytopathic effect (CPE) which is characterized by formation of plaques. The adenovirus-containing cells were then harvested. To prepare a crude viral lysate, the harvested cells were frozen at -80°C for at least 30 min and thawed at 37°C in water bath for 15 min. After repeating freezing and thawing twice, the cell lysates were centrifuged (3000rpm, 15 min, room temperature) and the supernatants were taken and stored at -80°C as adenoviral stock passage one.

The andenoviral stocks were amplified by infecting 293A cells. The infected cells were harvested 2-3 days after infection when 80-90% cells had rounded up or were floating. After repeating freezing-thawing, the cell lysates were centrifuged and the supernatants were collected and stored at -80°C as adenoviral stock passage two.

4.4.2.3   Titeration of adenoviral stocks

293A cells were seeded in 6-well plate at 37°C overnight (1 Mio cells per well). Adenoviral stocks were thawed and diluted ranging from 10^{-4} to 10^{-9} with complete culture medium to a final volume of 1 ml. The adenoviral dilutions were added to cells and incubated at 37°C overnight. The following day, the medium containing virus was gently replaced with agarose overlay (2 ml per well). After another 2 days, the cells were gently overlayed with an additional 1 ml of agarose overlay solution per well. Generally 8-12 days post-infection, MTT solution (5 mg/ml, 1/10 the volume of the agarose overlay) was layered the on top of the solidified agar and incubated for 3 hours at 37°C.
Plaques were counted to determine the titer of adenoviral stocks. Titers ranging from 1 x 10^8 to 1 x 10^9 pfu/ml are generally suitable for use in most applications.

4.4.2.4   Cell transduction with adenoviral stocks

The mammalian cells of choice were plated in appropriate complete media. On the day of transduction, the adenoviral stocks of passage 2 were thawed and mixed gently by pipetting. The culture medium of the cells were replaced with the supernatant of passge 2 of diverse adenoviral stocks. The plate was

swirled gently to disperse the medium and incubated at 37°C overnight. The following day, the medium containing viruses were replaced with fresh, complete culture medium. The cells were harvested 2 days post transduction and analyzed for the presence of the specific protein.

4.5 Molecular biology methods

4.5.1 Cloning of FMNL1α and FMNL1γ into pcDNA 3.1 vector

The plasmid pcDNA 3.1 containing FMNL1β and the FMNL1α and FMNL1γ DNA fragments were prepared by Elfriede Eppinger (in the research group of Angela Krackhardt). As decribed in Chapter 5.2, the three FMNL1 splice variants are only different at C-terminus of the amino acid sequence (Figure 5.7b). To prepare plasmids, pcDNA 3.1-FMNL1α and pcDNA 3.1-FMNL1γ, pcDNA 3.1-FMNL1β was digested by restrict enzyme Sbf I in the middle of FMNL1 inserts and Xba I at the 3` cloning site and exchanged the 3` terminus with FMNL1α and FMNL1γ (Figure 4.1).
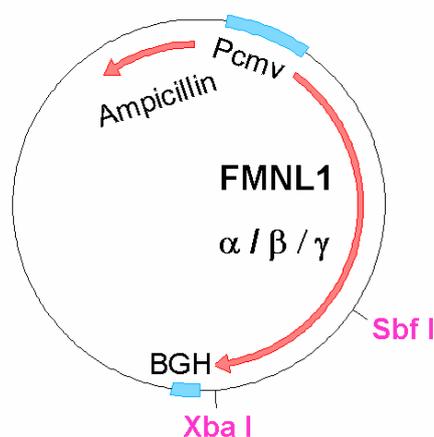
Figure 4.1:   FMNL1 α/β/γ in the pcDNA3.1 vector. Sbf I restrict enzyme site is in the middle of FMNL1 inserts and Xba I is at the 3` cloning site.

4.5.1.1   Amplification of 3` terminuses of FMNL1α and FMNL1γ

Although FMNL1α and FMNL1γ are different at the C terminus, the last 30 amino acids are exact the same (Figure 5.7b). Therefore, the same primers 5`C5B6 Sbf I and 3`C5B6 XbaI were used to amplify 3` terminuses of FMNL1α and FMNL1γ. The KOD Hot Start DNA Polymerase kit (Novagen) was used for the amplification. PCR products were amplified in 10 separated reaction tubes.

PCR mixture:

FMNL1 α 3` terminus		FMNL1 γ 3` terminus	
P-5` (100 pmol/ul)	1 µl	P-5` (100 pmol/ul)	1 µl
P-3` (100 pmol/ul)	1 µl	P-3` (100 pmol/ul)	1 µl
dNTP (2 mM)	5 µl	dNTP (2 mM)	5 µl
$MgSO_4$ (25 mM)	3 µl	$MgSO_4$ (25 mM)	3 µl
PCR buffer (10X)	5 µl	PCR buffer (10X)	5 µl
KOD-Polymerase (1U/µl)	1 µl	KOD-Polymerase (1U/µl)	1 µl
FMNL1 α (263 ng/µl)	2 µl	FMNL1 γ (524 ng/µl)	1 µl
DEPC-H_2O	to 50 µl	DEPC-H_2O	to 50 µl

PCR-program;			
	1. initial denaturation	94°C	2 min
	2. denaturation	94°C	30 sec
	3. annealing I	58°C	30 sec
	4. elongation	68°C	1 min
	5. terminal elongation	72°C	10 min
	6. cooling	4°C	

35 cycles form step 2 to step4

4.5.1.2   Gel electrophoresis and gel-extraction of the PCR production

The PCR products were diluted in a ratio of 5:1 with 6-fold Ladebuffer, loaded in a 1.5% agarose gel (with 0.7 g / ml ethidium bromide) and run in a gel electrophoresis chamber at a voltage of 120 mV over a period of approximately 50 min. The DNA ladder HyperLadder I (Bioline) was served as a size control. Amplified DNA products were visualized under a UV transilluminator. Appropriate bands were cut with a scalpel and eluted from the gel by using the NucleoSpin gel extraction kit (Macherey-Nagel Company), according to the manufacturer. The DNA quantity was measured on the spectrometer.

4.5.1.3   Digestion and purification of the inserts and vector

Both of the inserts (FMNL1α and FMNL1γ 3` termini) and the vector (pcDNA 3.1-FMNL1β) were digested with Sbf I and Xba I at 37°C for 3-4 hours and inactivated at 65°C for 20 minutes.

Digestion:

3` terminus of FMNL1 α/γ or pCDNA 3.1-FMNL1β	100 µg
Buffer NEB4 (10X)	10 µl
BSA (10X)	10 µl
Sbf I (10 U/ml)	3 µl
Xba I (20 U/ml)	4 µl
DEPC-H_2O	add to 100 µl

For purification, the digested vector were diluted in a ratio of 5:1 with loading buffer, loaded in a 1% agarose gel (with 0.7 g / ml ethidium bromide) and run in a gel electrophoresis chamber at a voltage of 120 mV over a period of approximately 50 min. The DNA ladder HyperLadder I (Bioline) was served as a size control. The appropriate band was eluted from the gel by using the NucleoSpin gel extraction kit (Macherey-Nagel Company), according to the manufacturer. The DNA quantity was measured on the spectrometer.

The digested inserts were purified by using phenol-chloroform extraction to remove enzymes and small DNA fragments. Each insert digestion was very well mixed with 500 µl of equilibrated phenol. After centrifugation (2 min, 14000 rpm), the upper aqueous phase was transferred into a new tube and added with 500 µl chloroform-isoamyl alcohol. After mixing and centrifugation (2 min, 14 000 rpm), the upper phase was again transferred into a new tube and mixed with 10 µl sodium acetate (3 M) and 1 ml ethanol (99%). After centrifugation (20 min, 14 000 rpm, 4 °C) the supernatant was discarded and the DNA sediment was solved in DEPC-H_2O after air drying. The DNA quantity was measured on the spectrometer.

4.5.1.4 Ligation
Digested and purified inserts and vectors were ligated in a ratio of insert : vector = 6 : 1. The DNA amount is calculated as follows:
Insert [ng] = 6 X (insert [bp]) X (vector [ng]) / (vector [bp])

Ligation mixture:

pcDNA 3.1-FMNL1α
3` terminus of FMNL1 α	1 µl (562 ng/µl 1:5 diluted)
pcDNA 3.1-FMNL1β (Sbf I / Xba I)	1 ul (99.5 ng/µl)
Ligation buffer (10X)	1 µl
T4 ligase	1 µl
DEPC-H_2O	to 10 µl

pcDNA 3.1-FMNL1γ
3` terminus of FMNL1 γ	1 µl (105 ng/µl)
pcDNA 3.1-FMNL1β (Sbf I / Xba I)	1 ul (99.5 ng/µl)
Ligation buffer (10X)	1 µl
T4 ligase	1 µl
DEPC-H_2O	to 10 µl

Reaction:	16°C	overnight
Inactivation:	65°C	20 min
Cooling:	4°C	
Stock:	-20°C	

4.5.1.5 Transformation to bacteria

Ligation products were transformed by heat shock into chemically competent E. *coli* , Escherichia *coli* One Shot TOP10 (Invitrogen). These bacteria were thawed on ice and 2 µl ligation products were added and stirred with a tip. After 30 min incubation on ice, the bacteria were incubated for 45 s at 42°C and immediately transferred on ice to cool. After the addition of 250 µl S.O.C medium (Invitrogen) the bacteria were shaked at 225 rpm for 1 h at 37°C, and placed on preheated LB agar plates with appropriate antibiotic additives (eg: Ampicilllin: Cend = 100 µg / ml) in two different volumes (50 µl, 100 µl). The plates were incubated at 37°C overnight and stocked at 4°C for maximum one week.

4.5.1.6 Selection of the transformed bacteria

Only the bacteria successfully transformed with the ligation products could grow on the agar plates since the ligation products contains antibiotic resistance. Individual colonies were picked with tips and transferred in 5 ml LB medium containing the same antibiotic, shaked overnight at 37 °C.

4.5.1.7 Plasmid-DNA-extraction and digestion

To check whether the ligation products were properly incorporated into the vector, plasmid DNA of 5-10 starter cultures were purified by using the "Jetstar Plasmid Purification Mini Kit" (Genomed) according to the manufacturer. After determining the DNA quantity, these mini-preparations were tested by digestion with specific restriction enzymes targeting a specific sequence within the insert (Sbf I and Xba I). Two bands of 7701 bp and 1079 bp should be visible after digestion of pcDNA 3.1-FMNL1α, two bands of 7701 bp and 1253 bp should be visible after digestion of pcDNA 3.1-FMNL1γ.

4.5.1.8 Plasmid sequencing and maxi-preparation

Plasmid with the fragments of the correct size had been sequenced by the company Sequiserve or MWG.

The corresponding starter culture, from which the plasmid of right sequence was obtained, was used to provide plasmid DNA of greater quantity. For this, 300 µl of starter cultures was transferred in 300 ml LB-medium (with antibiotic) and the bacteria were shacked overnight at 37 ° C for expanding. The Maxi preparation was performed with the "Jetstar Plasmid Purification Maxi Kit" (Genomed) according to the manufacturer. The DNA quantity was measured on the spectrometer and the plasmid was stocked at -20°C.

4.5.2 Cloning of Kozak sequence into pcDNA 3.1-FMNL1α/γ

To enhance the expression, a kozak sequence (CACC) was added before the 5` start coden of FMNL1α/γ in pcDNA 3.1 vector. To do this, pcDNA

3.1-FMNL1α/γ were digested by restrict enzyme Nhe I at the 5` cloning site and Xho I in the middle of FMNL1 inserts and exchanged the 5` terminus of FMNL1β containing kozak sequence (Figure 4.2), since the three FMNL1 splice variants are same at N-terminus of the amino acid sequence.
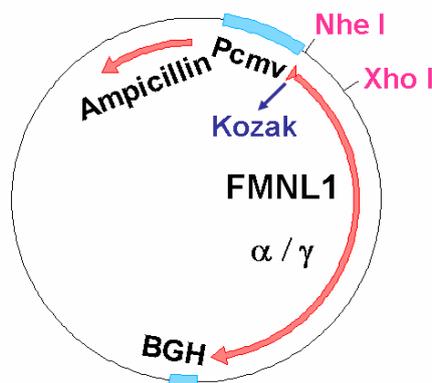
Figure 4.2: FMNL1 α/γ containing Kozak sequence in the pcDNA3.1 vector. Restrict enzyme Nhe I is at the 5` cloning site and Xho I site is in the middle of FMNL1 inserts.

4.5.2.1 Amplification of 5` terminuse of FMNL1β containing kozak sequence

The pEntr11-derived entry clone pACDC-FMNL1β including the kozak sequence was prepared by Elfriede Eppinger (in the research group of Angela Krackhardt). The primers 5`pCD-F-NheI KL2 and 3`FMNL1-Ins-Xho I and the KOD Hot Start DNA Polymerase kit (Novagen) were used to amplify 5` termini of FMNL1β containing kozak sequence. PCR products were amplified in 10 separated reaction tubes.

PCR mixture:

5` terminus of FMNL1 + Kozak

P-5` (15 pmol/ul)	1 µl
P-3` (15 pmol/ul)	1 µl
dNTP (2 mM)	5 µl
MgSO$_4$ (25 mM)	3 µl
PCR buffer (10X)	5 µl
KOD-Polymerase (1U/µl)	1 µl
pACDC-Kozak-FMNL1β	1 µg
DMSO	2.5µl
DEPC-H$_2$O	to 50 µl

PCR-program;	1. initial denaturation	94°C	2 min
	2. denaturation	94°C	30 sec
	3. annealing l	68°C	30 sec
	4. elongation	68°C	1 min
	5. terminal elongation	72°C	10 min
	6. cooling	4°C	

35 cycles form step 2 to step 4

The PCR products were used for gel electrophoresis and eluted from the gel as described before (Chapter 4.5.1.2). The DNA quantity was measured on the spectrometer.

4.5.2.2 Digestion and purification of the inserts and vector
Both of the inserts (5` terminus of FMNL1+ Kozak) and the vector (pcDNA 3.1-FMNL1α/γ) were digested with Nhe I and Xho I at 37°C for 3-4 hours and inactivated at 65°C for 20 minutes.

Digestion:

5` terminus of FMNL1+ Kozak or pcDNA 3.1-FMNL1α/γ	100 µg
Buffer NEB2 (10X)	10 µl
BSA (10X)	10 µl
Nhe I (10 U/ml)	2 µl
Xho I (20 U/ml)	2 µl
DEPC-H$_2$O	add to 100 µl

Purification of the digested insert and vectors was performed as described before (Chapter 4.5.1.3). DNA quantity was measured on the spectrometer.

4.5.2.3 Ligation
Digested and purified inserts and vectors were ligated in a ratio of insert: vector = 6 : 1.

Ligation mixture:

pcDNA 3.1-Kozak-FMNL1α

5` terminus of FMNL1 + Kozak	1 µl (52.24 ng/µl)
pcDNA 3.1-FMNL1α (Nhe I / Xho I)	1.5 ul (64.29 ng/µl)
Ligation buffer (10X)	1 µl
T4 ligase	1 µl
DEPC-H$_2$O	to 10 µl

pcDNA 3.1-Kozak-FMNL1γ

5` terminus of FMNL1 + Kozak	1 µl (52.24 ng/µl)
pcDNA 3.1-FMNL1γ (Nhe I / Xho I)	1.2 ul (80.42 ng/µl)
Ligation buffer (10X)	1 µl
T4 ligase	1 µl
DEPC-H$_2$O	to 10 µl

Reaction:	16°C overnight
Inactivation:	65°C 10 min
Cooling:	4°C
Stock:	-20°C

Bacteria are transformed by ligation products as described before (Chapter 4.5.1.5). On the second day, 5-10 clones of each ligation were select to make start cultures.

4.5.2.4 Plasmid-DNA-extraction and digestion

Starter cultures were purified by using the "Jetstar Plasmid Purification Mini Kit" (Genomed). After determining the DNA quantity, these mini-preparations were tested by digestion with Nhe I and Xho I. Two bands of 8353 bp and 431 bp should be visible after digestion of pcDNA 3.1-Kozak-FMNL1α, two bands of 8527 bp and 431 bp should be visible after digestion of pcDNA 3.1-Kozak-FMNL1γ.

Plasmid with the fragments of the correct size had been sequenced by the company Sequiserve or MWG.

The corresponding starter culture was expanded and the maxi preparation was performed with the "Jetstar Plasmid Purification Maxi Kit" (Chapter 4.5.1.8). The DNA quantity was measured on the spectrometer and the plasmid was stocked at -20°C.

4.5.3 Cloning of FMNL1α / γ into pACDC entry clone vector

To clone FMNL1α/γ from pcDNA 3.1 vector into pACDC entry clone vector, the restrict enzyme Bgl II site in pACDC entry clone vector was selected as the cloning site, which is however in the FMNL1α/γ sequence. Therefore, BamH I was added at the 5` and 3` ends of FMNL1α/γ which has the compatible end of Bgl II (Figure 4.3).
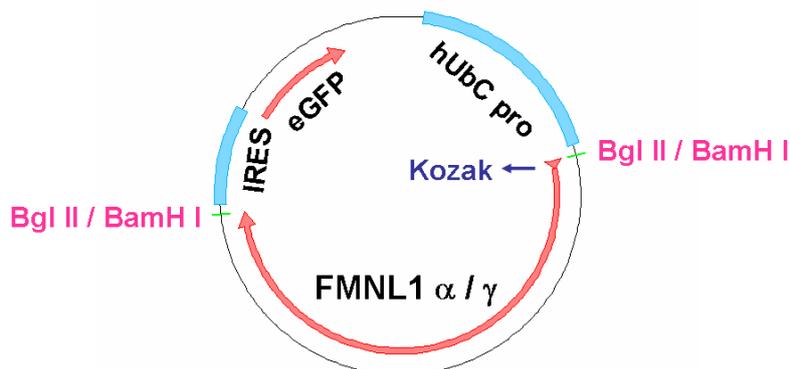
Figure 4.3: FMNL1 α/γ in the pACDC entry clone vector. Restrict enzyme BamH I at the 5` and 3` ends of FMNL1α/γ was ligated with Bgl II in poly cloning site of pACDC entry clone.

4.5.3.1 Amplification of FMNL1α/γ

The primers 5`Adeno-FMNL1-F and 3`Adeno-FMNL1-C5B6 and the KOD Hot Start DNA Polymerase kit (Novagen) were used to amplify FMNL1α/γ using pcDNA 3.1-Kozak-FMNL1 α/γ as templates. PCR products were amplified in 10 separated reaction tubes.

PCR mixture:

FMNL1α/γ

P-5` (100 pmol/ul)	1 µl
P-3` (100 pmol/ul)	1 µl
dNTP (2 mM)	5 µl
MgSO$_4$ (25 mM)	3 µl
PCR buffer (10X)	5 µl
KOD-Polymerase (1U/µl)	1 µl
pcDNA 3.1-Kozak-FMNL1α/γ	1 µg
DMSO	2.5 µl
DEPC-H$_2$O	to 50 µl

PCR-program;			
	1. initial denaturation	94°C	2 min
	2. denaturation	94°C	30 sec
	3. annealing l	72°C	30 sec
	4. elongation	72°C	4 min
	5. terminal elongation	72°C	10 min
	6. cooling	4°C	
	35 cycles form step 2 to step4		

The PCR products were used for gel electrophoresis and eluted from the gel as described before (Chapter 4.5.1.2). The DNA quantity was measured on the spectrometer.

4.5.3.2 Digestion and purification of the inserts and vector

The inserts (FMNL1α/γ + Kozak) was digested by BamH I at 37°C for 3-4 hours and inactivated at 65°C for 20 minutes.

Digestion:

FMNL1α/γ	100 µg
BamH I buffer with BSA (10X)	10 µl
BamH I (10 U/ml)	3 µl
DEPC-H$_2$O	to 100 µl

Purification of the digested insert was performed as described before (Chapter 4.5.1.3). DNA quantity was measured on the spectrometer. The Bgl II digestion and purification of vector (pACDC) was done by Elfriede Eppinger (in the research group of Angela Krackhardt).

4.5.3.3 Ligation

Digested and purified inserts and vectors were ligated in a ratio of insert: vector = 5 : 1.

Ligation mixture:

pACDC-FMNL1α

FMNL1α (BamH I)	2.6 µl (117 ng/µl)
pACDC (Bgl II)	0.5 ul (220 ng/µl)
Ligation buffer (10X)	1 µl
T4 ligase	1 µl
DEPC-H$_2$O	to 10 µl

pACDC-FMNL1γ

FMNL1γ (BamH I)	3 µl (104 ng/µl)
pACDC (Bgl II)	0.5 ul (220 ng/µl)
Ligation buffer (10X)	1 µl
T4 ligase	1 µl
DEPC-H$_2$O	to 10 µl

Reaction:	16°C	overnight
Inactivation:	65°C	10 min
Cooling:	4°C	
Stock:	-20°C	

Ligation products were transformed to bacteria as described before (Chapter 4.5.1.5). On the second day, 5-10 clones of each ligation were select to make starter cultures.

4.5.3.4 Plasmid-DNA-extraction and digestion

Starter cultures were purified by using the "Jetstar Plasmid Purification Mini Kit" (Genomed). After determining the DNA quantity, these mini-preparations were tested by digestion with EcoR I (in insert) and Kpn I (in vector). Two bands of 5302 bp and 3165 bp should be visible after digestion of pACDC-Kozak-FMNL1α, two bands of 5302 bp and 3339 bp should be visible after digestion of pACDC-Kozak-FMNL1γ.

Plasmid with the fragments of the correct size had been sequenced by the company Sequiserve or MWG.

The corresponding starter culture was expanded and the maxi preparation was performed with the "Jetstar Plasmid Purification Maxi Kit" (Chapter 4.5.1.8). The DNA quantity was measured on the spectrometer and the plasmid was stocked at -20°C.

4.5.4 Mutagenesis

Mutagenesis was performed by QuikChange$^{®}$ Site-Directed Mutagenesis Kit (STRATAGENE) which allows site-specific mutation in virtually any double-stranded plasmid. The QuikChange$^{®}$ site-directed mutagenesis method is performed using *PfuTurbo* DNA polymerase and a temperature cycler. The basic principle is that *PfuTurbo* DNA polymerase replicates both plasmid strands with high fidelity and without displacing the mutant oligonucleotide primers. The oligonucleotide primers, each complementary to opposite strands of the plasmid, are extended during temperature cycling to generate a mutated plasmid containing staggered nicks. Following temperature cycling, the product is treated with *Dpn* I (target sequence: 5´-Gm6ATC-3´) which is specific for methylated and hemimethylated DNA and is used to digest the parental DNA template and to select for mutation-containing synthesized DNA. DNA isolated from almost all *E. coli* strains is dam methylated and therefore susceptible to *Dpn* I digestion. The nicked vector DNA containing the desired mutations is then transformed into XL1-Blue supercompetent cells.

4.5.4.1 Mutagenesis of N-terminal myristoylation site in pACDC-FMNL1γ
To mutate the N-terminal myristoylation site (Chapter 5.4, Figure 5.15), the oligonucleotide primers G2TA4T and G2TA4T anti were designed using QuikChange$^{®}$ Primer Design Program available online (http://www.stratagene.com/qcprimerdesign). A four-step procedure to generate mutants was performed according to the introduction manual.

Reaction mixture:

P-G2TA4T (100 ng/ul)	1.25 µl
P-G2TA4T anti (100 ng/ul)	1.25 µl
dNTP mix	1 µl
Reacton buffer (10X)	5 µl
PfuTurbo DNA polymerase	1 µl
pACDC-FMNL1γ	1.925 µl (25ng)
DMSO	4 µl (Cend=8%)
DEPC-H$_2$O	to 50 µl

Cycling-program; 1. initial denaturation   95°C 2 min

                      2. denaturation   95°C 1 min

                      3. annealing I   68°C 1 min

                      4. elongation   68°C 9 min

                      18 cycles form step 2 to step4

After cycling, 1 µl of the *Dpn* I restriction enzyme (10 U/µl) was directly added to the amplified product and incubated at 37°C for 1 hour to digest the parental supercoiled dsDNA. After that, reaction was transformed into XL1-Blue supercompetent cells.

DNA was extracted from selected bacteria clones and digested by EcoR I and Kpn I. Plasmids with the fragments of the correct size were sent for sequencing by the company Sequiserve or MWG to check if correct mutants were obtained. The plasmid containing the correct mutant was named pACDC-G2TA4T.

4.5.4.2   Cloning of the N-terminal myristoylation site mutant into pcDNA 3.1-FMNL1γ

In order to clone the mutated N-terminal myristoylation site into pcDNA 3.1-FMNL1γ, pcNDA 3.1-FMNL1γ was digested by restrict enzyme Nhe I at the 5` cloning site and Xho I in the middle of FMNL1 inserts and exchanged the 5` terminus with G2TA4T containing the mutant N-terminal myristoylation site (Figure 4.2).

The primers 5`G2TA4T-Nhe I and 3`FMNL1-Ins-Xho I and the KOD Hot Start DNA Polymerase kit (Novagen) were used to amplify the 5` terminus sequence of G2TA4T using pACDC-G2TA4T as template. PCR products were amplified in 10 separated reaction tubes.

PCR mixture:

<u>5` terminus of G2TA4T</u>

P-5` (15 pmol/ul)	1 µl
P-3` (15 pmol/ul)	1 µl
dNTP (2 mM)	5 µl
MgSO$_4$ (25 mM)	3 µl
PCR buffer (10X)	5 µl
KOD-Polymerase (1U/µl)	1 µl
pACDC-FMNL1β	1 µg
DMSO	2.5 µl
DEPC-H$_2$O	to 50 µl

PCR-program;
1. initial denaturation	94°C	2 min
2. denaturation	94°C	30 sec
3. annealing I	68°C	30 sec
4. elongation	68°C	1 min
5. terminal elongation	68°C	10 min
6. cooling	4°C	

35 cycles form step 2 to step4

The PCR products were used for gel electrophoresis and eluted from the gel. After digestion with Nhe I and Xho I, the PCR products were ligated with pcDNA 3.1-FMNL1γ digested with the same enzymes in a ratio of 6:1.

Bacteria were transformed by ligation products. After DNA extraction, the plasmids with correct insert were selected by digestion with Nhe I and Xho I and sequencing. Maxi preparation was performed with the "Jetstar Plasmid Purification Maxi Kit" (Chapter 4.5.2). The DNA quantity was measured on the spectrometer and the plasmid was stocked at -20°C.

4.5.5 Cloning of FMNL1ΔDAD and G2TA4TΔDAD into pcDNA

3.1 vector and pACDC entry clone vector

4.5.5.1 Cloning of FMNL1ΔDAD and G2TA4TΔDAD into pcDNA 3.1

To Clone FMNL1ΔDAD into pcDNA 3.1, the restrict enzyme Nhe I and Xba I were selected as the cloning sites in pcDNA 3.1 vector (Figure 4.4). The primers 5`pcD-F-NheI KL2 and 3`pcD-F-C-Xba I 2 were used to amplify FMNL1ΔDAD sequence using pcDNA 3.1-Kozak-FMNL1γ as template. The amplification was performed by KOD Hot Start DNA Polymerase kit (Novagen). The gel-purified PCR production was used as template for further PCR reaction to obtain more product. PCR products were amplified in 10 separated reaction tubes.

PCR mixture:

<u>FMNL1ΔDAD</u>

P-5` (100 pmol/ul)	1 µl
P-3` (100 pmol/ul)	1 µl
dNTP (2 mM)	5 µl
MgSO$_4$ (25 mM)	3 µl
PCR buffer (10X)	5 µl
KOD-Polymerase (1U/µl)	1 µl
pcDNA3.1-FMNL1γ	1 µg
DMSO	2.5 µl
DEPC-H$_2$O	to 50 µl

PCR-program;	1. initial denaturation	94°C	2 min
	2. denaturation	94°C	30 sec
	3. annealing I	72°C	30 sec
	4. elongation	72°C	4 min
	5. terminal elongation	72°C	10 min
	6. cooling	4°C	

35 cycles form step 2 to step4

PCR products were used for gel electrophoresis and eluted from the gel. After digestion with Nhe I and Xba I, the PCR products were ligated with pcNDA 3.1 vector digested with the same enzymes in a ratio of 6:1.
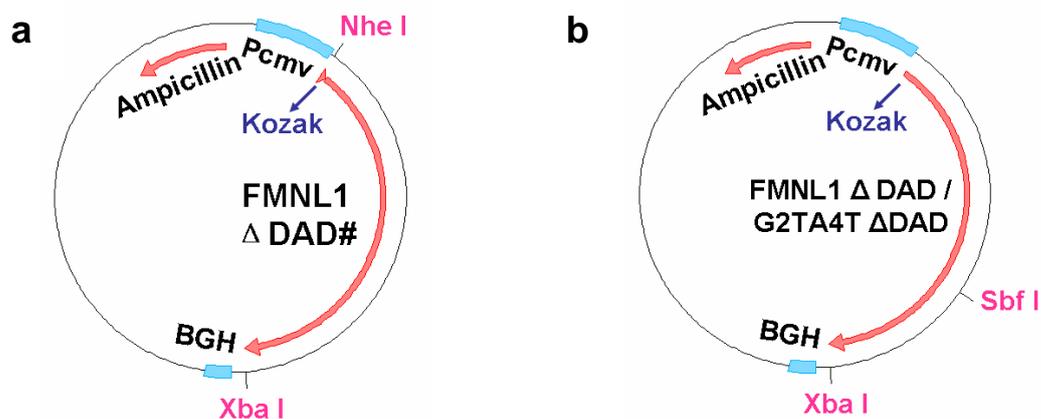
Figure 4.4: Cloning of FMNL1ΔDAD and G2TA4TΔDAD in the pcDNA 3.1 vector. a: FMNL1ΔDAD# containing mutants were cloned into pcDNA 3.1 vector by Nhe I at 5` and Xba I at 3` end. b: FMNL1ΔDAD and G2TA4TΔDAD were cloned into pcDNA 3.1 vector by using Sbf I to exchange the 3`terminus with FMNL1ΔDAD#.

Bacteria were transformed by ligation products. After DNA extraction, the plasmids with correct insert were selected by digestion with Nhe I and Xba I.

However, several mutatations were found in the FMNL1ΔDAD sequence before Sbf I restriction site by sequencing. Maxi preparation of pcDNA 3.1-FMNL1ΔDAD containing mutatations (pcDNA 3.1-FMNL1ΔDAD#) was performed with the "Jetstar Plasmid Purification Maxi Kit". The 3` terminus lacking DAD was cut out from FMNL1ΔDAD# by Sbf I and Xba I and exchanged with the 3`terminuses of FMNL1γ and G2TA3T in pcDNA 3.1 vector (Figure 4.4).

Digestion1:

pcDNA 3.1-FMNL1ΔDAD#	10 µg
Buffer NEB4 (10X)	10 µl
BSA (10X)	10 µl
Sbf I (10 U/ml)	3 µl
Xba I (20 U/ml)	3 µl
DEPC-H$_2$O	to 100 µl

The small fragment of 956 bp was extracted from the gel and used as insert for ligation (3`terminus of FMNL1ΔDAD).

Digestion2:

pcDNA 3.1-FMNL1γ / G2TA4T	20 µg
Buffer NEB4 (10X)	10 µl
BSA (10X)	10 µl
Sbf I (10 U/ml)	3 µl
Xba I (20 U/ml)	3 µl
DEPC-H$_2$O	add to 100 µl

The big fragments of 7705 bp were extracted from the gel and used as cut vector for ligation (pcDNA 3.1-FMNL1γ / G2TA4T (Sbf I / Xba I)).

Ligation (insert : vector = 6 : 1)

pcDNA 3.1-FMNL1ΔDAD:

3`terminus of FMNL1ΔDAD	0.83 µl (90.9 ng/µl)
pcDNA 3.1-FMNL1γ (Sbf I / Xba I)	1.55 ul (64.4 ng/µl)
Ligation buffer (10X)	1 µl
T4 ligase	1 µl
DEPC-H$_2$O	to 10 µl

pcDNA 3.1-GTA4TΔDAD:

3`terminus of FMNL1ΔDAD	0.83 µl (90.9 ng/µl)
pcDNA 3.1-G2TA4T (Sbf I / Xba I)	0.67 ul (148.5 ng/µl)
Ligation buffer (10X)	1 µl
T4 ligase	1 µl
DEPC-H$_2$O	to 10 µl

Reaction:	16°C	overnight
Inactivation:	65°C	10 min
Cooling:	4°C	

Bacteria were transformed by ligation products. After DNA extraction, the plasmids with correct insert were selected by digestion with Sbf I (in insert) and Mfe I (in vector). Two bands of 5723 bp and 2938 bp should be visible after digestion and gel-electrophoresis of both pcDNA 3.1-FMNL1ΔDAD and pcDNA 3.1-G2TA4TΔDAD.

Plasmids with the fragments of the correct size had been sequenced by the company Sequiserve or MWG.

The corresponding starter culture was expanded and the maxi preparation was performed with the "Jetstar Plasmid Purification Maxi Kit". The DNA quantity was measured on the spectrometer and the plasmid was stocked at -20°C.

4.5.5.2 Cloning of FMNL1ΔDAD and G2TA4TΔDAD into pACDC entry clone vector

To clone FMNL1ΔDAD and G2TA4TΔDAD from pcDNA 3.1 vector into pACDC entry clone vector, similar procedures have been performed as described in chapter 4.5.3.

The primers 5`Adeno-FMNL1-F and 3`FMNL1-C-BamH I 2 were used to amplify the FMNL1ΔDAD, while the FMNL1ΔDAD fragment was used as template which was cut out from pcDNA 3.1-FMNL1ΔDAD by Nhe I and Xba I and purified by gel extraction. The primers 5`-G2TA4T-BamH I 2 and 3`FMNL1-C-BamH I 2 were used to amplify G2TA4TΔDAD while the G2TA4TΔDAD fragment was used as template which was cut out from pcDNA 3.1- G2TA4TΔDAD by Nhe I and Xba I and purified by gel extraction. The amplification was performed by using the KOD Hot Start DNA Polymerase kit (Novagen). The product was amplified in 10 separated reaction tubes.

PCR mixture:

FMNL1ΔDAD:

		G2TA4TΔDAD:	
P-5` (100 pmol/ul)	1 µl	P-5` (100 pmol/ul)	1 µl
P-3` (100 pmol/ul)	1 µl	P-3` (100 pmol/ul)	1 µl
dNTP (2 mM)	5 µl	dNTP (2 mM)	5 µl
MgSO$_4$ (25 mM)	3 µl	MgSO$_4$ (25 mM)	3 µl
PCR buffer (10X)	5 µl	PCR buffer (10X)	5 µl
KOD-Polymerase (1U/µl)	1 µl	KOD-Polymerase (1U/µl)	1 µl
FMNL1ΔDAD insert	1 µl	G2TA4TΔDAD insert	1 µl
DMSO	2.5 µl	DMSO	2.5 µl
DEPC-H$_2$O	to 50 µl	DEPC-H$_2$O	to 50 µl

PCR-program;	1. initial denaturation	94°C	2 min
	2. denaturation	94°C	30 sec
	3. annealing l	72°C	30 sec
	4. elongation	72°C	4 min
	5. terminal elongation	72°C	10 min
	6. cooling	4°C	
	35 cycles form step 2 to step4		

The PCR products were used for gel electrophoresis and eluted from the gel and digested by BamH I at 37°C for 3-4 hours and inactivated at 65°C for 20 minutes.

Digestion:

FMNL1ΔDAD or G2TA4TΔDAD	100 µg
BamH I buffer with BSA (10X)	10 µl
BamH I (10 U/ml)	3 µl
DEPC-H$_2$O	to 100 µl

After purification, the digested inserts were ligated with the Bgl II digested and purified pACDC entry clone vector with a ratio of 6 : 1.

Ligation mixture:

pACDC-FMNL1ΔDAD

FMNL1ΔDAD (BamH I)	0.35 µl (1034 ng/µl)
pACDC (Bgl II)	0.5 ul (220 ng/µl)
Ligation buffer (10X)	1 µl
T4 ligase	1 µl
DEPC-H$_2$O	to 10 µl

<u>pACDC-G2TA4TΔDAD</u>

GTA4TΔDAD (BamH I)	1.3 µl (289 ng/µl)
pACDC (Bgl II)	0.5 ul (220 ng/µl)
Ligation buffer (10X)	1 µl
T4 ligase	1 µl
DEPC-H$_2$O	to 10 µl

Reaction:	16°C	overnight
Inactivation:	65°C	10 min
Cooling:	4°C	
Stock:	-20°C	

Bacteria were transformed by ligation products. After DNA extraction, the plasmids with correct insert were selected by double digestion.

Plasmid	Sbf I (ins)/Mfe I (vec)	EcoR I (ins)/Kpn I (vec)
pACDC-Kozak-FMNL1ΔDAD	5572 bp/2756 bp	5286 bp/3042 bp
pACDC-Kozak-G2TA4TΔDAD	5572 bp/2756 bp	5286 bp/3042 bp

Plasmid with the fragments of the correct size had been sequenced by the company Sequiserve or MWG. The corresponding starter culture was expanded and the maxi preparation was performed with the "Jetstar Plasmid Purification Maxi Kit". The DNA quantity was measured on the spectrometer and the plasmid was stocked at -20°C.

5 Results

5.1 Expression and localization of endogenous FMNL1 in hematopoietic lineage-derived cells and tumor cells

FMNL1 has been previously shown to be selectively expressed in PBMCs and overexpressed in CLL samples as well as in malignant cell lines (Figure 2.1) (Krackhardt, Witzens et al. 2002), suggesting FMNL1 to be an attractive target antigen for tumor immune responses. The expression of FMNL1 in was now investigated more in detail by western blot and confocal microscopy.

5.1.1 FMNL1 expression in tumor cell lines and in malignant cells derived from patients with acute lymphatic leukaemia

High protein expression of FMNL1 has been reported in native malignant cells from patients with lymphatic as well as myeloid leukemias and EBV-transformed B cells. FMNL1 protein expression has been also detected in lymphoma-derived cell lines and aberrant protein expression was found in renal cell carcinoma lines compared to normal embryonal kidney cells (Schuster, Busch et al. 2007).
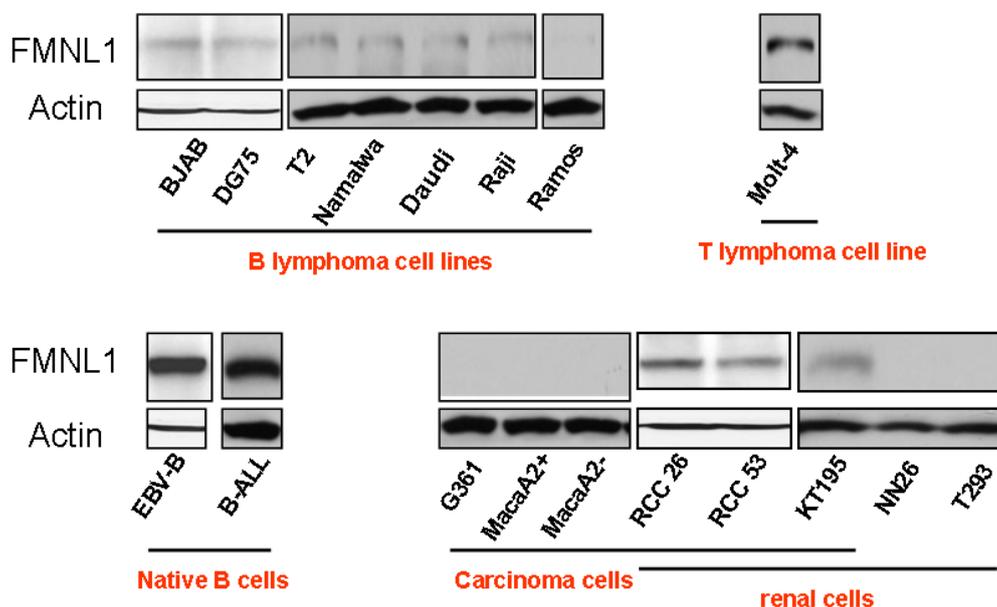
Figure 5.1 FMNL1 expression in transformed cells, tumor cell lines and in malignant cells derived from patients with acute lymphatic B cell leukaemia. 50 µg of total protein was used for SDS/PAGE. Probing with anti-actin antibody served as equal loading control.

In this study, analysis was extended in more lymphoma cells and carcinoma

cells. The expression of FMNL1 was observed by western blot in B lymphoma cell lines as BJAB, DG75, T2, Namalwa, Daudi and Raji cells but not in Ramos cells. The T lymphoma cell line Molt-4 had an enhanced expression. FMNL1 is highly expressed in malignant cells derived from the selected patient with acute lymphatic leukaemia (ALL) and in diverse EBV-transformed B cells. The expression of FMNL1 is not detectable in carcinoma cells like the melanoma cell line G361, the breast carcinoma cell line Maca A2+ /A2- and cell lines dericved from embryonal and normal renal cells like NN26 AND 293T. However, FMNL1 is clearly expressed in diverse renal carcinoma cells as RCC26, RCC53 and KT195 (Figure 5.1).

5.1.2 Expression and localization of endogenous FMNL1 in different subtypes of unstimulated and stimulated PBLs

To investigate the expression of endogenous FMNL1 in unstimulated and stimulated T cells, T cells were unspecificlly stimulated by LPS, TNFα, PMA combined with ionomycine and IL 2 combined with OKT-3. LPS from the outer membrane of Gram-negative bacteria is an endotoxin, and induces activation of B cells, macrophages and other APC. LPS could also stimulate proliferation of human T cell by accessory of LPS-primed monocytes and the costimulatory signals via the interaction between CD28 on T cells and it ligand CD80 on monocytes (Mattern, Flad et al. 1998). TNFα stimulates T cells through their receptors on the cell surface. PMA could activate the signal transduction enzyme protein kinase C (PKC), which triggers calcium release and mobilization resulting in the activation of T cells. Ionomycin is an ionophore which is usually used to raise the intracellular level of calcium in conjunction with PMA. IL-2 and the CD3-specific antibody OKT3 are T cell mitogens, responsible for T cell activation and proliferation. However, unspecific stimulation of T cells by OKT3 requires signals provided by accessory cells and is IL 2 dependent.
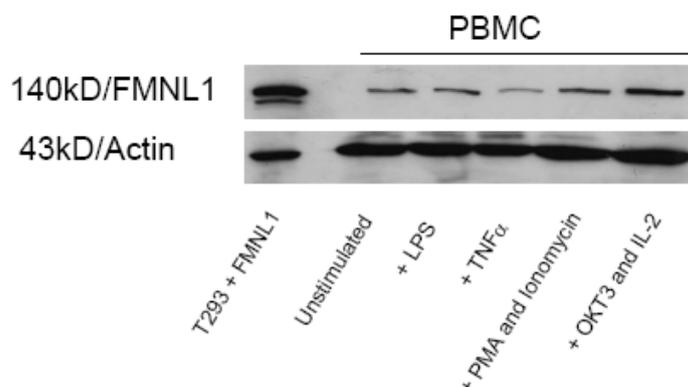
Figure 5.2 FMNL1 is naturally expressed in unstimulated T cells and the expression is up-regulated after stimulation with different stimuli. 50 µg of total protein was used for SDS/PAGE. Probing with anti-actin antibody served as equal loading control.

The most effective up-regulation of FMNL1 was induced by PMA combined with ionomycine and IL-2 combined with OKT-3 as shown by western blot for three different donors (Figure 5.2)

The localization of endogenous FMNL1 in different subtypes of PBLs was further investigated by confocal microscopy. FMNL1 showed a dot-like expression pattern in the cytoplasma of unstimulated and unspecifically stimulated T cells, B cells and malignant B cells from patients with CLL (Figure 5.3).
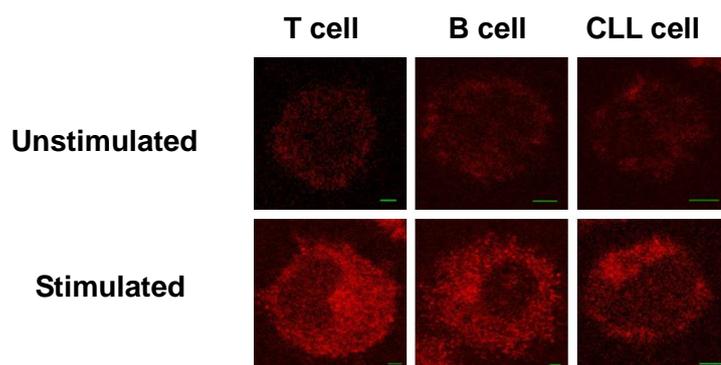
Figure 5.3 FMNL1 is expressed in diverse hematopoietic lineage-derived cells. FMNL1 was visualized in unstimulated and stimulated PBL subtypes as T cells, B cells and malignant B cells from patients with CLL by immunofluorescence staining with the rat FMNL1-specific antibody 6F2 followed by Cy3-labeled goat anti-rat antibody. T cells were stimulated with IL-2 and OKT3 and B cells as well as CLL cells were activated using soluble CD40-Ligand. Scale bars represent 2 µm.

5.1.3 The function-associated localization of endogenous FMNL1

In T cells, FMNL1 has been reported to be involved in reorientation of the MTOC towards the immunological synapse (Gomez, Kumar et al. 2007). Similar polarization of FMNL1 towards the immunological synapse was observed after targeting of FMNL1-PP2-specific T cells (Schuster, Busch et al. 2007) with peptide-pulsed T2 cells (Figure 5.4).
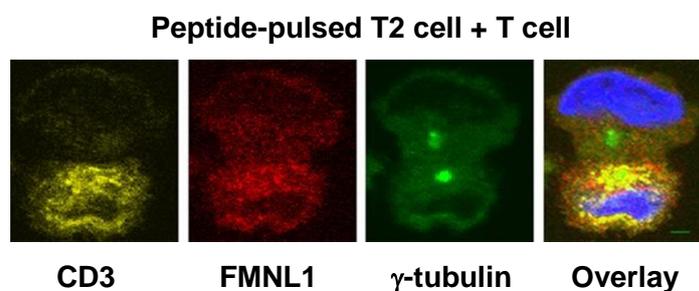
Figure 5.4 Polarization of FMNL1 towards the immunological synapse. To investigate FMNL1 expression in polarized T cells, the FMNL2-PP2-specific T cell

clone SK22 was incubated for 15 minutes with T2 cells pulsed with the peptide FMNL1-PP2 at 10 µmol. Cells were then fixed and stained with DAPI for nuclear staining (blue), rabbit anti-human CD3 antibody followed by Cy5-labeled goat anti rabbit antibody (yellow) for T cell identification and rat FMNL1-specific antibody 6F2 followed by Cy3-labeled goat anti-rat antibody (red). The MTOC was stained with mouse anti-human γ-tubulin antibody followed by Alexa Fluor 488-labeled goat anti mouse antibody (green). Enrichment of FMNL1 and CD3 was observed around the MTOC. Scale bars represent 2 µm.

Moreover, dividing T cells were investigated by confocal microscopy after unspecific stimulation with IL-2 combined with OKT-3. Colocalization of endogenous FMNL1 with α-tubulin at the cortex and mitotic spindles was observed in dividing T cells during metaphase, anaphase and especially telophase (Figure 5.5), suggesting an involvement of FMNL1 in mitosis and cytokinesis.

Dividing T cells
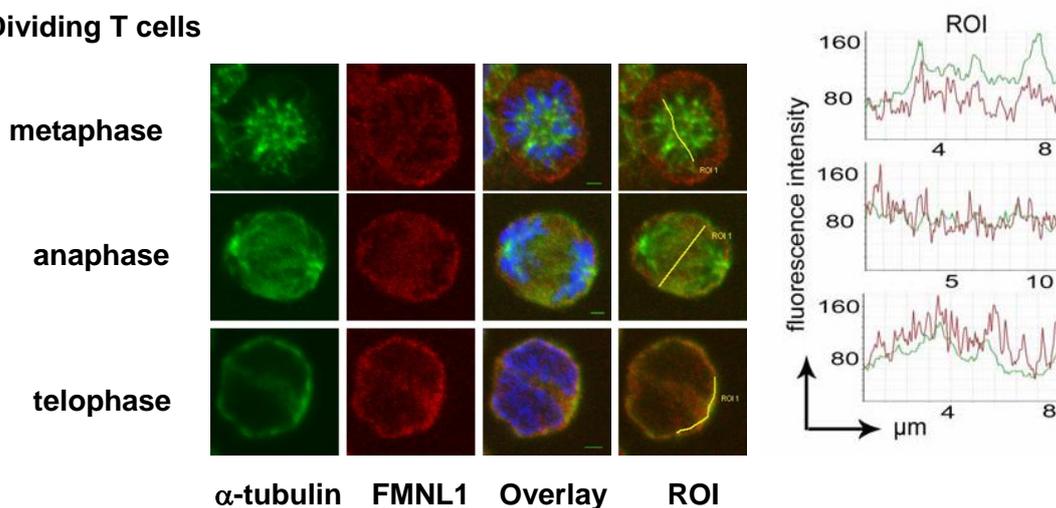
Figure 5.5 Colocalization of endogenous FMNL1 with α-tubulin at the cortex and mitotic spindles of dividing T cells. T cells were unspecifically stimulated with OKT3 and IL-2. Colocalization was observed at different time points of mitosis as metaphase, anaphase and telophase. FMNL1 was stained as described before (red), α-tubulin was stained with mouse anti-human α-tubulin followed by Alexa Fluor 488-labeled goat anti-mouse antibody (green), nuclei were stained with DAPI (blue). Colocalization was quantified and displayed as histograms using the Leica microsystems confocal software. ROI = region of interest.

In addition, the murine homologue FRL, which has 85% homology to the human counterpart, has been shown to be involved in Fc receptor-mediated phagocytosis (Yayoshi-Yamamoto, Taniuchi et al. 2000; Seth, Otomo et al. 2006). Function-associated localization of endogenous FMNL1 at the phagocytic cup of monocytes was also observed during phagocytosis of cells and platelets (Figure 5.6).
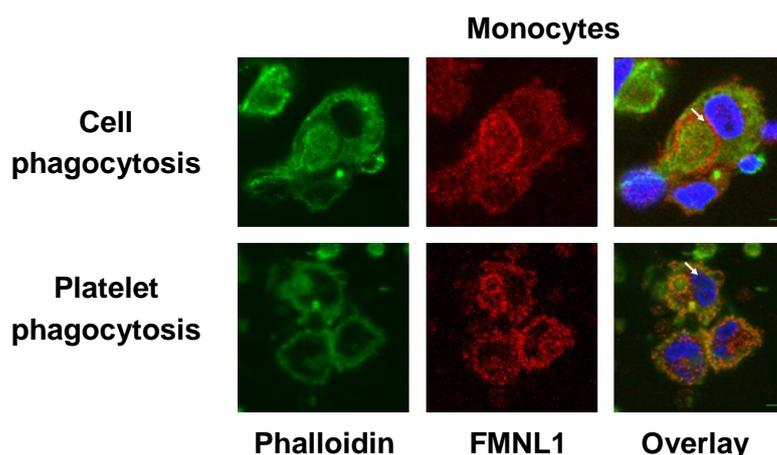
Monocytes

Figure 5.6 FMNL1 is localized at the phagocytic cup (white arrows) of monocytes during phagocytosis of cells and platelets. FMNL1 (red) was stained as figure 5.4, actin was stained by Alexa 488-conjugated Phalloidin (green) and nuclei were stained with DAPI (blue). Scale bars represent 2 µm.

5.2 FMNL1 splice variants and mutant investigated in this study

DRFs including FRL have been previously described to be regulated by autoinhibition which is dependent on the C-terminal DAD (Seth, Otomo et al. 2006). Using exon-specific primers for the C-terminal end of FMNL1, three different FMNL1 splice variants derived from cDNA of CLL cells and human lung carcinoma have been cloned by Elfriede Eppenger (in the research group of Angela Krackhardt) which result in varying C-terminal amino acid sequences (Figure 5.7a). Two splice variants are corresponding to the previously described murine splice variants, FRLα and FRLβ (Yayoshi-Yamamoto, Taniuchi et al. 2000; Harris, Li et al. 2004). An additional C-terminal splice variant FMNL1γ was identified which contains an intron retention but shares the final C-terminal end with FMNL1α (Figure 5.7b). To further investigate the DAD dependent autoinhibition mechanism, an FMNL1 mutant lacking the C-terminal DAD (FMNL1ΔDAD) was generated (Figure 5.7a).

(a)

(b)

```
                          AA
                          1047
                           |
FMNL1α      YESDRDGAIEDIITVIKTVPFTARTGKRTSRLLCEASLGEEMPL

FMNL1β      YESDRDGAIEDIITDLRNQPYIRADTGRRSARRRPPGPPLQVTSDLSL

FMNL1γ      YESDRDGAIEDIITGKGLARPWSYPQSVLLCFLLTQCAILWGTGCHTASCYLFCFSFLFPFSTPLHLP
            HPHSVIKTVPFTARTGKRTSRLLCEASLGEEMPL

FMNL1ΔDAD   YESDRDGAI
```

Figure 5.7 Identification of a novel FMNL1 splice variant (FMNL1γ) containing an intron retention at the C-terminal end. (a) Schematic diagrams of FMNL1α, FMNL1β, FMNL1γ and FMNL1ΔDAD constructs used in this study. (b) Amino acid sequences of the C-termini of FMNL1α and β corresponding to murine FRLα and β, as well as of the novel isoform FMNL1γ containing an C-terminal intron retention but sharing the final C-terminal amino acids with FMNL1α. The identical C-terminal amino acids in FMNL1α and FMNL1γ are underlined.

5.3 Function associated localization of FMNL1γ and FMNL1ΔDAD

5.3.1 FMNL1γ and FMNL1ΔDAD are located at the cell membrane and induce membrane blebbing

All three different FMNL1 splice variants were transfected into 293T cells and investigated by confocal microscopy. 293T cells transfected with FMNL1α and FMNL1β showed mainly intracellular cytoplasmatic distribution of FMNL1, whereas cells transfected with FMNL1γ showed a distinct membranous FMNL1 localization as well as extensive polarized membrane protrusions and blebs (Figure 5.8a). Similar membrane protrusions were observed after adenoviral transduction of K562 cells with FMNL1γ but not with the other splice variants. However, in these cells the shape of the blebs was different and a more prominent enrichment of FMNL1 γ at the cell cortex has been observed (Figure 5.8b). Similarly, 293T cells and K562 cells transfected or transduced with FMNL1ΔDAD showed similar membranous localization of FMNL1 and extensive polarized membrane protrusions and blebs (Figure 5.8 a,b) indicating that deregulation of autoinhibition is responsible for membrane localization and blebbing observed in cells overexpressing the splice variant FMNL1γ. Increase of blebbing was less obvious in HT1080 and MDA-MB 231 cells after adenoviral transduction of FMNL1γ. However, these cell lines also demonstrated FMNL1γ localization at the cell membrane and especially enrichment of FMNL1γ at intracellular vesicles whereas cells transduced with the other two splice variants had a more dispersed distribution within the cytoplasma (Figure 5.8c). Similar localization was also observed in HT1080 and MDA-MB 231 cells after adenoviral transduction of FMNL1ΔDAD.

(a) **293T**

DIC

FMNL1

Overlay

FMNL1α   FMNL1β   FMNL1γ   FMNL1 Δ DAD

(b) **K562**

DIC

FMNL1

Overlay

FMNL1α   FMNL1β   FMNL1γ   FMNL1 Δ DAD

(c)

HT1080

MDA-MB 231

FMNL1α   FMNL1β   FMNL1γ   FMNL1 Δ DAD
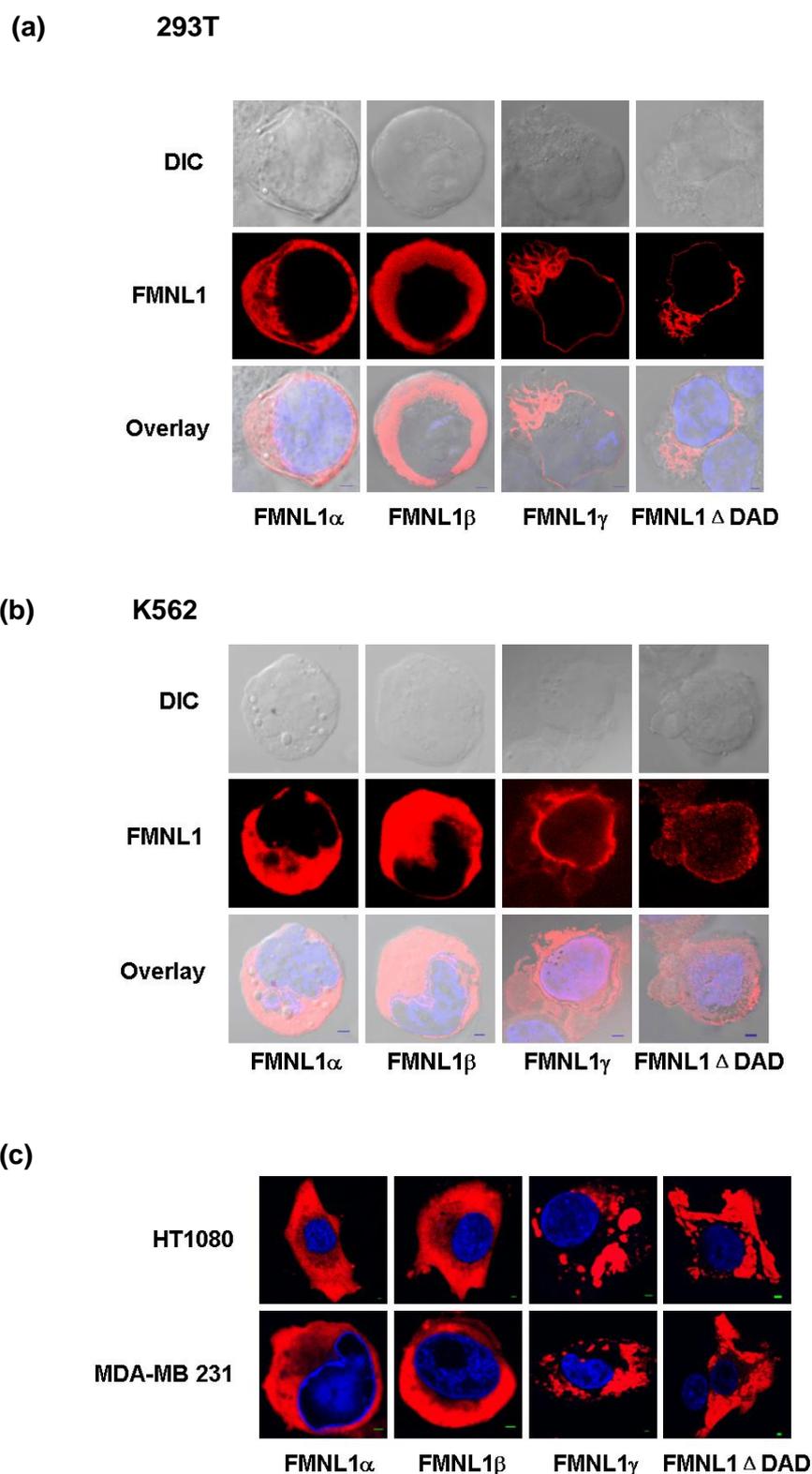
Figure 5.8 FMNL1γ and FMNL1ΔDAD are located at the cell membrane and cortex and induce extensive cell blebbing. (a) FMNL1γ and FMNL1ΔDAD induce extensive blebbing in 293T cells. 293T cells were transfected with the pcDNA3.1 vector containing different isoforms of FMNL1 and analyzed by confocal microscopy after immunofluorescence staining with the rat FMNL1-specific antibody

6F2 followed by Cy3-labeled goat anti-rat antibody (red). Nuclei were stained with DAPI (blue). Scale bars represent 2 µm. DIC = differential interference contrast. (b) FMNL1γ and FMNL1ΔDAD induce blebbing in K562 cells. FMNL1 isoforms were adenovirally transduced into K562 cells and analyzed by confocal microscopy as described above. Scale bars represent 2 µm. (c) FMNL1γ and FMNL1ΔDAD are enhanced in intracellular vesicles of HT1080 and MDA-MB 231 cells. FMNL1 isoforms were adenovirally transduced into HT1080 and MDA-MB 231 cells and analyzed by confocal microscopy as described above. Scale bars represent 2 µm.

Significant increase of membrane blebbing in 293T and K562 cells after transduction with FMNL1γ and FMNL1ΔDAD in comparison to the other splice variants was quantified by independent counting experiments (Figure 5.9).
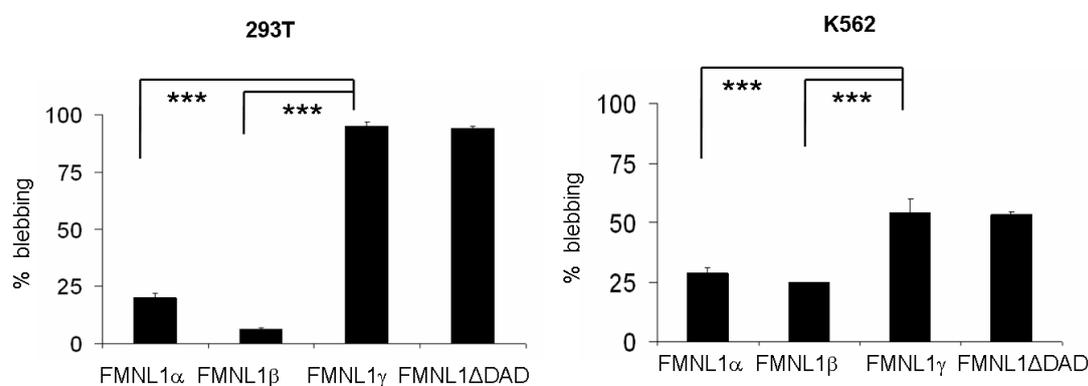
Figure 5.9 Cell blebbing was quantified by counting hundred FMNL1-transduced cells in 293T cells and K562 cells. By independent counting experiments (n ≥ 3), the results indicate a significant increase of blebbing in cells expressing FMNL1γ and FMNL1ΔDAD (*** $p < 0.001$).

5.3.2 FMNL1γ co-localizes with actin, ezrin and myosin IIb on the cell membrane and cortex

FMNL1γ colocalized with actin in FMNL1γ-transfected 293T cells as shown by Phalloidin staining demonstrating actin assembly activity of FMNL1γ (Figure 5.10).

293T-FMNL1γ

FMNL1γ   Phalloidin   Overlay
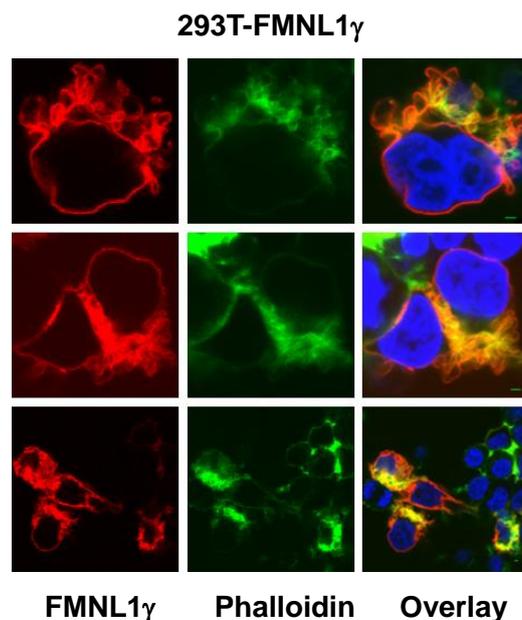
Figure 5.10 FMNL1γ colocalizes with actin in 293T cells. 293T cells were transfected with the pcDNA3.1 vector containing FMNL1γ and stained with Alexa 488-conjugated Phalloidin (green) as well as with the FMNL1-specific antibody FMNL1 6F2 followed by rat Cy3-labeled goat anti-rat secondary antibody (red). Nuclei were stained with DAPI (blue). Scale bars represent 2 µm.

Bleb expansion is driven by intracellular pressure transiently generated by myosin II contraction at the actin cortex (Charras 2008). Ezrin links the actin cytoskeleton to the membrane and localizes to bleb membrane when bleb expansion slows (Charras, Hu et al. 2006). We have investigated if Ezrin and myosin IIb colocalzes with FMNLγ at the membrane of blebbing cells. In fact, we observed colocalization of FMNL1γ with ezrin and myosin IIb especially at the cortex of blebbing K562 cells by confocal microscopy (Figure 5.11). Moreover, K562 cells transduced with FMNL1γ often demonstrated a polarized circular accumulation of FMNL1γ at one pole of the cell showing also small blebbing. FMNL1γ colocalizes especially with ezrin and myosin IIb in this area (Figure 5.11).

K562-FMNL1γ   **K562-FMNL1γ**

FMNL1   Ezrin   Overlay   FMNL1   Myosin IIb   Overlay
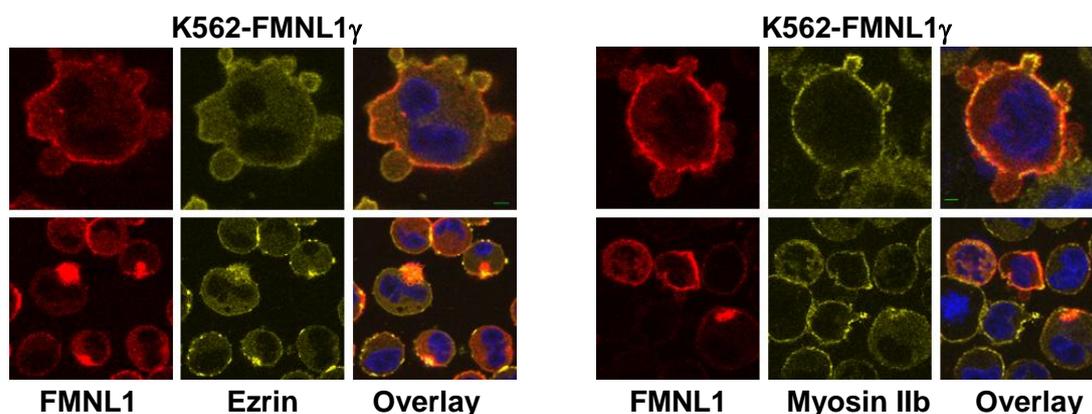
Figure 5.11 FMNL1γ colocalizes with ezrin and myosin IIb particularly at the cortex of blebbing K562 cells. K562 cells were transduced with adenoviral vector containing the FMNL1γ isoform. Cells were then stained with the FMNL1-specific antibody 6F2 followed by rat Cy3-labeled goat anti-rat (red), as well as with rabbit anti-human ezrin and rabbit anti-human myosin IIb followed by Cy5-conjugated goat anti-rabbit (yellow). Nuclei were stained with DAPI (blue). Scale bars represent 2 µm.

5.3.3 FMNL1γ does not induce apoptosis in K562 cell

Plasma membrane blebbing has long been observed as an early event in apoptosis. More recently, non-apoptotic blebbing was identified to play roles in distinct cellular processes such as cytokine release, cytokinesis or cancer cell invasion (Charras, Yarrow et al. 2005; Fackler and Grosse 2008). As blebbing may occur during apoptosis, I investigated if FMNL1γ expression increases apoptosis by Annexin V and propidium iodide staining. K562 cells were adenovirally transduced with FMNL1 isoforms as well as vector control. Vincristine was added to cells to induce cell apoptosis as a positive control. Three days later, cells were harvested and stained with Annexin V and propidium iodide to analyze apoptotic cell death. The result demonstrated that FMNL1γ does not induce apoptosis in K562 cell compared to wild type cells, vector control and other isoforms of FMNL1 (Figure 5.12).
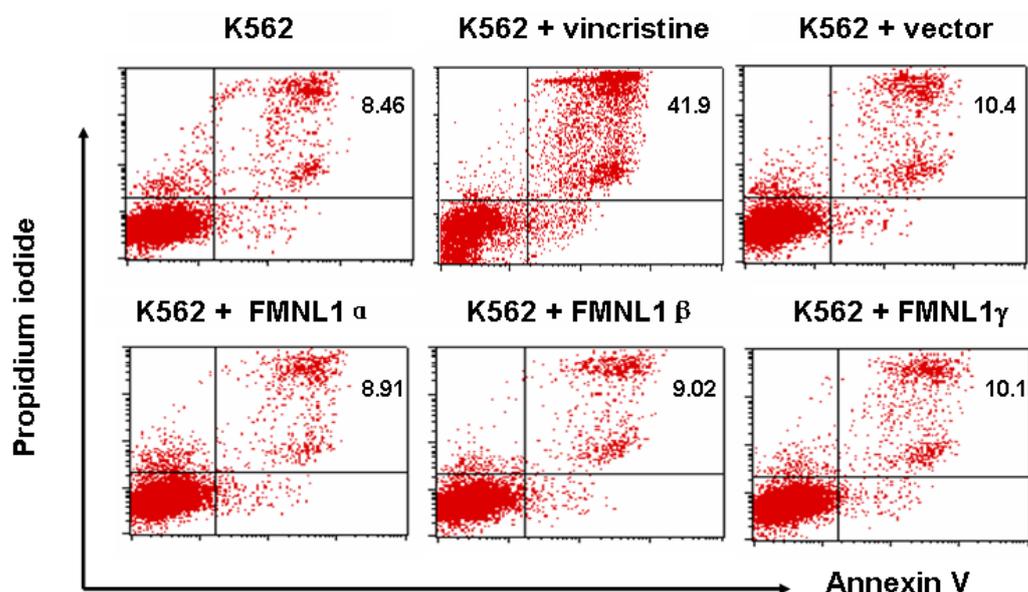
Figure 5.12 FMNL1γ does not induce apoptosis in K562 cell. Non-treated K562 cells, K562 cells incubated with vincristine and K562 cells transduced with vector alone or FMNL1 isoforms were stained with APC conjugated to annexin V together with propidium iodide. Vincristine was used to induce cell apoptosis as a positive control.

5.3.4 Blebbing induced by FMNL1γ or FMNL1ΔDAD is independent of Src and ROCK but depends on myosin, actin and tubulin integrity

Plasma membrane blebbing has been previously shown to be induced by FHOD1 when co-expressed with ROCK1 (Hannemann, Madrid et al. 2008). Moreover, blebbing induced by FHOD1 requires Src activity (Hannemann, Madrid et al. 2008). Our former results demonstrated the association of blebbing induced by FMNL1γ with F-actin and myosin IIb. It has also been previously reported that tubulins were involved in blebbing and associated in formin-associated functions. Nocodazole has been previously described to inhibit leishmania-derived HASPB induced blebbing although no colocalization of microtubuli and HASPB was observed (Tournaviti, Hannemann et al. 2007). However, the formin mDia has been demonstrated to be involved in organization of microtubules (Ishizaki, Morishima et al. 2001) and to interact with the microtubule binding protein CLIP-170 (Lewkowicz, Herit et al. 2008).

To further investigate components involved in plasma membrane blebbing induced by FMNL1γ, 293T cells were transfected with FMNL1γ and different substances were added which are known to inhibit membrane blebbing. According to previous publications, concentrations of inhibitors were selected as follows: 50 µM Src inhibitor PP1, 90 µM ROCK inhibitor Y-27632, 100 µM myosin II inhibitor Blebbistatin, 25 µM F-actin inhibitor Latrunculin B and 200 µM tubulin inhibitor Nocodazole (Eisenmann, Harris et al. 2007; Tournaviti, Hannemann et al. 2007; Hannemann, Madrid et al. 2008). PP1 and Y-27632 had only minimal effects on membrane blebbing as investigated by confocal microscopy. However, membrane blebbing was grossly reduced by addition of Latrunculin B, Blebbistatin and Nocodazole (Figure 5.13a,b), demonstrating that the mechanism of blebbing induced by FMNL1γ was not mediated by Src and ROCK but dependent on actin, myosin and tubulin integrity. Similar data were obtained by FMNL1ΔDAD-transfected 293T cells (Figure 5.13a,b).

(a)   293T
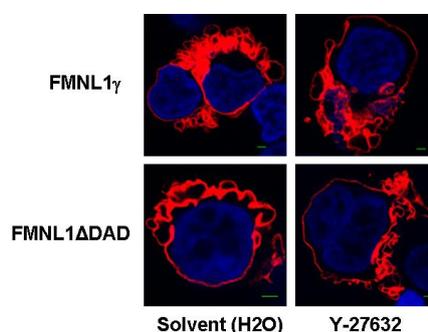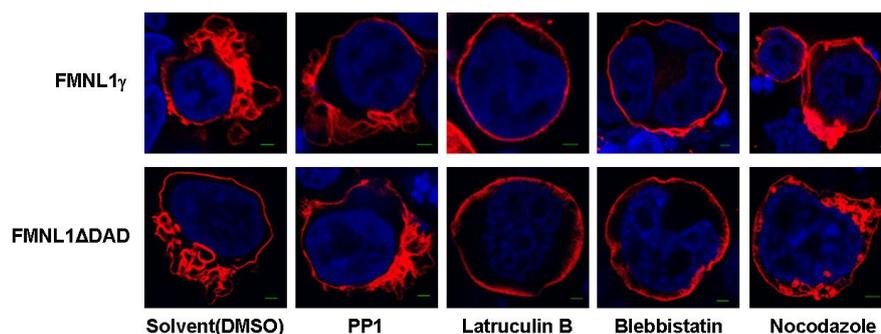
(b)   293T- FMNL1γ
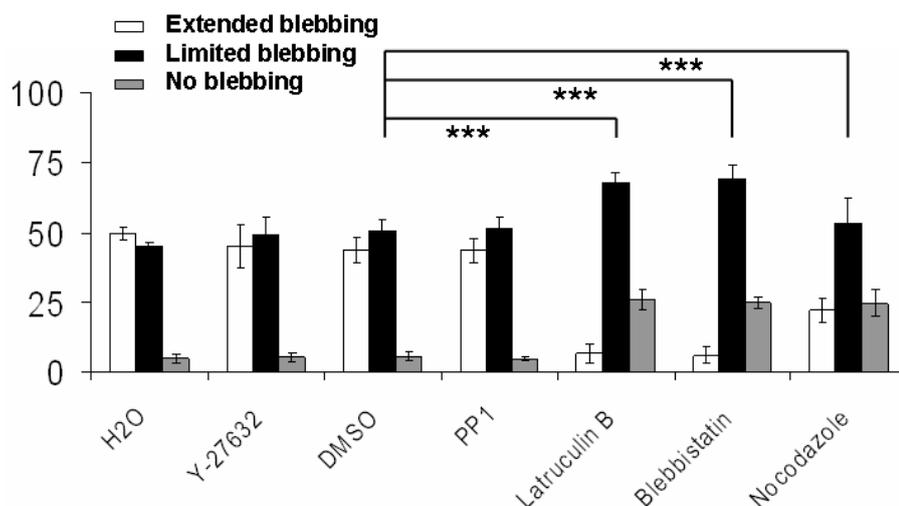
Figure 5.13 Blebbing induced by FMNL1γ or FMNL1ΔDAD is independent of ROCK and Src but depends on actin, myosin and microtubules. 293T cells were transfected with the pcDNA3.1 vector containing FMNL1γ or FMNL1ΔDAD and treated with different inhibitors of blebbing as well as solvent controls. After 2 days cells were stained with the rat FMNL1-specific antibody 6F2 followed by Cy3-labeled goat anti-rat antibody (red). Nuclei were stained with DAPI (blue). Scale bars represent 2 µm. Blebbing cells were analyzed by confocal microscopy as previously described (a). Cell blebbing was quantified by counting hundred FMNL1γ-transduced cells in three independent experiments (b) classifying them as cells exhibiting extensive blebs (white bars), limited blebs (black bars) or none (grey bars). Standard deviation of independent counting experiments is shown (n=3, *** p<0.001).

Furthermore, FMNL1γ transduced 293T cells were treated with Latrubulin B, Blebbistatin and Nocodazole of gradient concentrations demonstrating that blebbing induced by FMNL1γ could be inhibited at very low concentration (Figure 5.14 a,b).

(a)

293T-FMNL1γ + Latruculin B

F-actin

FMNL1

Overlay

DMSO　　1 µM　　10 µM　　25 µM

293T-FMNL1γ + Blebbistatin

Myosin IIb

FMNL1

Overlay

DMSO　　10 µM　　50 µM　　100 µM

293T-FMNL1γ + Nocodazole

α-tubulin

FMNL1

Overlay

DMSO　　1 µM　　10 µM　　100 µM　　200 µM
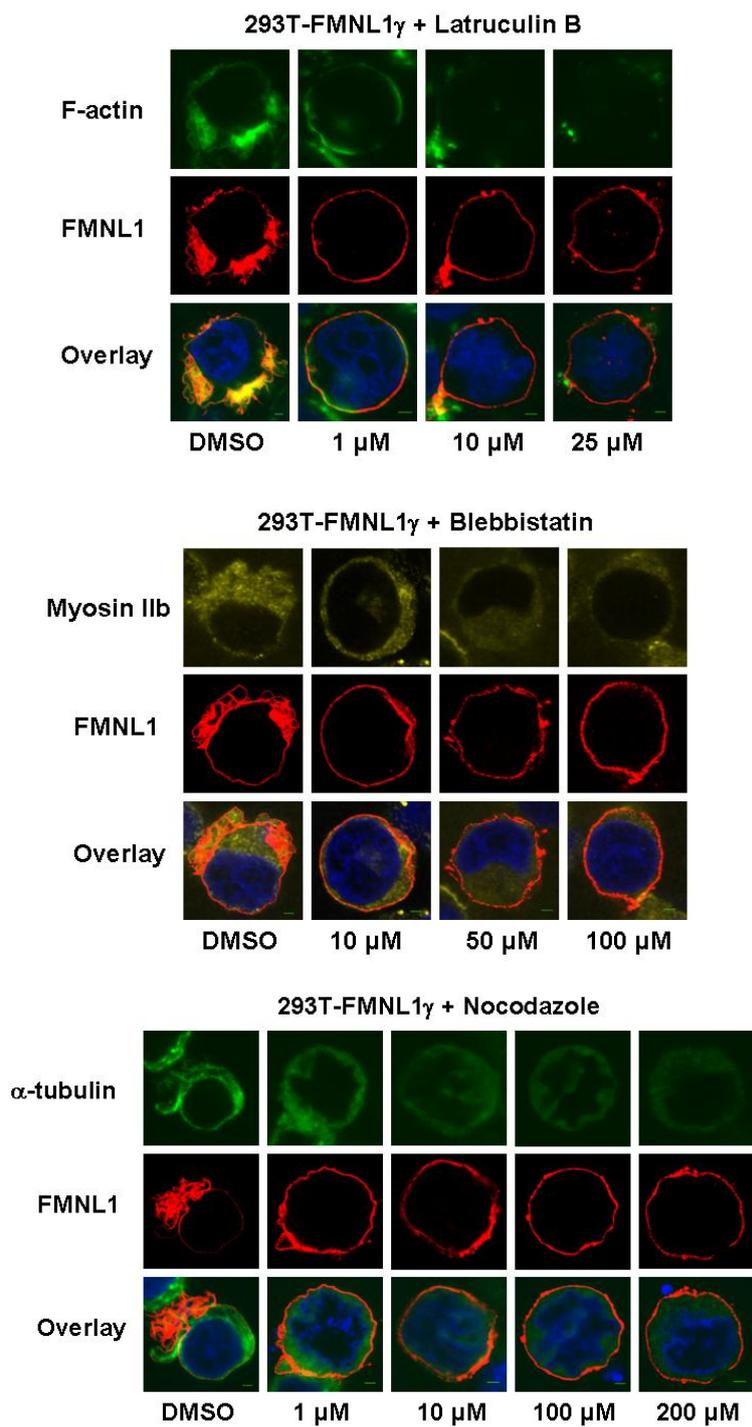
(b)
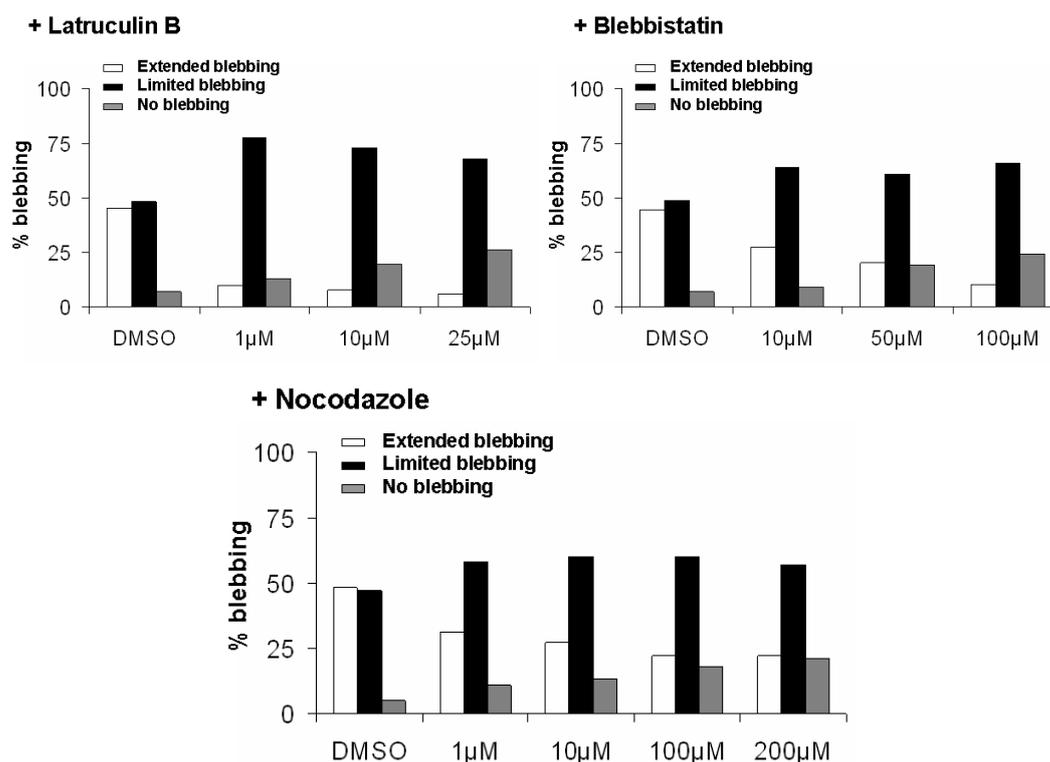
Figure 5.14 Inhibition of blebbing induced by FMNL1γ by Latrubulin B, Blebbistatin and Nocodazole was analyzed using gradient concentrations of inhibitors. 293T cells were transfected with the pcDNA3.1 vector containing FMNL1γ and treated with different bleb-inhibitors at gradient concentrations as well as DMSO controls. After 2 days cells were stained with the rat FMNL1-specific antibody 6F2 followed by Cy3-labeled goat anti-rat antibody (red). Myosin IIb was stained with a rabbit anti-myosin IIb antibody followed by Cy5-labeled goat anti-rabbit antibody (yellow). F-actin was stained with Alexa 488-conjugated Phalloidin (green) and α-tubulin was stained with a mouse anti- α -tubulin antibody followed by Alexa 488-conjugated goat anti-mouse antibody (green). Nuclei were stained with DAPI (blue). Scale bars represent 2 μm (a). Cell blebbing was quantified by counting hundred FMNL1γ-transduced cells (b), classifying them as cells exhibiting extensive blebs (white bars), limited blebs (black bars) or none (grey bars).

5.4 Identification of the mechanism of membranous localization induced by FMNL1γ and FMNL1ΔDAD

Membrane localization of FMNL1 was a predominant feature in 293T cells transfected with the splice variant FMNL1γ and FMNL1ΔDAD. The mechanism how FMNL1 is located to the cell membrane remains elusive. Investigation of the FMNL1 amino acid sequence by prediction analyses

revealed a potential N-terminal myristoylation site (http://elm.eu.org). This N-terminal myristoylation motif is highly specific for the leukocyte-specific formins FMNL1, 2 and 3 in man and mouse but not present in other formin proteins. To investigate whether FMNL1γ is indeed a myristoylated protein, glycine (G) at position 2 and alanine (A) at position 4 were mutated to threonine (T) within FMNL1γ (Figure 5.15).

```
                        AA
                         1
                         |
FMNL1        ATG GGC AAC GCG GCC GGC AGC
              M   G   N   A   A   G   S

G2TA4T       ATG ACC AAC ACG GCC GGC AGC
              M   T   N   T   A   G   S
```
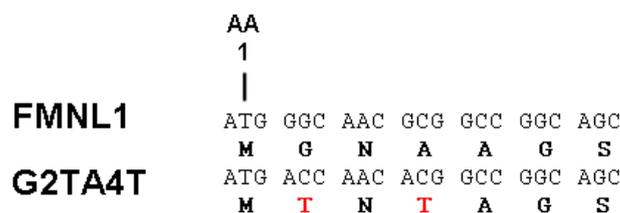
Figure 5.15 Schematic view of the N-terminus of FMNL1. The predicted N-terminal myristoylation site was mutated on position 2 and 4, glycine and alanine to threonine (red), respectively.

5.4.1 FMNL1γ contains an N-terminal myristoylation site

To further confirm that FMNL1 contains a myristoylation site, 293T cells were transfected with FMNL1γ or G2TA4T mutant and then metabolically labeled with [3H]-myristic acid. Total proteins were immunoprecipitated with the FMNL1-specific antibody 8A8 detecting an N-terminal epitope not including the N-terminal myristoylation site. Immunoprecipitated probes were investigated by immunoblot using the FMNL1-specific antibody 6F2 to examine for expression of FMNL1γ or G2TA4T mutant (Figure 5.16a) as well as autoradiography to analyze incorporation of [3H]-myristic acid (Figure 5.16b). Both FMNL1γ protein and G2TA4T mutant were sufficiently immunprecipitated by FMNL1-specific antibody 8A8, however only FMNL1γ, but not G2TA4T, was myristoylated in 293T cells. These results provide clear evidence that FMNL1γ is indeed a myristoylated protein.

(a) Blot: anti- FMNL1

(b) ^{3}H- Myristate
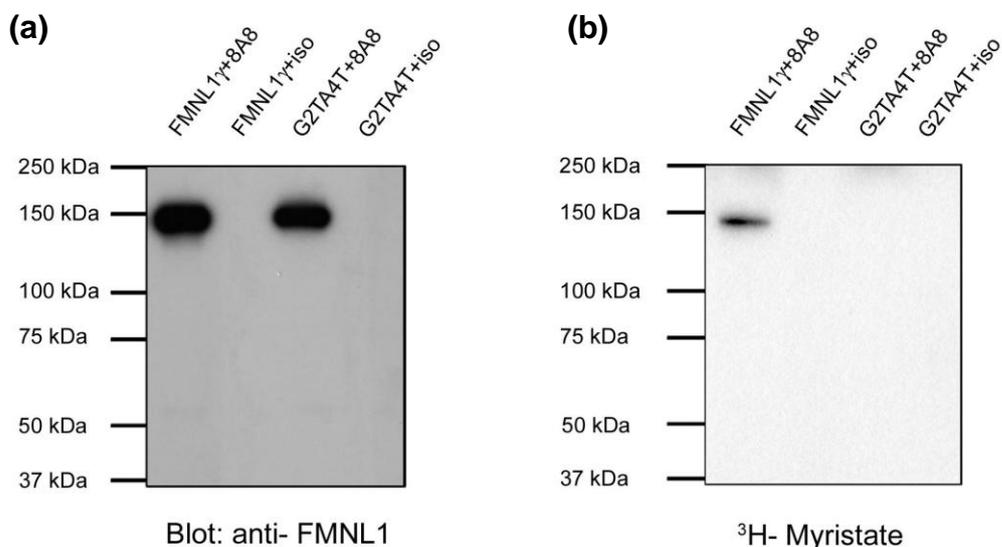
Figure 5.16 FMNL1 contains an N-terminal myristoylation site. Metabolic labelling of FMNL1 with [3H]-myristic acid. 293T cells transfected with FMNL1γ or G2TA4T were cultured for 16 h with [3H]-myristic acid. FMNL1 proteins were immunoprecipitated with 8A8 antibody or the isotype control, analysed by SDS/PAGE, followed by immunoblotting with anti-FMNL1 mAb 6F2 (a) or autoradiography (b). Molecular mass sizes are indicated in kDa.

5.4.2 Membrane localization and blebbing of FMNL1 is mediated by N-terminal myristoylation

To investigate if N-terminal myristoylation plays a role in FMNL1 function and membrane localization, cells were transfected with FMNL1γ or the G2TA4T mutant. The mutant G2TA4T, in fact, abolished membranous and cortical localization of FMNL1γ after transfection of the mutant splice variant in 293T cells as well as after genetic transfer of this mutant in other cell lines (Figure 5.17a). Similarly, mutation of the N-myristoylation site in the FMNL1ΔDAD (G2TA4TΔDAD) also abrogated membranous localization of FMNL1ΔDAD (Figure 5.17b). Membrane localization of FMNL1γ and FMNL1ΔDAD could be also inhibited by adding 2-Hydroxymyristate, a potent inhibitor of protein myristoylation (Paige, Zheng et al. 1990), further confirming that plasma membrane localization of FMNL1 is dependent on N-terminal myristoylation (Figure 5.18).
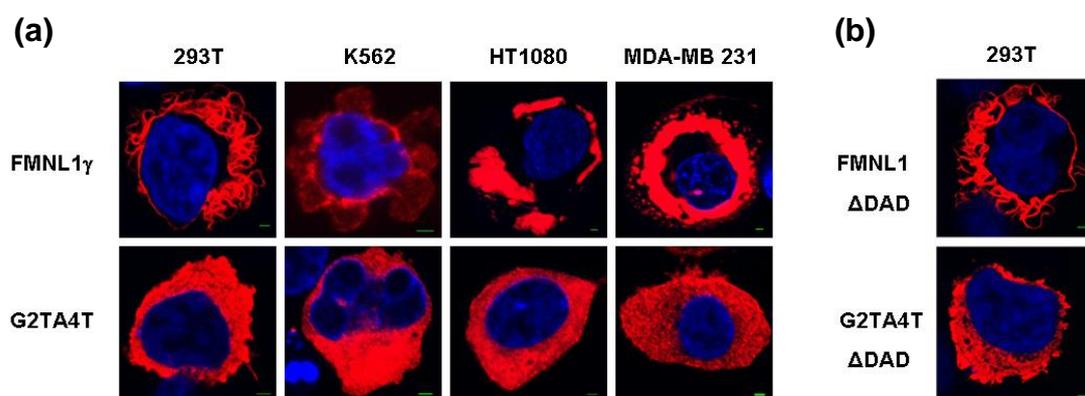
Figure 5.17 Mutation of the N-myristoylation site abrogated membranous localization of FMNL1γ and FMNL1ΔDAD. (a) Localization of FMNLγ at the membrane or intracellular vesicles is abrogated by mutation of the N-terminal myristoylation motif. Different cell lines were transfected or adenovirally transduced with either FMNL1γ or the mutant G2TA4T followed by staining with the rat FMNL1-specific antibody 6F2 and Cy3-labeled goat anti-rat antibody (red). Nuclei were stained with DAPI (blue). Scale bars represent 2 μm. (b) Localization of FMNL1ΔDAD at the membrane is abrogated by mutation of the N-terminal myristoylation motif. 293T cell lines were transfected with either FMNL1ΔDAD or the mutant G2TA4TΔDAD followed by staining with the rat FMNL1-specific antibody 6F2 and Cy3-labeled goat anti-rat antibody (red). Nuclei were stained with DAPI (blue). Scale bars represent 2 μm.

293T

Figure 5.18 Membrane localization of FMNL1γ and FMNL1ΔDAD could be inhibited by adding 2-Hydroxymyristate. 293T cells transfected with the isoform FMNL1γ and FMNL1ΔDAD were treated with the inhibitor 2-hydroxy-myristic acid, a potent inhibitor of protein myristoylation and stained as described in Figure 5.17. Scale bars represent 2 μm.

Blebbing was significantly reduced in 293T cells after transfection with G2TA4T or G2TA4TΔDAD in comparison to FMNL1γ or FMNL1ΔDAD (Figure 5.19), indicating that membrane or cortical localization mediated by N-terminal myristoylation is important for membrane blebbing induced by FMNL1γ. Furthermore, we observed an increase in multinucleated cells in T293 cells transduced with the mutated FMNL1 (Figure 5.20).
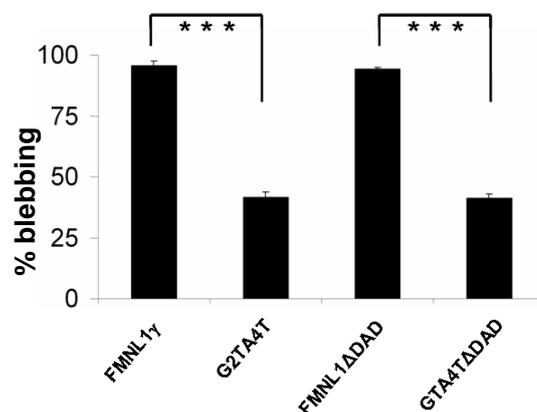
Figure 5.19 Mutation of the N-terminal myristoylation motif reduced membrane blebbing induced by FMNL1γ or FMNL1ΔDAD in 293T cells. Hundred transduced cells were analyzed for investigation of cell blebbing. The bars show the standard deviation of independent counting experiments (n=3; *** p< 0.001).
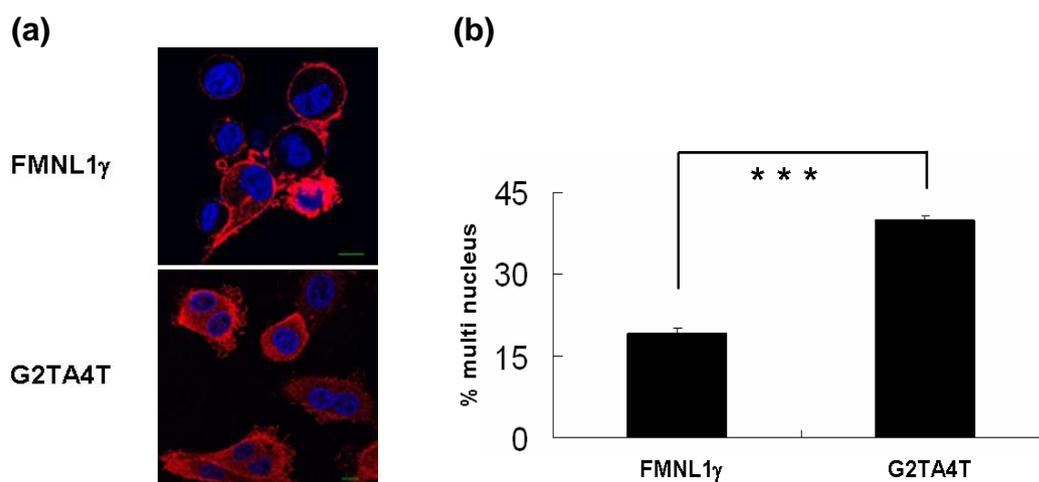
Figure 5.20 Mutation of the N-terminal myristoylation motif increased cells with multiple nuclei. (a) 293T cells were transfected with pcDNA vector contiaing FMNLγ or G2TA4T mutant. Cells were stained with the rat FMNL1-specific antibody 6F2 followed with Cy3-labeled goat anti-rat antibody (red). Nuclei were stained with DAPI (blue). Scale bars represent 2 µm. (b) For investigation of cells with multiple nuclei, hundred transfected cells were analyzed. The bars show the standard deviation of independent counting experiments (n=3; *** p< 0.001).

5.5 Expression of FMNL1γ moderately increases cell proliferation

Blebbing has been previously shown to be associated to cytokinesis (Charras 2008). By analyzing cell numbers after transfection of 293T cells or transduction of K562, MDA-MB 231 and HT1080 cells with different splice variants of FMNL1, moderately increased cell counts were observed in cells transfected or transduced with FMNL1γ in comparison to the other isoforms or the GFP mock control (Figure 5.21).
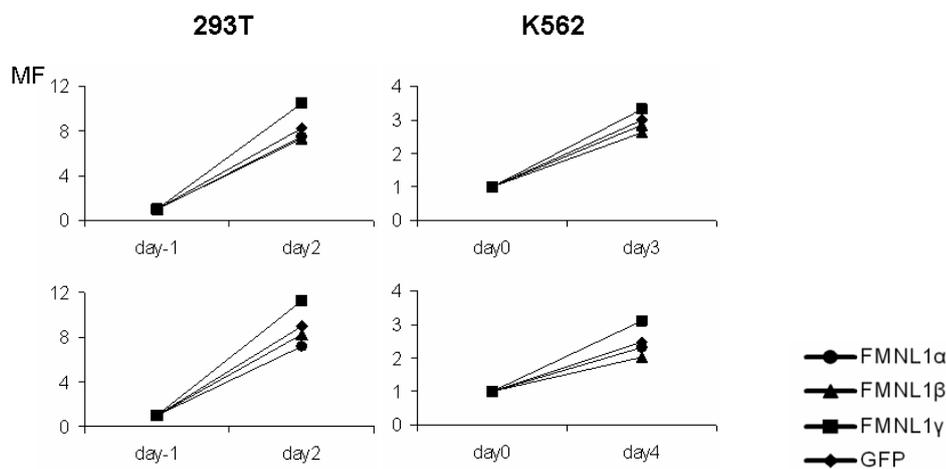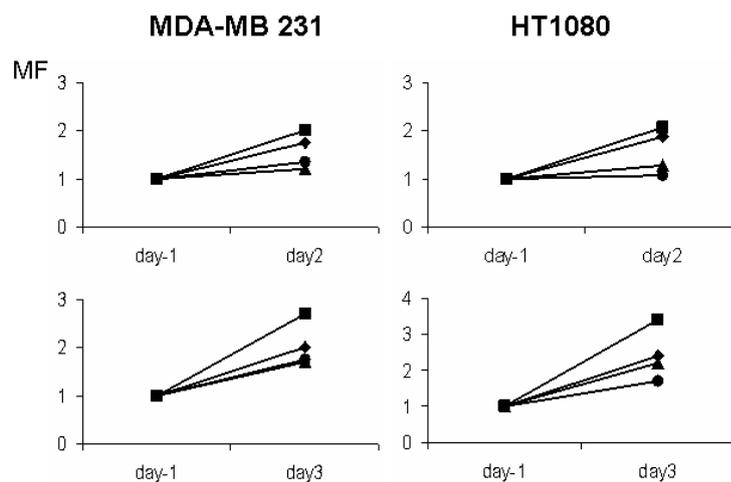
Figure 5.21 Cell counts after transfection of 293T cells or transduction of K562, MDA-MB 231 and HT1080 cells with different splice variants of FMNL1. Counting of cells after transduction with different FMNL1 isoforms revealed a moderate increase in cell proliferation after transfection or transduction with FMNL1γ in comparison to FMNL1α, FMNL1β and GFP. All single counting experiments showed an increase in cell counts after transduction of this isoform in different cell lines as 293T, K562, HT1080 and MDA-MB 231. The multiplication factor (MF) of cell counts after transduction in comparison to day -1 or day 0, when adenoviral transduction was performed, is shown.

As HT1080 and MDA-MB 231 cells are highly genetically transducible by adenoviral infection as seen by GFP expression (> 90%), we used these cell lines for further investigation of proliferation by seminaphtorhodafluor-1 carboxylic acid, acetate and succinimidyl ester (SNARF-1) staining. SNARF-1 worked similarly as Carboxyfluorescein diacetate succinimidyl ester (CFSE), but conjugated with fluorescence PE instead of Fitc. SNARF-1 is retained by the cells and is shared by the daughter cells at each division, resulting in multimodal flow cytometric SNARF-1 histograms, with each cell generation clustering around half the fluorescence intensity of the previous one. Cells transduced with FMNL1γ demonstrated an enhanced decrease of SNARF-1 stain correlating with increased cell proliferation (Figure 5.21a). Similar results were obtained after 5`-bromo-2`-deoxyuridine (BrdU) incorporation followed by anti-BrdU and 7-amino-Actinomycin D (7-AAD) staining of HT1080 cells transduced with different splice variants (Figure 5.22b). In these experiments we did not observe major differences in single cell cycle phases. However, despite of a reduced number of cells entering the cell cycle after adenoviral infection similar for all conditions, we repeatedly observed a significant BrdU positive population at G0/G1 phase 3 days after transduction with FMNL1γ in comparison to the other isoforms or GFP control indicating an accelerated passage through the cell cycle (Figure 5.22b).
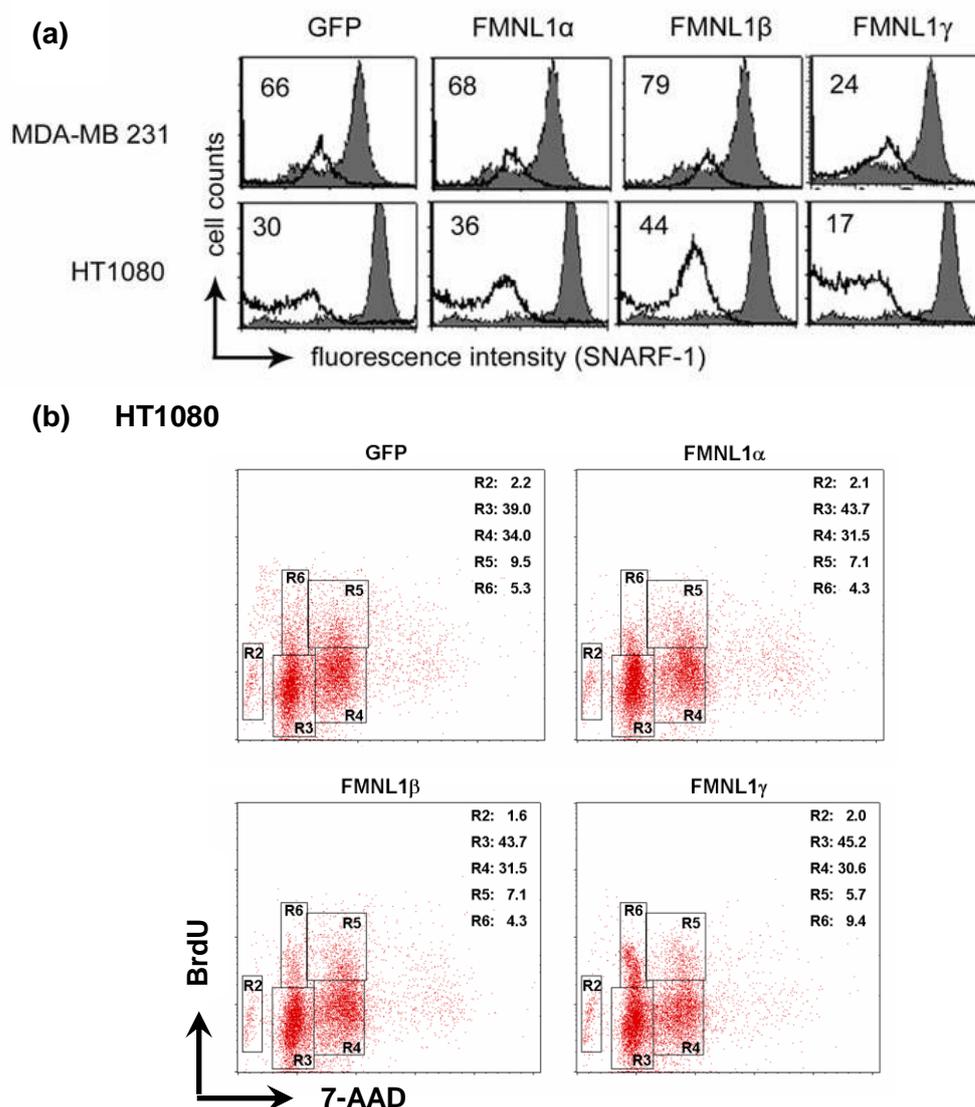
Figure 5.22 FMNL1γ moderately enhances cell proliferation in transduced cell lines. (a) Increase of proliferation was confirmed by SNARF-1 staining using MDA-MB 231 and HT1080. Cells were stained by SNARF-1 and then adenovirally transduced with the three different FMNL1 isoforms as well as GFP control. The filled grey curves show the fluorescence at 620 nm at day 0 and the black transparent curves at day 4 after transduction. The mean fluorescence of SNARF-1 after 4 days is indicated within the graph. One of three similar experiments is shown. (b) Accelerated proliferation in HT1080 cells after transduction of FMNL1γ was additionally confirmed by BrdU uptake without significant differences in single cell cycle phases analyzed by DNA-staining with 7-AAD. HT1080 cells were seeded overnight and transduced the next day with different FMNL1 isoforms and GFP vector control. After 24 hours 10 µM BrdU was added and 48 hours later cells were harvested fixed and stained with APC-conjugated anti-BrdU antibody and 7-AAD. R1: life gate within forward and side scatter (not shown), R2: apoptotic cells, R3: cells in G0/G1 without BrdU uptake, R4: cells in S phase without BrdU uptake, R5 cells in G2/M with BrdU uptake, R6: cells in G0/G1 with BrdU uptake after cycling.

Investigation by confocal microscopy has demonstrated that, like the endogenous FMNL1 in T cells, FMNL1γ located at contractile ring and cortex of mitotic FMNL1γ transfected 293T cells (Figure 5.23). This result suggested that the involvement of FMNL1γ in acceleration of cell proliferation may be associated to the involvement of FMNL1γ in cytokinesis.

293T-FMNL1γ
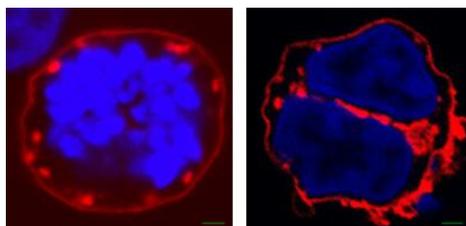
Figure 5.23 FMNL1γ was located at contractile ring and cortex of mitotic cells. 293T cells were transfected with FMNLγ and stained with the rat FMNL1-specific antibody 6F2 followed by Cy3-labeled goat anti-rat antibody (red). Nuclei were stained with DAPI (blue). Scale bars represent 2 µm.

5.6 FMNL1 increases free intracellular Calcium after stimulation

By matrix-assisted laser desorption/ionization (MALDI), several candidates have been isolated in the group of Angela Krackhardt (unpublished data) as interaction partners of FMNL1 including the protein AHNAK. AHNAK is a scaffold protein which has been reported to be critical for calcium signaling during T cell activation. AHNAK deficiency in CD4+ T cells resulted in a reduced calcium influx upon TCR crosslinking and subsequent poor activation of the transcription factor NFAT (Matza, Badou et al. 2008). We therefore transfected or transduced different cell lines with FMNL1 isoforms and measured the calcium influx after activating these cells with ionomycine or A23187 (Figure 5.24a-c).

293T cells were transfected with FMNL1 isoforms as well as the vector control and activated by 10 µg/ml ionomycine. In two experiments, FMNL1 isoforms increased free intracellular calcium level compared to the vector control. Two additional cell lines MDA-MB 231 cells and HT1080 cells were adenovirally transduced with FMNL1 isoforms as well as vector conrol. MDA-MB 231 cells were activated by 10 µg/ml ionomycine while HT1080 cells were activated with 10µg/ml A23187, which is also known as calcium ionophore used to increase intracellular Ca^{2+} levels. Similar results have been obtained indicating that all splice variants of FMNL1 induced an increase of

free intracellular calcium compared to vector and WT controls. At the same time, immunoblotting was performed to confirm expression of FMNL1. These experiments suggested that N-terminal myristoylation may not play a role in increasing intracellular calcium as no difference between cell transfected with FMNL1 isoforms or G2TA4T mutant was observed in all experiments performed.

(a)

Exp1: 293T + ionomycine 10 µg/ml

	MF
FMNL1 Δ DAD	1,01
FMNL1γ	0,94
G2TA4T	0,98
FMNL1α	0,9
Vector	0,78

Exp2: 293T + ionomycine 10 µg/ml

	MF
FMNL1 Δ DAD	0,85
FMNL1γ	0,86
G2TA4T	0,86
FMNL1α	0,88
Vector	0,61

Exp2:

(b)

Exp3: MDA-MB 231 + ionomycine 10 µg/ml

	MF
G2TA4T	0.76
FMNL1ΔDAD	0.8
FMNL1γ	0.77
FMNL1β	0.78
FMNL1α	0.66
Vector	0.59
WT	0.55

(c)
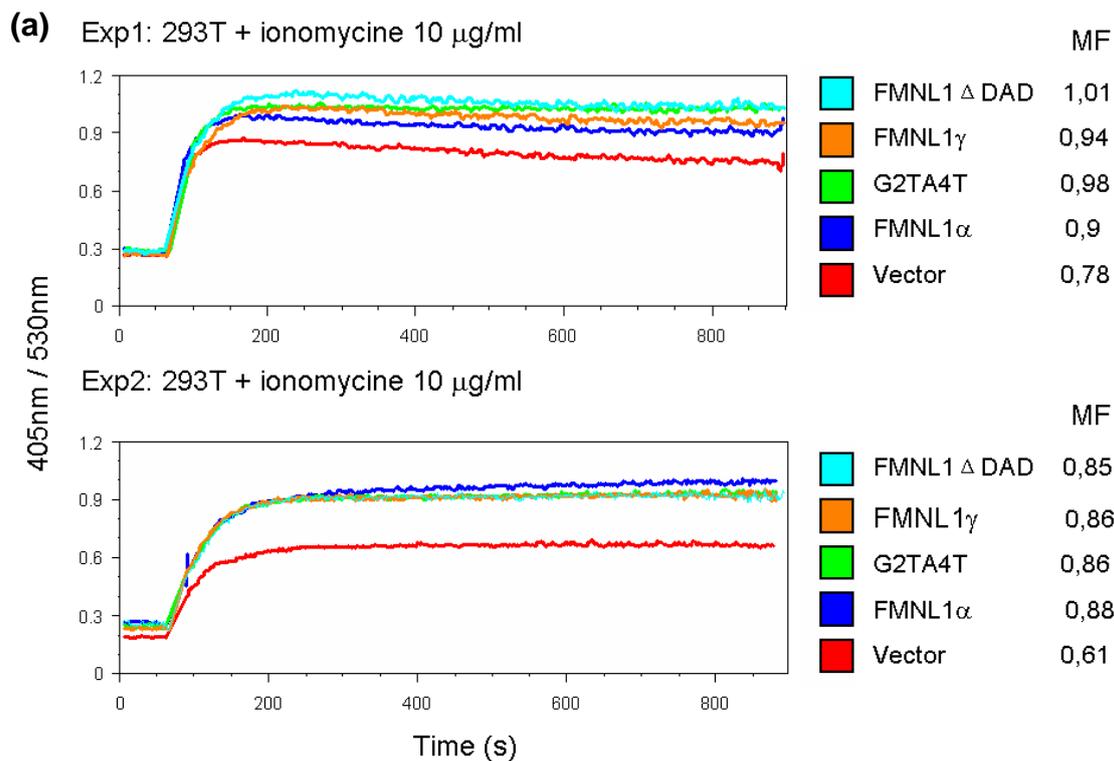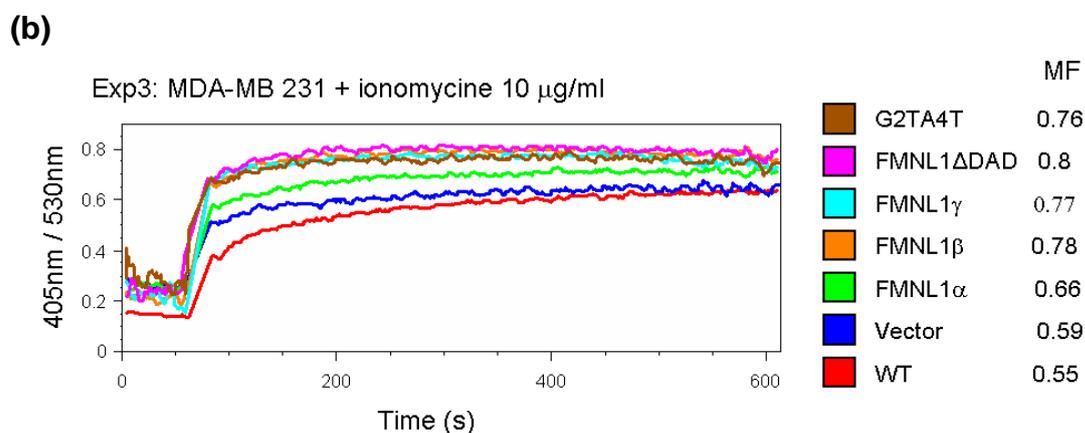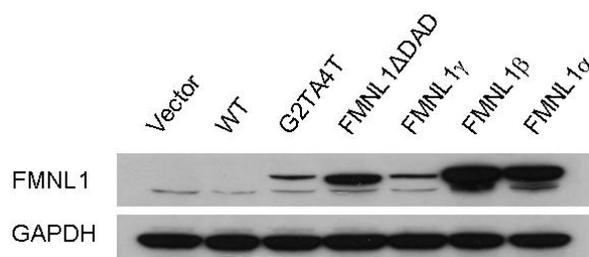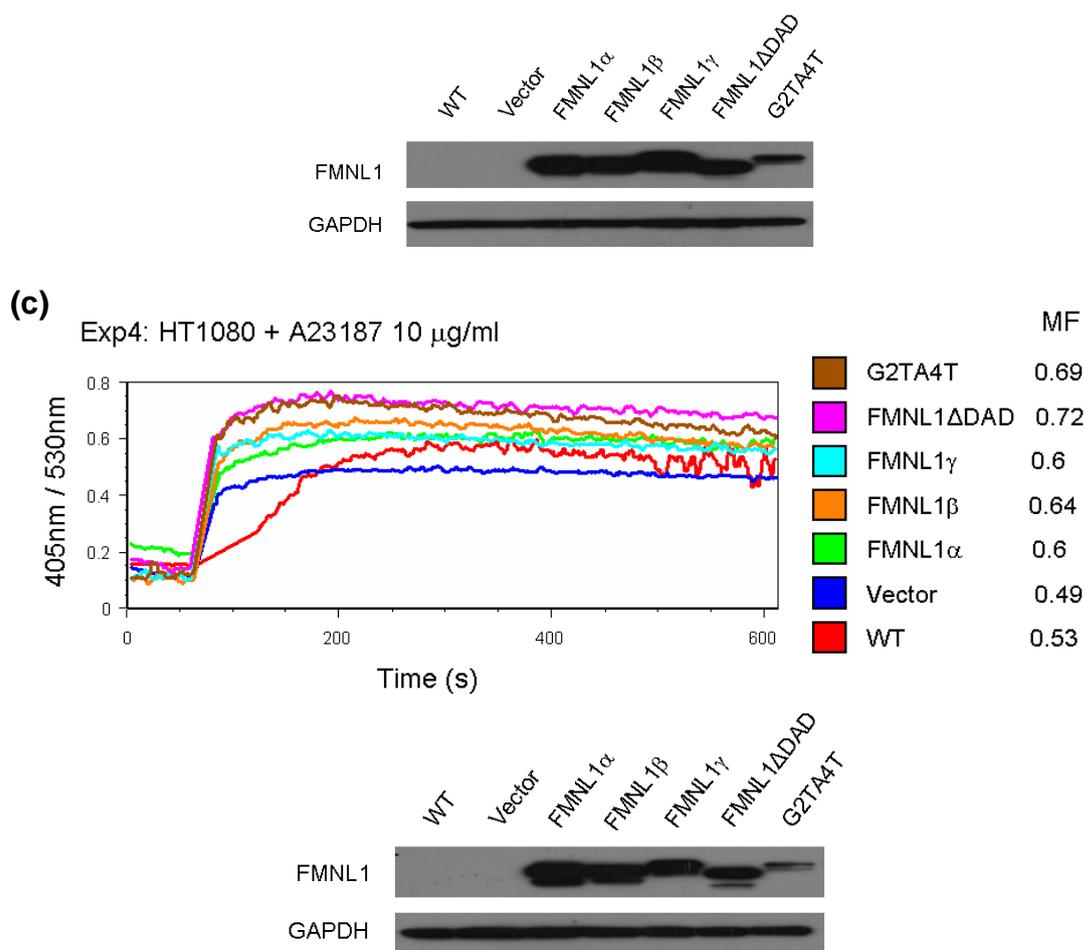
Figure 5.24 FMNL1 induces increased calcium influx after cell activation. 293T cells (a) were transfected with pcDNA vector containing FMNL1 isoforms as well as the vector control. MDA-MB 231 cells (b) and HT1080 cells (c) were adenovirally transduced with FMNL1 isoforms as well as vector conrol. 2 days later, cells were harvested and activated by 10 µg/ml ionomycine (a,b) or 10µg/ml A23187 (c). Calcium concentration was measured by a ratiometric method using indo-1 as probe. MF= mean fluorescence. The expression of FMNL1 isoforms was investigated by immunoblotting using the FMNL1 specific antibody 6F2.

6 Discussion

Immunotherapies against cancer using T cells or antibodies specific for tumor antigens are attractive alternative and complementary treatment modalities of malignant diseases. One major advantage is the high specificity and limited toxicity of these agents. Several therapeutic monoclonal antibodies have been already approved by the US Food and Drug Administration (FDA) for use in oncology (Adams and Weiner 2005; Weiner, Dhodapkar et al. 2009). Adoptive cell therapy (ACT) using autologous tumor-infiltrating lymphocytes has been considered as the most effective treatment for patients with metastatic melanoma since it can induce approximate 50% regression in patients with target cancer (Rosenberg, Restifo et al. 2008). The emphasis of the development of immunotherapies has shifted from discovery and identification of tumor antigens to the utilizating these antigens to mediate the destruction of tumor in humans (Rosenberg 1999). However, it might be also important to carefully investigate expression and function of tumor-associated antigens in order to estimate potential side effect when targeting them (Theoret et. al.2008).

The hematopoietic lineage-specific formin FMNL1 is a tumor-associated antigen which has been previously identified using the SEREX technology. FMNL1 is overexpressed in malignant cells derived from patients with CLL and other lymphomas as well as some solid tumors. In healthy tissue, it is almost exclusively expressed in hematopoietic cells suggesting this TAA to be a suitable target antigen for immune-mediated therapies in a transplant setting. However, function and role of FMNL1 have not been well characterized. Formin proteins have been described to promote the formation of actin networks and to be involved in regulation of essential cellular functions as cell division, migration, adhesion and intracellular trafficking.

In this work, we first investigated the expression of FMNL1 by western blot and confirmed the previous data that FMNL1 could be detected in native malignant cells from patients with lymphatic as well as myeloid leukemias and EBV-transformed B cells. FMNL1 is also expressed in lymphoma-derived cells and renal carcinoma cells (Schuster, Busch et al. 2007). Moreover, we continued to investigate the localization of FMNL1 by confocal microscopy. We found a dot-like cytoplasmic localization of native human FMNL1 in different hematopoietic lineage-derived cells and observed stimulation-specific polarization of endogenous FMNL1 to the immunological synapse of T cells and to the phagocytotic cup of monocytes which is in common with previous observations for human FMNL1 and the murine counterpart (Yayoshi-Yamamoto, Taniuchi et al. 2000; Seth, Otomo et al. 2006; Gomez, Kumar et al. 2007). We additionally noticed colocalization of FMNL1 at the mitotic spindle and cortex of dividing T cells, especially at the telephase,

suggesting involvement of FMNL1 involved in mitosis and cytokinesis (discussed in Chapter 6.4).

To further investigate the functional role of FMNL1, we have isolated three different FMNL1 splice variants from cDNA of CLL cells and human lung carcinoma, which result in varying C-terminal amino acid sequences (Figure 5.7a). FMNL1α and FMNL1β are corresponding to the previously described murine splice variants, FRLα and FRLβ (Yayoshi-Yamamoto, Taniuchi et al. 2000; Harris, Li et al. 2004). However, the novel identified splice variant (FMNL1γ) contains an intron retention of 58 amino acids at the C-terminal end affecting the DAD but sharing the last 30 amino acids of C-terminal end with FMNL1α (Figure 5.7b). FMNL1γ showed increased mRNA-expression in bone marrow, thymus, fetal brain and diverse hematopoietic lineage-derived cells. We also observed a high expression of FMNL1γ in malignant cells of a subset of CLL patients. Detailed analyses of systematically isolated and processed patient samples need to be performed in order to clarify if overexpression of FMNL1γ in CLL samples is associated with an activated malignant cell status and/or patient prognosis and will be a focus of further studies.

Overexpression of FMNL1γ shows that it is specifically located at the cell membrane and cortex in diverse cell lines which is similar as observed for a mutant lacking the DAD domain (FMNL1ΔDAD) indicating that deregulation of autoinhibition is effective in FMNL1γ. Both expression of FMNL1γ and FMNL1ΔDAD induces polarized non-apoptotic blebbing which is dependent on actin, tubulin and myosin integrity but independent of Src and ROCK activity, which are reported to be crucial for bleb formation induced by other formins (discussed in Chapter 6.2). Moreover, we described N-terminal myristoylation as a regulative mechanism of FMNL1 responsible for membrane trafficking potentially involved in a diversity of polarized processes of cells including proliferation.

6.1 Deregulation of autoinhibition in FMNL1γ

Although a role of the novel isolated splice variant FMNL1γ in malignant transformation could not be ascertained in this study, it showed distinct functional properties similar to the FMNL1 mutant missing the DAD sequence with deregulated autoinhibition. Both of them showed membrane localization and distinct functional properties as actin assembly activity and blebbing. This is in common with a previous publication demonstrating that deregulation of autoinhibition by deletion of the DAD region induces membrane localization and actin assembly activity in FRLα (Seth, Otomo et al. 2006).

A complex regulation network seems to be responsible for activation and

different functions of formin proteins. A central regulative tool for DRFs is autoregulation which can be released by interaction with active Rho-GTPases and potentially additional factors (Faix and Grosse 2006). Splicing has been also shown to result in differential functionality of formin proteins (Gasman, Kalaidzidis et al. 2003). The protein autoinhibition is induced by binding of the DAD peptide region to the DID armadillo repeat structure which has been reported to be mainly dependent of hydrophobic interaction (Nezami, Poy et al. 2006; Lammers, Meyer et al. 2008). The core of the DAD segment is an amphipathic helix. As described for mDia1 by Nezami et al, the Gly1180 at its N terminus and Gly1192 at its C terminus bind to the concave surface of DID which is formed by the central B helices of the five armadillo repeats. The hydrophobic face of the DAD helix, defined by Val1181, Met1182, Leu1185, and Leu1189, packs in a shallow groove on the DID. DAD residue Met1182 makes particularly extensive contact; it inserts into a pocket formed by a ring of hydrophobic residues on DID (Nezami, Poy et al. 2006).

The DAD binding surface on the DID domain is highly conserved among most Diaphanous related formins. 5 surface residues (Asn217, Asn218, Ala256, Asn310, and Gln352) were demonstrated to be most conserved participating in DAD recognition. This is based on mapping of conserved residues on the surface of the DID domain of DRFs (Nezami, Poy et al. 2006). Moreover, The DAD residues in the binding interface are also conserved among most DRFs, including the residues of Met 1182, Leu1185, Leu1186 and Leu1189 (Figure 6.1) (Alberts 2001; Nezami, Poy et al. 2006).
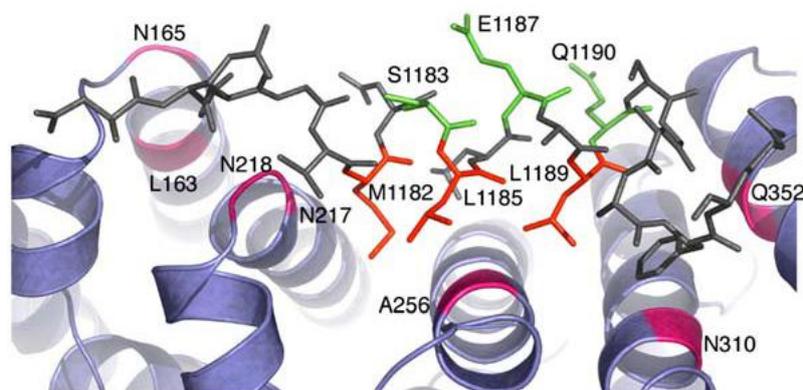
Figure 6.1 Conservation at the DID/DAD Interface. Highly conserved residues of DID interacting with DAD are shown in pink. Previous structure/function analysis (Alberts, 2001) of the DAD segment reveals that residues Met1182, Leu1185 and Leu1189 (red side chains) are required for autoinhibition, but Ser1183, Glu1187, and Gln1190 are not required (green side chains). (Nezami, Poy et al. 2006)

In figure 6.2, we have compared the conserved DAD residues of FMNL1α, FMNL1β and FMNL1γ with mammalian formins mDia, Daam1 (Dishevelledassociated activator of morphogenesis-1), the yeast formin Bnr1p,

the mammalian formin FRL1, FRL2, and FRL3 (Higgs and Peterson 2005; Nezami, Poy et al. 2006). It shows that Ile1059, Ile1062 and Ile1066 in FMNL1α and Ile1059, Ile1062 and Leu1066 in FMNL1β are corresponding to Met1182, Leu1185, and Leu1189 in mDia, which are considered to be responsible for protein autoinhibition. However, FMNL1γ contains an intron retention of 58 amino acids at the C-terminus but shares the last 30 amino acids with FMNL1α. This intron retention affects the DAD sequence and results in a positive charged polar amino acid Lys1066 instead of the non polar amino acids Ile1066 or Leu1066 present in FMNL1α or FMNL1β. This polar lysine could be responsible for release of hydrophobic reaction between DID and DAD and further release of autoinhibition of FMNL1γ resulting in a constitutively activated form.

```
mDia1     1180  GVMDSLLEALQSGAAFR
mDia2     1180  GVMDSLLEALQSGAAFR
mDia3     1180  GVMDNLLEALQSGAAFR
Daam1     1180  GEFDDLVSALRSGEVFD
Bnr1p     1180  DAVDLLISKLR---EVK
FRL1      1064  GAIEDIITVIKTVPFTA
FRL2       991  GTIEDIITGLHCQPMVV
FRL3      1049  GAIEDIITDLRNQPYRR
FMNL1α    1047  GAIEDIITVIKTVPFTA
FMNL1β    1047  GAIEDIITDLRNQPYIR
FMNL1γ    1047  GAIEDIITGKGLARPWS
```

Figure 6.2 Multiple sequence alignment of residues at the DAD interface in DRF formins. Residues involved in the autoinhibitory interaction are indicated in red. High conservation of these residues in all mDia formins as well as mammalian Daam1, FRL1, FRL2, FRL3, FMNL1 splice variants and yeast Bnr1p points to a similar mechanism of autoinhibition in these formins. However, FMNL1γ contains an intron retention affecting the DAD sequence and resulting in a positive charged polar amino acid Lys1066 instead (in blue), which may be responsible for the release of autoinhibition in FMNL1γ.

In fact, the splice variant FMNL1γ, in common with FMNL1ΔDAD, was specifically located at the membrane and cortex of different cell lines and induced bleb formation. It points to the fact that the incapability of DID binding to DAD is responsible for deregulation of autoinhibition and membrane localization and bleb formation by FMNL1γ. It is very interesting that FRL2 has been also reported to be a constitutively activated formin protein because of its capability to accumulate actin stress fibers. However, FRL2 is located in the cytoplasma as its autoinhibited counterpart FRL3. The DAD of FRL2 could still

bind to the DID without any inhibition (Vaillant, Copeland et al. 2008). It could be explained by the presence of only non polar amino acids at the highly conserved position of DAD in FRL2, which insures the interaction between the two domains. However, this interaction failed to inhibit FRL2 activity suggesting an additional regulator for formin autoinhibition.

6.2   Regulation of blebbing induced by FMNL1γ

Blebbing is a common feature of cell physiology during cell movement, cytokinesis, cell spreading and apoptosis. Blebs are spherical protrusions of the cell membrane which form and disappear in seconds (Charras, Yarrow et al. 2005). Usually, the blebs induced by apoptosis are larger and more transparent and their growth is independent of actomyosin contractions (Barros, Kanaseki et al. 2003). Unlike them, other blebs depend on actomyosin contractions of the cortex, which cause either detachment of the cell membrane from the actin cortex (Charras, Yarrow et al. 2005) or a local rupture in the actin cortex (Paluch, Piel et al. 2005) to form blebbs. In the former way, a local shortening of the actin cortex caused by myosin contraction gives rises to a centripetal compression of the cytoplasm and induces a transient increase in intra-cellular pressure. This high local intra-cellular pressure tears the membrane from the actin cortex and pushed cytosol from cell body by into blebs. Alternatively, myosin contraction stretchs the actin cortex and increases local tension, leading to the final rupture of actin cortex and the expelling of cytosol which inflates the cell membrane. During growth, the plasma membrane is transiently devoid of an actin cytoskeleton and lipids flow into the bleb through the neck of blebs. Furthermore, after growth has stalled, an actin cortex is reconstituted under the plasma membrane (Charras 2008). During the blebs expansion and cortex regrowth, regulatory proteins of the actin cytoskeleton are present at the cell membrane, the first of which is the ERM protein ezrin, which links the actin cytoskeleton to the cell membrane. Shortly after the recruitment of ezrin, actin appeared at the bleb membrane forming a cage-like structure underneath the bleb membrane. Finally, myosin II motors powered bleb retraction (Charras, Hu et al. 2006; Charras 2008).

In this work, we have observed that FMNL1γ could induce non-apoptotic cell blebbing in 293T cells and K562 cells. Moreover, FMNL1γ colocalized with the indicated regulatory proteins such as actin, ezrin and myosin IIb on cell membrane and cortex to blebs. The colocalization FMNL1γ with F-actin in bleb protrusions suggests the property of FMNL1γ to induce actin assembly. Blebbing but not membrane localization of FMNL1γ was totally abrogated by Latrunculin B further confirming regulation of actin assembly and actin-mediated polarized bleb formation by FMNL1γ. To further investigate the mechanism of bleb formation induced by FMNL1γ, FMNL1γ transduced 293T cells were incubated in medium containing Myosin II-ATPase inhibitor

Blebbistatin and microtubuli inhibitor Nocodazole. Bleb formation was significantly inhibited by these inhibitors confirming a substantial role of myosin and microtubules in FMNL1γ-induced blebbing. These results are in common with previous reports demonstrating that bleb induction by the Leishmania parasite virulence factor HASPB depends on the integrity of F-actin and requires myosin II function as well as microtubule networks (Tournaviti, Hannemann et al. 2007). Tournaviti also demonstrated that although blebbing induced by HASPB is dependent on the integrity of microtubule, no specific association of microtubule with the blebs was observed (Tournaviti, Hannemann et al. 2007). In contrast, we additionally observed colacolization of α-tubulin with FMNL1γ to FMNL1γ-induced blebs in 293T cells. It suggested that, unlike HASPB, FMNL1γ may directly associate with microtubule to induce bleb formation. However, it needs to be confirmed by protein immunoprecipitation.

Moreover, the formins FHOD1, mDia1 and mDia2 have been also associated to blebbing (Eisenmann, Harris et al. 2007; Kitzing, Sahadevan et al. 2007; Hannemann, Madrid et al. 2008). Bleb formation induced by these formins required Rho-kinase (ROCK) and Src activity. It has been previously reported that the small GTPase Rho and its downstream effector ROCK play an essential role in governing cell cortex contraction (Coleman, Sahai et al. 2001; Etienne-Manneville and Hall 2002). The activation of GTPase Rho and ROCK leads to both actin polymerization and myosin II recruitment during cytokinesis and chemotaxis (Lee, Katakai et al. 2004; Bement, Benink et al. 2005; Kamijo, Ohara et al. 2006). Rho directly activates formins, which as an actin-nucleating protein hold onto growing barbed ends (Higashida, Miyoshi et al. 2004), and activates myosin II by regulation of its phosphorylation state through Rho-kinase (Totsukawa, Yamakita et al. 2000). How might Src signalling regulate blebbing? Ezrin which is a membrane-actin crosslinks protein, is subject to regulation by Src (Elliott, Qiao et al. 2004; Srivastava, Elliott et al. 2005). Additionally, Src functionally cooperates with formin protein family which might also govern bleb retraction (Tominaga, Sahai et al. 2000; Gasman, Kalaidzidis et al. 2003; Koka, Minick et al. 2005). However, in contrast to former publications, blebbing induced by FMNL1γ is independent of Src and ROCK as the Src inhibitor PP1 and the ROCK inhibitor Y-27632 did not reduce blebbing in our experiments. This might be explained by the constitutive activation of FMNL1γ and suggest a novel regulation of blebbing induced by formin proteins beside the activation of Rho GTPase, ROCK and Src.

Futrthermore, the shape and extent of blebs varied in different cell lines. FMNL1γ-induced blebbing was less obvious in HT1080 and MDA-MB 231 cells. However, these cell lines especially demonstrated enrichment of FMNL1γ at intracellular vesicles beside the localization at the cell membrane. HT1080 has mesenchymal characteristics and MDA-MB 231 cells are epithelial cells,

indicating that cell type-specific interaction partners additionally play an important role in function and bleb shape. In these cell lines, FMNL1 could play a role in vesicles transferring and autophagocytosis. Unlike them, the K562 cells are hematopoietic origin, which could probably represent a more natural recipient cell for investigation of FMNL1γ. K562 cells transduced with FMNL1γ often demonstrated a polarized uropod-like circular. Uropod formation of leukocytes has been reported to be involved in cell migration, activation and cell-cell interaction. This polarized structure has distinct function in the immune response as it could help T cell to form the immunological synapse when interacting with target cells (Fais and Malorni 2003). The involvement of FMNL1γ in the cell polarization is in common with the investigation of endogenous FMNL1 in specific targeted T cell.

6.3   N-terminal myristoylation

To further evaluate the mechanism of membrane localization and bleb-induction by FMNL1γ, we analyzed the protein sequence motifs of FMNL1 and identified a myristoylation site at the N-terminus of human FMNL1 and murine FRL with glycine at position 2 representing an essential requirement for myristoylation.

N-terminal myristoylation of proteins stand for the covalent attachment of myristate, a 14-carbon saturated fatty acid, to the N-terminal glycine of eukaryotic and viral proteins (Farazi, Waksman et al. 2001). This transfer is catalyzed by myristoyl-CoA:protein N-myristoyltransferase (Nmt) (Towler, Adams et al. 1987). N-terminal myristoylation sites have been reported to direct membrane association by interaction with negatively charged phospholipids enriched in the cytoplasmic leaflet of cellular membranes (Peitzsch and McLaughlin 1993). The model of how the N-terminal myristoylated protein, tyrosine kinase c-Src, anchors to the membrane is shown in Figure 6.3 (Murray, Ben-Tal et al. 1997): 10 carbon fatty acids penetrate the hydrocarbon core of the membrane while the other four insert into the polar head group region. The N-terminal glycine is located just outside the envelope of the polar head group region.
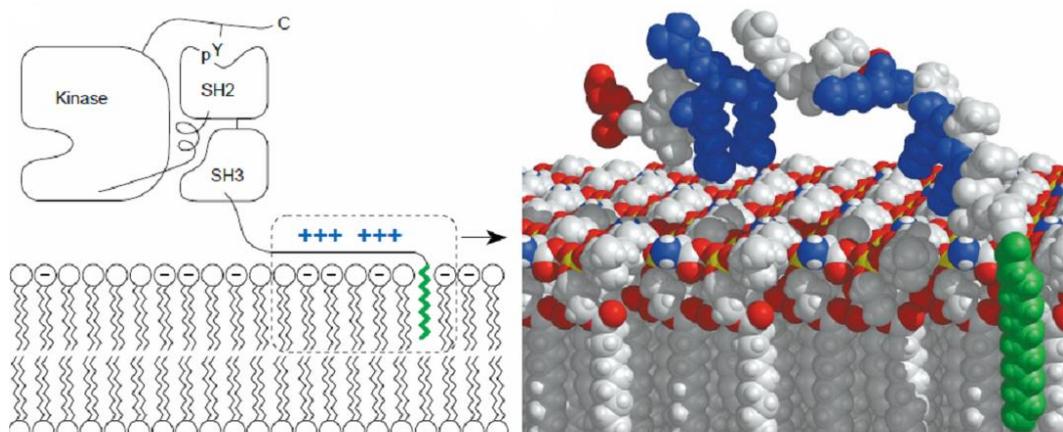
Figure 6.3 Schematic view of interaction of N-myristoalated protein Src with membrane. (a) The N-terminal portion of Src which contains the two motifs required for membrane association: the myristate (colored green) and a cluster of basic residues (blue plus signs), which are shown in more detail in (b) The myristate of Src protein is colored green, basic residues blue and acidic residues red. In the membrane, the acidic lipid, phosphatidylserine, is identified by its exposed nitrogen, colored blue. (Murray, Ben-Tal et al. 1997)

Some proteins containing an N-termial glycine at position two are not myristoylated, probably because of some sequence requirements that are not fulfilled by those proteins. The sequence at the N-terminal myristoylatrion site of the protein substrates should contain more than the glycine at the N-terminus (Boutin 1997). The most important sequence might be the second and sixth residue (Boutin 1997). A serine or a threonine residue at the sixth position favours the myristoylation (Johnson, Bhatnagar et al. 1994). FMNL1 does have a glycine at N-terminus at position two and the favourable asparagines at position three, however lacks the serine or threonine at position six (Figure 5.15). FMNL1γ contains another glycine at position s, which is also common in some myristoylated proteins like ARF3, c-abl and Rat lipase (Boutin 1997). To confirm if FMNL1γ is an N-myristoylated protein, a myristic acid uptake assay was performed. Cells transfected with FMNL1γ or G2TA4T mutant were metabolically labeled with [3H]-myristic acid and immunoprecipitated by FMNL1-specific antibody. Autoradiography analysis demonstrated that FMNL1γ, but not G2TA4T, was myristoylated in 293T cells which provides direct evidence that FMNL1γ is indeed an N-terminal myristoylated protein. FMNL1γ and FMNL1ΔDAD but not the mutant G2TA4T was shown to be located to the plasma membrane. Moreover, myristoylation could be inhibited by 2-Hydroxymyristate, a potent inhibitor of myristoylation (Paige, Zheng et al. 1990), resulting in loss of membrane localization. As described before, FMNL1 splice variants just differ at the C-terminus. Therefore, FMNL1α and FMNL1β also contain N-terminal myristoylation site. However, the complex formed by the interaction between DID and DAD in the

autoinhibited state may impede membrane localization regulated by N-terminal myristoylation.

N-terminal myristoylated proteins have diverse functions and intracellular destinations. They are crucial in signal transduction, cellular transformation, and oncogenesis (Shrivastav, Varma et al. 2008). This motif is typically present in the SH4 domain of Src tyrosine kinases and myristoylation has been shown to be critical for malignant transformation of v-Src (Cross, Garber et al. 1984; Kamps, Buss et al. 1985). Myristate is required for Src membrane binding which, in turn, is required for Src to function, since nonmyristoylated v-Src mutants are found in the cytoplasm but do not transform cells, even though the kinase activity of the protein is unaffected. It may because some critical targets for Src activity are located at or near the cell membrane (Kamps, Buss et al. 1985; Buss, Kamps et al. 1986). In this work, we investigated that blebbing induced by FMNL1γ is dependent on N-terminal myristoylation since the mutation of glycine at position 2 significantly reduced blebbing. We therefore propose that activation of FMNL1 is regulated not only by binding of a Rho-GTPase but additionally by an increase of intracellular Ca^{2+} or a specific ligand binding. This may cause a myristoyl switch and therefore induces extrusion of the myristoyl group enabling it to quickly and reversibly interact with lipid bilayer membranes as previously described for other myristoylated proteins (Seykora, Myat et al. 1996; Ames, Ishima et al. 1997). It was proposed that the myristoyl group is sequestered in the calcium-free form of the protein and becomes exposed in the calcium-bound form, enabling it to insert into a lipid bilayer of membrane or a hydrophobic site of a target protein (Zozulya and Stryer 1992; Ames, Ishima et al. 1997). These data suggested that myristoyl groups are not simply hydrophobic anchors, but can serve as dynamic partners in signaling (Ames, Ishima et al. 1997). We have observed that calcium binding slightly increases the membrane localization of the autoinhibited FMNL1α and FMNL1β (preliminary data) suggesting that FMNL1 could also be activated through the calcium- myristoyl switch. Furthermore, stimulation of ionomycine will induce higher concentration of intracellular calcium in FMNL1 transduced cells potentially reprtesenting a self-activating loop, which will be discussed later in chapter 6.5.

6.4   Acceleration of cell proliferation induced by FMNL1γ

As we have shown by Annexin V and propidium iodide staining that blebbing induced by FMNL1γ was not associated to apoptosis (Figure 5.12). We continued to investigate other cellular processes which have been described to be involved in cell blebbing such as cytokinesis. By analyzing cell numbers in independent counting experiments, we observed that cells derived from different cell lines transfected or transduced with FMNL1γ revealed slightly

enhanced cell numbers compared to the other splice variants and the mock control. Moderately accelerated cell proliferation induced by FMNL1γ was confirmed by SNARF-1 staining in two cell lines, HT1080 and MDA-MB 231, which are highly genetically transducible by adenoviral infection as seen by GFP expression (> 90%). Similar results were obtained through a cell cycle experiment by BrdU incorporation followed by anti-BrdU and 7-AAD staining of HT1080 cells transduced with different FMNL1 splice variants demonstrating a significant BrdU positive population at G0/G1 phase 3 days after transduction with FMNL1γ which was not present in the other isoforms or GFP control. This experiment did not show major differences in single cell cycle phases, however indicated an accelerated passage of cells transduced by FMNLγ through the cell cycle.

Murine formin FRL has been shown to be involved in regulation of cell survival (Yayoshi-Yamamoto et al., 2000). This group demonstrated that macrophages overexpressing the FRL-FH3 truncated protein (only contains N-terminal FH3 domain but not FH1 and FH2 domians) were inhibited in cell growth and were prone to cell apoptosis. This may be explained by the direct binding of FRL-FH3 truncated protein to Rho GTPase Rac, which interfered with the Rac binding to endogenous FRL; thus, the normal function of FRL was inhibited. However, a direct effect on proliferation has not been demonstrated so far. In this work, we have observed by confocal microscopy that FMNL1γ located at contractile ring and cortex of mitotic FMNL1γ transfected 293T cells. Futhermore, proliferation of cells transduced with G2TA4T was still enhanced although slightly reduced in comparison to the non-mutated FMNL1γ (data not shown). Meanwhile, cells transduced with G2TA4T showed an enhancement of multinucleated cells compared to cells transduced with non-mutated FMNL1γ. Multinucleation was also observed in spermatids of male flies, when the formin diaphanous mutants resulted in a failure in cell division during spermatogenesis (Goode and Eck 2007). Our relsults give rise for the hypothsis that the accelerated cell proliferation induced by FMNL1γ may because of its involvement in cell cytokinesis and N-terminal myristoylation may play a role in cell seperation.

The effect on cell proliferation induced by FMNL1γ was moderate but constantly observed. This may correlate with the slow increase in malignant cell burden often observed in patients with CLL and highly encourages the further investigation of the role of FMNL1 in CLL cells. In addition, we observed colocalization of endogenous FMNL1 to the microtubules and midzone cortex of dividing T cells pointing to a possible involvement of FMNL1 in mitosis of T cells.

To further confirm the involvement of FMNL1γ in cell proliferation, a FMNL1γ specific siRNA would be required to knockdown the endogenous FMNL1γ in

hematopoietic lineage-derived cells, for example T cells, and then analyzes cell proliferation. A FMNL1γ specific antiboby would also be required to detect the colocalization of endogenous FMNL1γ to the microtubuli at the cortex and mitotic spindles in dividing cells. On the other hand, the endogenous FMNL1 may be generally involved in enhanced cell proliferation since knock down of FMNL1 in T cells showed slight inhibition of T cell proliferation (unpublished data of the group of Dr. Angela Krackhardt). Furthermore, FMNL1 could increase intracellular calcium concentration after stimulation which is a sufficient signal for cell activation and subsequent gene expression and proliferation through the nuclear factor-κB (NF-κB) pattway (Dolmetsch, Lewis et al. 1997). Analysis of interaction partners of FMNL1 could also be required to characterize the complete sigaling pathway.

6.5 Intracellular calcium concentration

The intracellular calcium is one of the most fundamental signalling substances which controls diverse cell functions, including adhesion, motility, gene expression and proliferation. It has also been reported to be involved in cell morphological oscillations such as blebbing (Pletjushkina, Rajfur et al. 2001; Blaser, Reichman-Fried et al. 2006). Cyclic intra-cellular calcium changes are accompanied with cortical contractility, but whether these calcium oscillations are the cause or a consequence of the enhanced contractility is unclear. Chelation of extracellular calcium could inhibit blebbing. Therefore elevated intra-cellular calcium may cause the myosin contractions that give rise to blebs. Conversely, calcium could also enter the cells as a consequence of increased membrane tension in blebs.

On the other hand, a cooperation partner of FMNL1, AHNAK, which has been identified as an interaction partner of FMNL1 by our group, has been reported to be critical for calcium signaling during T cell activation. AHNAK deficiency in CD4+ T cells resulted in a reduced calcium influx upon TCR crosslinking and subsequent poor activation of the transcription factor NFAT (Matza, Badou et al. 2008). In our preliminary experiments, AHNAK, like FMNL1, was polarized at the immunosynapse in specifically stimulated T cells and colocalized with CD3. Moreover, AHNAK was colocalized with FMNL1γ at cell membrane and blebs in FMNL1γ transduced cells.

In this work, different cell lines were transfected or transduced with FMNL1 isoforms and stained with indo-1 AM. Immediately after activation with ionomycine or A23187, the intracellular calcium concentrations in these cells were measured during a time of 10 minutes. The results demonstrated a higher intracellular calcium concentration in cells transfected or transduced with different isoforms of FMNL1 compared to vector and wildtype control.

However, there is no difference of enhancement of intracellular calcium concentration among different isoforms of FMNL1 including the mutant G2TA4T. Thus, the increase of intracellular calcium concentration seems to be independent of N-terminal myristoylation. Further experiments need to be performed to investigate the role of FMNL1 in calcium signaling pathways.

In conclusion, this project provides novel information about expression and specific localization of human endogenous FMNL1 in a diversity of polarized processes of hematopoietic lineage-derived cells suggesting FMNL1 to be a pluripotent effector protein. Moreover, the newly identified splice variant FMNL1γ represents a constitutively active form of FMNL1 which localizes at the membrane and induces bleb formation. FMNL1γ also associates FMNL1 to mitosis and cell growth. We identified N-terminal myristoylation as an important regulatory tool for FMNL1 necessary for bleb formation, enabling fast and reversible membrane localization compatible with diverse functions of hematopoietic lineage-derived cells. Thus our results suggest FMNL1 to be a promise potential target antigen for anti-tumor immunotherapy as it is potentially involved in cellular transformation and tumor progression. The identification of interaction partners of FMNL1 in diverse hematopoietic-derived cells as well as the further characterization of splice variants will be highly interesting to identify key molecules regulating different FMNL1 functions potentially revealing possibilities for specific therapeutic interaction in malignant and inflammatory disease.

7 Reference

Adams, G. P. and L. M. Weiner (2005). "Monoclonal antibody therapy of cancer." <u>Nat Biotechnol</u> **23**(9): 1147-57.

Alberts, A. S. (2001). "Identification of a carboxyl-terminal diaphanous-related formin homology protein autoregulatory domain." <u>J Biol Chem</u> **276**(4): 2824-30.

Ames, J. B., R. Ishima, et al. (1997). "Molecular mechanics of calcium-myristoyl switches." <u>Nature</u> **389**(6647): 198-202.

Banchereau, J., F. Briere, et al. (2000). "Immunobiology of dendritic cells." <u>Annu Rev Immunol</u> **18**: 767-811.

Barros, L. F., T. Kanaseki, et al. (2003). "Apoptotic and necrotic blebs in epithelial cells display similar neck diameters but different kinase dependency." <u>Cell Death Differ</u> **10**(6): 687-97.

Bement, W. M., H. A. Benink, et al. (2005). "A microtubule-dependent zone of active RhoA during cleavage plane specification." <u>J Cell Biol</u> **170**(1): 91-101.

Blaser, H., M. Reichman-Fried, et al. (2006). "Migration of zebrafish primordial germ cells: a role for myosin contraction and cytoplasmic flow." <u>Dev Cell</u> **11**(5): 613-27.

Boutin, J. A. (1997). "Myristoylation." <u>Cell Signal</u> **9**(1): 15-35.

Brichard, V., A. Van Pel, et al. (1993). "The tyrosinase gene codes for an antigen recognized by autologous cytolytic T lymphocytes on HLA-A2 melanomas." <u>J Exp Med</u> **178**(2): 489-95.

Bubenik, J., P. Perlmann, et al. (1970). "Cellular and humoral immune responses to human urinary bladder carcinomas." <u>Int J Cancer</u> **5**(3): 310-9.

Buss, J. E., M. P. Kamps, et al. (1986). "The absence of myristic acid decreases membrane binding of p60src but does not affect tyrosine protein kinase activity." <u>J Virol</u> **58**(2): 468-74.

Cantwell, M., T. Hua, et al. (1997). "Acquired CD40-ligand deficiency in chronic lymphocytic leukemia." <u>Nat Med</u> **3**(9): 984-9.

Chames, P., M. Van Regenmortel, et al. (2009). "Therapeutic antibodies: successes, limitations and hopes for the future." <u>Br J Pharmacol</u> **157**(2): 220-33.

Chapman, P. B. (2004). "T-cell chauvinists versus antibody advocates--can't we all just

get along?" J Clin Oncol **22**(22): 4446-8.

Charras, G. T. (2008). "A short history of blebbing." J Microsc **231**(3): 466-78.

Charras, G. T., C. K. Hu, et al. (2006). "Reassembly of contractile actin cortex in cell blebs." J Cell Biol **175**(3): 477-90.

Charras, G. T., J. C. Yarrow, et al. (2005). "Non-equilibration of hydrostatic pressure in blebbing cells." Nature **435**(7040): 365-9.

Chen, Y. T., E. Stockert, et al. (1996). "Serological analysis of Melan-A(MART-1), a melanocyte-specific protein homogeneously expressed in human melanomas." Proc Natl Acad Sci U S A **93**(12): 5915-9.

Chhabra, E. S. and H. N. Higgs (2007). "The many faces of actin: matching assembly factors with cellular structures." Nat Cell Biol **9**(10): 1110-21.

Coleman, M. L., E. A. Sahai, et al. (2001). "Membrane blebbing during apoptosis results from caspase-mediated activation of ROCK I." Nat Cell Biol **3**(4): 339-45.

Copeland, S. J., B. J. Green, et al. (2007). "The diaphanous inhibitory domain/diaphanous autoregulatory domain interaction is able to mediate heterodimerization between mDia1 and mDia2." J Biol Chem **282**(41): 30120-30.

Coulie, P. G., V. Brichard, et al. (1994). "A new gene coding for a differentiation antigen recognized by autologous cytolytic T lymphocytes on HLA-A2 melanomas." J Exp Med **180**(1): 35-42.

Cox, A. L., J. Skipper, et al. (1994). "Identification of a peptide recognized by five melanoma-specific human cytotoxic T cell lines." Science **264**(5159): 716-9.

Cross, F. R., E. A. Garber, et al. (1984). "A short sequence in the p60src N terminus is required for p60src myristylation and membrane association and for cell transformation." Mol Cell Biol **4**(9): 1834-42.

Disis, M. L., H. Bernhard, et al. (2009). "Use of tumour-responsive T cells as cancer treatment." Lancet **373**(9664): 673-83.

Dolmetsch, R. E., R. S. Lewis, et al. (1997). "Differential activation of transcription factors induced by Ca2+ response amplitude and duration." Nature **386**(6627): 855-8.

Dreger, P., P. Corradini, et al. (2007). "Indications for allogeneic stem cell transplantation in chronic lymphocytic leukemia: the EBMT transplant consensus." Leukemia **21**(1): 12-7.

Dreger, P. and E. Montserrat (2002). "Autologous and allogeneic stem cell transplantation for chronic lymphocytic leukemia." Leukemia **16**(6): 985-92.

Dreger, P., S. Stilgenbauer, et al. (2004). "The prognostic impact of autologous stem cell transplantation in patients with chronic lymphocytic leukemia: a risk-matched analysis based on the VH gene mutational status." Blood **103**(7): 2850-8.

Eisenmann, K. M., E. S. Harris, et al. (2007). "Dia-interacting protein modulates formin-mediated actin assembly at the cell cortex." Curr Biol **17**(7): 579-91.

Elliott, B. E., H. Qiao, et al. (2004). "Co-operative effect of c-Src and ezrin in deregulation of cell-cell contacts and scattering of mammary carcinoma cells." J Cell Biochem **92**(1): 16-28.

Emens, L. A. and E. M. Jaffee (2005). "Leveraging the activity of tumor vaccines with cytotoxic chemotherapy." Cancer Res **65**(18): 8059-64.

Etienne-Manneville, S. and A. Hall (2002). "Rho GTPases in cell biology." Nature **420**(6916): 629-35.

Evangelista, M., K. Blundell, et al. (1997). "Bni1p, a yeast formin linking cdc42p and the actin cytoskeleton during polarized morphogenesis." Science **276**(5309): 118-22.

Fackler, O. T. and R. Grosse (2008). "Cell motility through plasma membrane blebbing." J Cell Biol **181**(6): 879-84.

Fais, S. and W. Malorni (2003). "Leukocyte uropod formation and membrane/cytoskeleton linkage in immune interactions." J Leukoc Biol **73**(5): 556-63.

Faix, J. and R. Grosse (2006). "Staying in shape with formins." Dev Cell **10**(6): 693-706.

Farazi, T. A., G. Waksman, et al. (2001). "The biology and enzymology of protein N-myristoylation." J Biol Chem **276**(43): 39501-4.

Favaro, P. M., F. Traina, et al. (2006). "High expression of FMNL1 protein in T non-Hodgkin's lymphomas." Leuk Res **30**(6): 735-8.

Finn, O. J. (2008). "Cancer immunology." N Engl J Med **358**(25): 2704-15.

Foster, A. E., M. K. Brenner, et al. (2008). "Adoptive T-cell immunotherapy of chronic lymphocytic leukaemia." Best Pract Res Clin Haematol **21**(3): 375-89.

Gasman, S., Y. Kalaidzidis, et al. (2003). "RhoD regulates endosome dynamics through

Diaphanous-related Formin and Src tyrosine kinase." Nat Cell Biol **5**(3): 195-204.

Giannopoulos, K. and M. Schmitt (2006). "Targets and strategies for T-cell based vaccines in patients with B-cell chronic lymphocytic leukemia." Leuk Lymphoma **47**(10): 2028-36.

Gomez, T. S., K. Kumar, et al. (2007). "Formins regulate the actin-related protein 2/3 complex-independent polarization of the centrosome to the immunological synapse." Immunity **26**(2): 177-90.

Goode, B. L. and M. J. Eck (2007). "Mechanism and function of formins in the control of actin assembly." Annu Rev Biochem **76**: 593-627.

Graziano, D. F. and O. J. Finn (2005). "Tumor antigens and tumor antigen discovery." Cancer Treat Res **123**: 89-111.

Hamblin, A. D. and T. J. Hamblin (2008). "The immunodeficiency of chronic lymphocytic leukaemia." Br Med Bull **87**: 49-62.

Hannemann, S., R. Madrid, et al. (2008). "The Diaphanous-related Formin FHOD1 associates with ROCK1 and promotes Src-dependent plasma membrane blebbing." J Biol Chem **283**(41): 27891-903.

Harris, E. S., F. Li, et al. (2004). "The mouse formin, FRLalpha, slows actin filament barbed end elongation, competes with capping protein, accelerates polymerization from monomers, and severs filaments." J Biol Chem **279**(19): 20076-87.

Hellstrom, K. E., I. Hellstrom, et al. (1982). "Human tumor-associated antigens identified by monoclonal antibodies." Springer Semin Immunopathol **5**(2): 127-46.

Higashida, C., T. Miyoshi, et al. (2004). "Actin polymerization-driven molecular movement of mDia1 in living cells." Science **303**(5666): 2007-10.

Higgs, H. N. (2005). "Formin proteins: a domain-based approach." Trends Biochem Sci **30**(6): 342-53.

Higgs, H. N. and K. J. Peterson (2005). "Phylogenetic analysis of the formin homology 2 domain." Mol Biol Cell **16**(1): 1-13.

Ho, W. Y., J. N. Blattman, et al. (2003). "Adoptive immunotherapy: engineering T cell responses as biologic weapons for tumor mass destruction." Cancer Cell **3**(5): 431-7.

Ishizaki, T., Y. Morishima, et al. (2001). "Coordination of microtubules and the actin cytoskeleton by the Rho effector mDia1." Nat Cell Biol **3**(1): 8-14.

Johnson, D. R., R. S. Bhatnagar, et al. (1994). "Genetic and biochemical studies of protein N-myristoylation." Annu Rev Biochem **63**: 869-914.

Kalil, N. and B. D. Cheson (1999). "Chronic lymphocytic leukemia." Oncologist **4**(5): 352-69.

Kamijo, K., N. Ohara, et al. (2006). "Dissecting the role of Rho-mediated signaling in contractile ring formation." Mol Biol Cell **17**(1): 43-55.

Kamps, M. P., J. E. Buss, et al. (1985). "Mutation of NH2-terminal glycine of p60src prevents both myristoylation and morphological transformation." Proc Natl Acad Sci U S A **82**(14): 4625-8.

Kao, H., A. A. Amoscato, et al. (2001). "A new strategy for tumor antigen discovery based on in vitro priming of naive T cells with dendritic cells." Clin Cancer Res **7**(3 Suppl): 773s-780s.

Kato, K., M. J. Cantwell, et al. (1998). "Gene transfer of CD40-ligand induces autologous immune recognition of chronic lymphocytic leukemia B cells." J Clin Invest **101**(5): 1133-41.

Kawakami, Y., S. Eliyahu, et al. (1994). "Identification of a human melanoma antigen recognized by tumor-infiltrating lymphocytes associated with in vivo tumor rejection." Proc Natl Acad Sci U S A **91**(14): 6458-62.

Kitzing, T. M., A. S. Sahadevan, et al. (2007). "Positive feedback between Dia1, LARG, and RhoA regulates cell morphology and invasion." Genes Dev **21**(12): 1478-83.

Koka, S., G. T. Minick, et al. (2005). "Src regulates the activity of the mammalian formin protein FHOD1." Biochem Biophys Res Commun **336**(4): 1285-91.

Korman, A. J., K. S. Peggs, et al. (2006). "Checkpoint blockade in cancer immunotherapy." Adv Immunol **90**: 297-339.

Kovar, D. R., J. R. Kuhn, et al. (2003). "The fission yeast cytokinesis formin Cdc12p is a barbed end actin filament capping protein gated by profilin." J Cell Biol **161**(5): 875-87.

Krackhardt, A. M., M. Witzens, et al. (2002). "Identification of tumor-associated antigens in chronic lymphocytic leukemia by SEREX." Blood **100**(6): 2123-31.

Kuppers, R. (2009). "The biology of Hodgkin's lymphoma." Nat Rev Cancer **9**(1): 15-27.

Lammers, M., S. Meyer, et al. (2008). "The specificity of interactions between mdia-isoforms and rho proteins." J Biol Chem.

Lee, J. H., T. Katakai, et al. (2004). "Roles of p-ERM and Rho-ROCK signaling in lymphocyte polarity and uropod formation." J Cell Biol **167**(2): 327-37.

Lewkowicz, E., F. Herit, et al. (2008). "The microtubule-binding protein CLIP-170 coordinates mDia1 and actin reorganization during CR3-mediated phagocytosis." J Cell Biol **183**(7): 1287-98.

Li, F. and H. N. Higgs (2003). "The mouse Formin mDia1 is a potent actin nucleation factor regulated by autoinhibition." Curr Biol **13**(15): 1335-40.

Mattern, T., H. D. Flad, et al. (1998). "Stimulation of human T lymphocytes by LPS is MHC unrestricted, but strongly dependent on B7 interactions." J Immunol **160**(7): 3412-8.

Matza, D., A. Badou, et al. (2008). "A scaffold protein, AHNAK1, is required for calcium signaling during T cell activation." Immunity **28**(1): 64-74.

Montserrat, E. and C. Moreno (2008). "Chronic lymphocytic leukaemia: a short overview." Ann Oncol **19 Suppl 7**: vii320-5.

Moreno, C., N. Villamor, et al. (2005). "Allogeneic stem-cell transplantation may overcome the adverse prognosis of unmutated VH gene in patients with chronic lymphocytic leukemia." J Clin Oncol **23**(15): 3433-8.

Morris, E. C., G. M. Bendle, et al. (2003). "Prospects for immunotherapy of malignant disease." Clin Exp Immunol **131**(1): 1-7.

Moseley, J. B., I. Sagot, et al. (2004). "A conserved mechanism for Bni1- and mDia1-induced actin assembly and dual regulation of Bni1 by Bud6 and profilin." Mol Biol Cell **15**(2): 896-907.

Murray, D., N. Ben-Tal, et al. (1997). "Electrostatic interaction of myristoylated proteins with membranes: simple physics, complicated biology." Structure **5**(8): 985-9.

Nezami, A. G., F. Poy, et al. (2006). "Structure of the autoinhibitory switch in formin mDia1." Structure **14**(2): 257-63.

Otomo, T., C. Otomo, et al. (2005). "Structural basis of Rho GTPase-mediated activation of the formin mDia1." Mol Cell **18**(3): 273-81.

Otomo, T., D. R. Tomchick, et al. (2005). "Structural basis of actin filament nucleation and processive capping by a formin homology 2 domain." Nature **433**(7025): 488-94.

Paige, L. A., G. Q. Zheng, et al. (1990). "Metabolic activation of 2-substituted derivatives of myristic acid to form potent inhibitors of myristoyl CoA:protein N-myristoyltransferase." Biochemistry **29**(46): 10566-73.

Paluch, E., M. Piel, et al. (2005). "Cortical actomyosin breakage triggers shape oscillations in cells and cell fragments." Biophys J **89**(1): 724-33.

Parmiani, G., A. De Filippo, et al. (2007). "Unique human tumor antigens: immunobiology and use in clinical trials." J Immunol **178**(4): 1975-9.

Peitzsch, R. M. and S. McLaughlin (1993). "Binding of acylated peptides and fatty acids to phospholipid vesicles: pertinence to myristoylated proteins." Biochemistry **32**(39): 10436-43.

Pletjushkina, O. J., Z. Rajfur, et al. (2001). "Induction of cortical oscillations in spreading cells by depolymerization of microtubules." Cell Motil Cytoskeleton **48**(4): 235-44.

Pruyne, D., M. Evangelista, et al. (2002). "Role of formins in actin assembly: nucleation and barbed-end association." Science **297**(5581): 612-5.

Quintas-Cardama, A. and S. O'Brien (2009). "Targeted therapy for chronic lymphocytic leukemia." Target Oncol **4**(1): 11-21.

Ribas, A., D. C. Hanson, et al. (2007). "Tremelimumab (CP-675,206), a cytotoxic T lymphocyte associated antigen 4 blocking monoclonal antibody in clinical development for patients with cancer." Oncologist **12**(7): 873-83.

Rivero, F., T. Muramoto, et al. (2005). "A comparative sequence analysis reveals a common GBD/FH3-FH1-FH2-DAD architecture in formins from Dictyostelium, fungi and metazoa." BMC Genomics **6**(1): 28.

Rose, R., M. Weyand, et al. (2005). "Structural and mechanistic insights into the interaction between Rho and mammalian Dia." Nature **435**(7041): 513-8.

Rosenberg, S. A. (1995). "The development of new cancer therapies based on the molecular identification of cancer regression antigens." Cancer J Sci Am **1**(2): 90-100.

Rosenberg, S. A. (1996). "Development of cancer immunotherapies based on identification of the genes encoding cancer regression antigens." J Natl Cancer Inst **88**(22): 1635-44.

Rosenberg, S. A. (1999). "A new era for cancer immunotherapy based on the genes that encode cancer antigens." Immunity **10**(3): 281-7.

Rosenberg, S. A., N. P. Restifo, et al. (2008). "Adoptive cell transfer: a clinical path to effective cancer immunotherapy." Nat Rev Cancer **8**(4): 299-308.

Rozman, C. and E. Montserrat (1995). "Chronic lymphocytic leukemia." N Engl J Med **333**(16): 1052-7.

Sahin, U., O. Tureci, et al. (1997). "Serological identification of human tumor antigens." Curr Opin Immunol **9**(5): 709-16.

Schirle, M., W. Keilholz, et al. (2000). "Identification of tumor-associated MHC class I ligands by a novel T cell-independent approach." Eur J Immunol **30**(8): 2216-25.

Schuster, I. G., D. H. Busch, et al. (2007). "Allorestricted T cells with specificity for the FMNL1-derived peptide PP2 have potent antitumor activity against hematologic and other malignancies." Blood **110**(8): 2931-9.

Seth, A., C. Otomo, et al. (2006). "Autoinhibition regulates cellular localization and actin assembly activity of the diaphanous-related formins FRLalpha and mDia1." J Cell Biol **174**(5): 701-13.

Seykora, J. T., M. M. Myat, et al. (1996). "Molecular determinants of the myristoyl-electrostatic switch of MARCKS." J Biol Chem **271**(31): 18797-802.

Shrivastav, A., S. Varma, et al. (2008). "Requirement of N-myristoyltransferase 1 in the development of monocytic lineage." J Immunol **180**(2): 1019-28.

Srivastava, J., B. E. Elliott, et al. (2005). "Src-dependent ezrin phosphorylation in adhesion-mediated signaling." Mol Biol Cell **16**(3): 1481-90.

Theobald, M., J. Biggs, et al. (1997). "Tolerance to p53 by A2.1-restricted cytotoxic T lymphocytes." J Exp Med **185**(5): 833-41.

Theoret, M. R., C. J. Cohen, et al. (2008). "Relationship of p53 Overexpression on Cancers and Recognition by Anti-p53 T Cell Receptor-Transduced T Cells." Hum Gene Ther **19**(11): 1219-32.

Tominaga, T., E. Sahai, et al. (2000). "Diaphanous-related formins bridge Rho GTPase and Src tyrosine kinase signaling." Mol Cell **5**(1): 13-25.

Totsukawa, G., Y. Yamakita, et al. (2000). "Distinct roles of ROCK (Rho-kinase) and MLCK in spatial regulation of MLC phosphorylation for assembly of stress fibers and focal adhesions in 3T3 fibroblasts." J Cell Biol **150**(4): 797-806.

Tournaviti, S., S. Hannemann, et al. (2007). "SH4-domain-induced plasma membrane

dynamization promotes bleb-associated cell motility." <u>J Cell Sci</u> **120**(Pt 21): 3820-9.

Towler, D. A., S. P. Adams, et al. (1987). "Purification and characterization of yeast myristoyl CoA:protein N-myristoyltransferase." <u>Proc Natl Acad Sci U S A</u> **84**(9): 2708-12.

Trojan, A., J. L. Schultze, et al. (2000). "Immunoglobulin framework-derived peptides function as cytotoxic T-cell epitopes commonly expressed in B-cell malignancies." <u>Nat Med</u> **6**(6): 667-72.

Urban, J. L. and H. Schreiber (1992). "Tumor antigens." <u>Annu Rev Immunol</u> **10**: 617-44.

Vaillant, D. C., S. J. Copeland, et al. (2008). "Interaction of the N- and C-terminal autoregulatory domains of FRL2 does not inhibit FRL2 activity." <u>J Biol Chem</u> **283**(48): 33750-62.

van der Bruggen, P., C. Traversari, et al. (1991). "A gene encoding an antigen recognized by cytolytic T lymphocytes on a human melanoma." <u>Science</u> **254**(5038): 1643-7.

Vavylonis, D., D. R. Kovar, et al. (2006). "Model of formin-associated actin filament elongation." <u>Mol Cell</u> **21**(4): 455-66.

Watanabe, N. and C. Higashida (2004). "Formins: processive cappers of growing actin filaments." <u>Exp Cell Res</u> **301**(1): 16-22.

Watanabe, N., P. Madaule, et al. (1997). "p140mDia, a mammalian homolog of Drosophila diaphanous, is a target protein for Rho small GTPase and is a ligand for profilin." <u>EMBO J</u> **16**(11): 3044-56.

Weiner, L. M., M. V. Dhodapkar, et al. (2009). "Monoclonal antibodies for cancer immunotherapy." <u>Lancet</u> **373**(9668): 1033-40.

Weinzierl, A. O., C. Lemmel, et al. (2007). "Distorted relation between mRNA copy number and corresponding major histocompatibility complex ligand density on the cell surface." <u>Mol Cell Proteomics</u> **6**(1): 102-13.

Wendtner, C. M., D. M. Kofler, et al. (2004). "The potential of gene transfer into primary B-CLL cells using recombinant virus vectors." <u>Leuk Lymphoma</u> **45**(5): 897-904.

Wolfel, T., M. Hauer, et al. (1995). "A p16INK4a-insensitive CDK4 mutant targeted by cytolytic T lymphocytes in a human melanoma." <u>Science</u> **269**(5228): 1281-4.

Yayoshi-Yamamoto, S., I. Taniuchi, et al. (2000). "FRL, a novel formin-related protein,

binds to Rac and regulates cell motility and survival of macrophages." Mol Cell Biol **20**(18): 6872-81.

Zozulya, S. and L. Stryer (1992). "Calcium-myristoyl protein switch." Proc Natl Acad Sci U S A **89**(23): 11569-73.

8   Abbreviations

7-AAD	7- amino-Actinomycin D
ACT	Adoptive cell therapy
ALL	acute lymphatic leukaemia
APCs	antigen-presenting cells
BrdU	5`-bromo-2`-deoxyuridine
CD	cluster of differentiation
cDNA	complememtary-DNA
CFSE	Carboxyfluorescein diacetate succinimidyl ester
CLL	chronic lymphocytic leukemia
Ci	Curie
CPE	cytopathic effect
CTL	cytotoxic T-lymphocyte
CTLA-4	cytotoxic T-lymphocyte–associated antigen 4
DAD	Diaphanous autoregulatory domain
DC	Dendritic cells
DD	dimerization domain
DEPC	Diethylpyrocarbonat
DID	Diaphanous-inhibitory domain
DMEM	Dulbecco's modified Eagle's medium
DMSO	Dimethyl Sulfoxide
dNTP	Desoxinucleosidtriphosphate
DRF	diaphanous-related forming
DTT	dithiothreitol
EBV	Epstein-Barr virus
FACS	fluorescence-activated cell sorting
FCS	Fetal calf serum
FH	formin homology
FMNL1	formin-like 1
GBD	GTPase binding domain
GFP	Green fluorescent protein
GM-CSF	Granulocyte Macrophage Colony Stimulating Factory
HBSS	Hanks Balanced Salt Solution
HD	Hodgkin disease
IMDM	Iscove's Modified Dulbecco's Medium
INFγ	Interferone-γ
Ig	Immunoglobulin
IL	Interleukin
LPS	Lipopolysaccharide

MALDI	matrix-assisted laser desorption/ionization
mDia1	mammalian diaphanous 1
MHC	major histocompatibility complex
min	minute
Mio	miollion
MTOC	microtubule organizing center
NHL	non-Hodgkin lymphoma
PBL	peripheral blood leukocytes
PBMC	Peripheral blood mononuclear cells
PBS	Phosphate buffered saline
PCR	polymerase chain reaction
PFA	Paraformaldehyd
PG	Prostaglandin
PI	Prodium Iodide
PMA	phorbol 12-myristate 13-acetate
PMSF	Pheylmethanesulfonyl
RCC	renal cell carcinoma
rpm	rounds per minute
SNARF-1	Seminaphtorhodafluor-1carboxylic acid, acetate and succinimidyl ester
TA	tumor antigens
TAA	tumor-associated antigens
TAE	Tris-acetat-EDTA buffer
TBS	Tris buffered saline
TILs	tumor-infiltrating lymphocytes
TNF α	Tumor necrosis factor α

9   Acknowledgments

First of all I would like to sincerely thank Dr. Angela Krackhardt for entrusting me and providing me with such an exciting opportunity to accomplish my doctor thesis. She has opened a new academic field for me and assisted me to go deeply into this field step by step. During the past three years, she always gave me help in time and answered my questions kindly and patiently. Her instruction helped me get more knowledge the immunology and biological chemistry. And by her supports, I had the chances to learn many advanced experiments technology. In addition to her help on my research, she has also helped a lot on my daily life. She picked me up at the Munich airport at dawning, accompanied me to my temporary residence and helped me to find an apartment. Moreover, she gave me quite a lot encouragements and supports to apply the visa of my husband to come to Munich and live together with me. I will always keep these in my heart.

I highly appreciate Prof. Dolores Schendel to give me this chance to work in institute of molecular immunology in Helmholtz Zentrum Muenchen for my doctor thesis. I would like to acknowledge the laboratories of Dr. Elisabeth Kremmer and Dr. Vigo Heissmeyer for kindly providing antibodies, the entry clone vectors and instruction for adenoviral transduction technology. I also would thank Dr. Joachim Ellwart for performing the intracellular calcium concentration measurement by the *MoFlow*™ and Manuel Deutsch for operating the confocal microscopy.

I am very happy to work together with all the members in our laboratory. They were so nice to me and helped me a lot. Elfriede Eppinger taught me many methods of technology with great patience; Ingrid Schuster, Luise Weigand and Xiaoling Liang helped me perform many experiments, encouraged me and gave me many advices both in experiments and daily life. And the members from other laboratory also were friendly to me. They gave me useful suggestions and advices.

Furthermore, I would like to give special thanks to Prof. Reinhard Zeidler from the University Munich for agreeing to be my doctor supervisor.

My husband Nan Luo is the most important support for me. He took good care of me and encouraged me which gave me power to overcome all the difficulties I faced in my experiments and living in a foreign country. My parents also helped me a lot. I would also thank my American friend Mr. Ely gilliam who read my whole dissertation carefully and revised mistakes of English. Last but not least I want to thank my respecting friend in Germany Mrs.Traute Aharia who made my life in Munich warm and happy.

10 Curriculum Vitae

PERSONAL DETAILS:

Name	Yanyan Han
Sex	Female
Date of Birth	23 November 1982
Place of birth	Nanjing, P. R. China
Marital Status	married

EDUCATION BACKGROUND:

10.2006-present	PhD student at Institute of Molecular Immunology, Helmholtz Zentrum München - German Research Center for Environmental Health. Supervisor: Dr. Angela Krackhardt External Promotion of the Ludwig-Maximilians-University Munich, Faculty of Medicine. Supervisor: Prof. Reinhard Zeidler Title of PhD thesis: Functional characterization of Formin-like 1 (FMNL1) as potential target for novel anti-tumor therapies.
09.2004-07.2006	Postgraduate student at Dept. Epidemiology and Preventive Veterinary Medicine, College of Veterinary Medicine, Nanjing Agricultural University. Supervisor: Prof. Ping Jiang Title of Master thesis: Study on indirect ELISA to antibody against Encephalomyocarditis virus (EMCV) with recombinant VP1 epitope protein.
09.2000-07.2004	Undergraduate student at College of Veterinary Medicine, Nanjing Agricultural University. Title of Bachelor thesis: Establishment of the prokaryote expressional vector of the epitope gene of Encephalomyocarditis virus.

09.1997-07.2000   Student in Nanjing No.1 Middle School.
Scores of all nine courses in the final examination are A.

LIST OF PUBLICATION:

Yanyan Han, Elfriede Eppinger, Ingrid G. Schuster, Luise U. Weigand, Xiaoling Liang, Elisabeth Kremmer, Christian Peschel and Angela M. Krackhardt
  Formin-like 1 (FMNL1) is regulated by N-terminal myristoylation and induces polarized membrane blebbing.
  The Journal of biological chemistry; 2009; 284(48): 33409–33417

HAN Yan-yan LI Yu-feng GU Xiao-xue JIANG Ping
  Development of an indirect ELISA with recombinant antigen for detecting antibody against Encephalomyocarditis virus.
  Animal husbandry & veterinary medicine, 2007; 39(12)

GU Xiao-xue JIANG Ping **HAN Yan-yan** LI Yu-feng
  Development of an indirect ELISA assay for detecting antibody to porcine reproductive and respiratory syndrome (PRRS) with recombinant GST-GP5AB protein.
  Animal husbandry & veterinary medicine, 2007; 39(2)

Han Yanyan, Jiang Ping,Gu Xiaoxue and Li Yufeng
  Expression and antigenicity of the epitope of VP1 gene of Encephalomyocarditis virus（EMCV） in *E. coli.*
  The Journal of Nanjing Agricultural University, 2005; 28(4):100-103

Formin-like 1 (FMNL1) Is Regulated by N-terminal Myristoylation and Induces Polarized Membrane Blebbing*[s]

Yanyan Han[‡1], **Elfriede Eppinger**[‡1], **Ingrid G. Schuster**[‡], **Luise U. Weigand**[‡], **Xiaoling Liang**[‡], **Elisabeth Kremmer**[‡], **Christian Peschel**[§], and **Angela M. Krackhardt**[‡§2]

From the ‡Helmholtz Zentrum München, National Research Center for Environment and Health, Institute of Molecular Immunology, Marchioninistrasse 25, 81377 Munich and the §III Medizinische Klinik, Klinikums Rechts der Isar, Technische Universität München, Ismaningerstrasse 15, 81675 Munich, Germany

The formin protein formin-like 1 (FMNL1) is highly restrictedly expressed in hematopoietic lineage-derived cells and has been previously identified as a tumor-associated antigen. However, function and regulation of FMNL1 are not well defined. We have identified a novel splice variant (FMNL1γ) containing an intron retention at the C terminus affecting the diaphanous autoinhibitory domain (DAD). FMNL1γ is specifically located at the cell membrane and cortex in diverse cell lines. Similar localization of FMNL1 was observed for a mutant lacking the DAD domain (FMNL1ΔDAD), indicating that deregulation of autoinhibition is effective in FMNL1γ. Expression of both FMNL1γ and FMNL1ΔDAD induces polarized nonapoptotic blebbing that is dependent on N-terminal myristoylation of FMNL1 but independent of Src and ROCK activity. Thus, our results describe N-myristoylation as a regulative mechanism of FMNL1 responsible for membrane trafficking potentially involved in a diversity of polarized processes of hematopoietic lineage-derived cells.

Formins represent a protein family indispensable for many fundamental actin-dependent processes, including migration, vesicle trafficking, morphogenesis, and cytokinesis (1). Because these polarized processes are also involved in inflammation, deregulated proliferation, and metastasis, formins have been suggested to represent attractive drug targets for inflammatory and malignant diseases. Formin-like 1 (FMNL1)[3] is expressed restrictedly in hematopoietic lineage-derived cells and overexpressed in malignant cells of different origin. This restricted expression suggests FMNL1 to be an attractive target for novel immunotherapies in malignant and inflammatory diseases (2, 3). However, function and regulation of FMNL1 are less well characterized. Previous work has shown involvement of FMNL1 in the reorientation of the microtubule-organizing center toward the immunological synapse and cytotoxicity of T cells (4). The murine homolog FRL, which has 85% homology to the human counterpart, has been additionally shown to be involved in cell adhesion and motility of macrophages as well as Fcγ receptor-mediated phagocytosis (5, 6). To date, it is not clear how these different membrane-associated processes are regulated.

Formins are defined by a unique and highly conserved C-terminal formin homology (FH) 2 domain that mediates the effects on actin (7–11). The FH2 domain is proceeded by a proline-rich FH1 domain that binds with low micromolar affinity to profilin (12, 13). In a conserved subfamily of formins known as diaphanous-related formins (DRFs), the FH1 and FH2 domains are flanked by an array of regulatory domains at the N terminus and by a single C-terminal diaphanous autoregulatory domain (DAD) (14). The large N-terminal regulatory region includes a binding domain for small G proteins like Rho-GTPase followed by an adjacent diaphanous-inhibitory domain (DID) and a dimerization domain (13, 15–17). The DAD, which comprised only a small stretch of amino acid residues, binds to the DID. Interaction of DAD and DID is responsible for autoinhibition of DRFs. The mammalian diaphanous 1 (Dia1) as well as the macrophage-enriched murine formin-like protein 1 (FRL) are both regulated by autoinhibition in a DAD-dependent manner (5, 6, 18, 19).

In addition to the domain-specific functions, formin proteins seem to be intensively regulated by splicing. Splicing at the N terminus has been demonstrated to be involved in distinct protein regulation and function of Dia2 (20). The DAD domain is also a hotspot of splicing. Within this area, two splice variants have been characterized for FRL, although functional differences have not been observed (19). In contrast, abrogation of autoinhibition in mutants lacking the C terminus in Dia1 and FRL specifically induces peripheral and plasma membrane localization (5, 21). The exact mechanism of how DRFs locate to the plasma membrane is, however, currently unknown.

We identified a novel splice variant and constitutively active form of FMNL1 with distinct membrane localization. We demonstrate that this novel splice variant (FMNL1γ) directly mediates intensive blebbing that is independent of Src and ROCK activity. In contrast, FMNL1-mediated membrane trafficking

---

[s] The on-line version of this article (available at http://www.jbc.org) contains supplemental Fig. S1.

[1] Both authors contributed equally to this work.

[2] To whom correspondence should be addressed: Helmholtz Zentrum München, National Research Center for Environment and Health, Institute of Molecular Immunology, Marchioninistr. 25, 81377 Munich, Germany. Tel.: 49-89-7099360; Fax: 49-89-7099300; E-mail: HTUangela.krackhardt@helmholtz-muenchen.deUTH.

[3] The abbreviations used are: FMNL1, formin-like 1; Chaps, 3-[(3-cholamidopropyl)dimethylammonio]-1-propanesulfonic acid; CLL, chronic lymphocytic leukemia; DAD, diaphanous autoregulatory domain; DID, diaphanous inhibitory domain; DRF, diaphanous-related formin; FH, formin homology; FRL, murine formin-like protein 1; PBMC, peripheral blood mononuclear cell.

and bleb formation are dependent on N-terminal myristoylation of FMNL1γ, potentially representing a general mechanism involved in diverse membrane-associated functions of FMNL.

EXPERIMENTAL PROCEDURES

Cells and Cell Lines—Peripheral blood mononuclear cells (PBMCs) from healthy donors as well as patients with chronic lymphocytic leukemia (CLL) were collected with donors' and patients' informed consent following the requirements of the local ethical board. Patients had diagnosis of CLL by morphology, flow cytometric analysis, and cytogenetics. PBMCs were obtained by density gradient centrifugation on Ficoll/Hypaque (Biochrom). PBMC subpopulations from healthy donors were isolated by negative or positive magnetic depletion (Invitrogen). A T cell clone (SK22) with specificity for the FMNL1-derived peptide PP2 was used to analyze polarized T cells (3). For polarization experiments, T2 cells were pulsed with the specific peptide followed by incubation with SK22 for 15 min before staining. Unspecific stimulation of PBMCs was induced by interleukin-2 (50 units/ml; Chiron Vaccines International) and OKT3 (30 ng/ml; ATCC) for 3 days. B cells and CLL cells were activated by soluble CD40-ligand (1 μg/ml; Tebu-bio). The following cell lines were used for expression and analysis of FMNL1 splice variants after adenoviral transfer: chronic myelogenous leukemia cell line K562 (ATCC CCL-243), breast carcinoma cell line MDA-MB 231 (CLS), the human fibrosarcoma cell line HT1080 (ATCC CCL-121), and HEK293T embryonal kidney cells (ATCC CRL-1573). In addition, 293A (Invitrogen) cells were used for production of adenoviral supernatant.

Detection of FMNL1 Splice Variants and Sequence Analysis—The DAD region of FMNL1 in CLL cells was analyzed using the following exon-overlapping primers: forward, GTGCTGCAGGAGCTAGACATG, and reverse, CCCTCTAGCCCCTCAGATCTG. Gel electrophoresis of PCR amplicons revealed PCR products of two different sizes, 1312 and 1489 (NCBI FJ534522), representing the C termini of FMNL1α and FMNL1γ, respectively. The PCR products were cloned into pCR 2.1 using the Topo cloning kit (Invitrogen) followed by transformation of Top10 *Escherichia coli* (Invitrogen). Growing clones were analyzed by sequencing (Sequiserve) revealing two different C-terminal sequences. In addition, the C terminus representing FMNL1β was derived from human lung carcinoma cDNA clone IMAGp958M162704Q2 (RZPD). The three splice variants are shown in Fig. 2*B*.

Quantitative Reverse Transcription-PCR—To evaluate quantitative mRNA expression of FMNL1γ compared with overall FMNL1 expression, total RNA was extracted from normal PBMCs and malignant cells from patients with CLL and cell lines (22), and cDNA was synthesized by Superscript II reverse transcriptase (Invitrogen) according to the manufacturer's instructions. In addition, cDNA derived from normal tissues pooled from different donors (Clontech) was used. Detection of splice variant-specific FMNL1 mRNA was conducted using the Light Cycler PCR Master Mix (Roche Applied Science). The following exon-overlapping primers were used for overall FMNL1 detection, resulting in a 299-bp amplicon: 5'-CAAGAACCCCAGAACCAAGGCTCTGG and 3'-CTGCAGGT-CGTACGCCTCAATGGC. In addition, exon-overlapping FMNL1γ splice variant-specific primers were applied, resulting in a 254-bp amplicon: 5'-GCAGCAGAAGGAGCCACTCAT-TTATGAGAGC and 3'-GCACCGTCTTGATCACTGAGT-GGGGGTGG. These primers resulted in high cycle threshold values (>26) in 293T cells overexpressing FMNL1α and β (see Fig. 2*D*). The amplicons were detected by fluorescence (530 nm) using a double-stranded DNA-binding dye, SYBR Green I with the Light Cycler instrument. 18 S rRNA was processed as a control for relative quantification. Relative quantitative expression was calculated using the Δ-Δ cycle threshold method (23). Skeletal muscle was used as reference tissue because it showed the highest cycle threshold for detection of FMNL1 and FMNL1γ (cycle threshold for overall FMNL1 expression in skeletal muscle, 25; for FMNL1γ expression in skeletal muscle, 30).

Cloning of FMNL1 Splice Variants and Mutants—DNA of different splice variants was cloned into pcDNA3.1 and a pEntr11/pACDC-derived entry clone containing the complete FMNL1β sequence using the single SbfI restriction site within FMNL1 to exchange the C termini with the sequences of FMNL1α and FMNL1γ. The pEntr11/pACDC-derived entry clone additionally contains the green fluorescent protein gene. This vector was used for recombination into pAD/PL-DEST adenoviral vector, digested with PacI, and transfected into a 293A adenoviral producer cell line according to the manufacturer's instructions (Invitrogen). Amplification of adenoviral stocks resulted in titers of 10^7–10^9 particles/ml. Virus supernatants were used to transiently infect different cell lines for transduction of FMNL1 splice variants. Transduction efficiency was analyzed by green fluorescent protein expression of infected cells and was 90–100% for HT1080 and MDA-MB 231 but only 20–40% for K562. In addition, pcDNA3.1 vectors containing different FMNL1 splice variants were transfected into 293T cells by calcium phosphate transfection as indicated, resulting in transfection rates of approximately 40–50%. Mutation of the hypothetical N-terminal myristoylation site was performed using the QuikChange mutagenesis kit (Stratagene) according to the manufacturer's instructions. The G2T/A4T mutations were performed at the N terminus (see Fig. 5*A*).

Mutants lacking the DAD were generated for FMNL1 and the mutant G2TA4T by PCR and cloned in pcDNA3.1 using the following primers: FMNL1, 5'-ATTGCTAGCCACCATGGG-CAACGCGGCCGGCAGCGCCGAGC; G2T/A4T, 5'-ATTG-CTAGCCACCATGACCAACACGGCCGGCAGCGCCGAG; and FMNL1ΔDAD, 3'-ATTCTAGACTAGCTCTCATAAAT-GAGTGGCTCCTTCTGCTG. The FMNL1 lacking DAD was also cloned in pEntr11/pACDC-derived entry clone using the following primers: FMNL1, 5'-ATGGATCCCACCATGGGC-AACGCGGCCGGCAGCGCCGAGCAGC; and FMNL1ΔDAD, 3'-AAGGATCCCTAGCTCTCATAAATGAGTGGCTCCTT-CTGCTG.

Reagents and Antibodies—The previously described C-terminal FMNL1-specific rat anti-human antibody 6F2 recognizing the peptide KKEAAAQEAGADT was used to detect FMNL1 by immunofluorescence microscopy and Western blotting. Specificity for FMNL1 has been demonstrated previously by immunoprecipitation and mass spectrometry (3).

We generated an additional N-terminal FMNL1-specific rat anti-human antibody (8A8) recognizing the peptide PAAPPP-KQPAPPKQP which was used for immunoprecipitation of FMNL1. In addition, the following primary and secondary antibodies were used: rabbit anti-human CD3 polyclonal antibody (Dako), mouse anti-human α-tubulin monoclonal antibody (Santa Cruz Biotechnology), mouse anti-human γ-tubulin monoclonal antibody (Sigma), and rabbit anti-human myosin IIb antibody (Sigma). Appropriate secondary antibodies with minimal cross-reactivity and conjugation to Cy3, Cy5 (Jackson), and Alexa Fluor 488 (Invitrogen) were applied as indicated. Alexa Fluor 488-labeled phalloidin (Invitrogen) was used to stain actin. For immunoblotting, horseradish peroxidase-conjugated secondary antibodies to rat and mouse were used. For inhibition of different targets involved in blebbing the following reagents were used: blebbistatin (Calbiochem) at 1 μM, 50 μM and 100 μM; PP1 (Calbiochem) at 50 μM; latrunculin B (Calbiochem) at 1 μM, 10 μM, and 25 μM; Y-27632 (Sigma) at 90 μM; and nocodazole (Calbiochem) at 1 μM, 10 μM, 100 μM, and 200 μM. 2-Hydroxymyristic acid (Biozol) was used for inhibition of N-terminal myristoylation at a concentration of 1 mM.

Immunofluorescence—Nonadherent cells were dropped on poly-L-lysine-coated coverslips, and adherent cells were settled on sterilized coverslips overnight. Cells were fixed in 3% paraformaldehyde for 30 min. Cells were then washed (phosphate-buffered saline, 0.5% Nonidet P-40, 0.01% NaN$_3$), blocked with 10% fetal calf serum for 20–30 min and stained with specific primary and secondary antibodies as indicated. DAPI (Molecular Probes) was used for nuclear staining. Glass coverslips were mounted on the cells in mounting medium (Molecular Probes) and investigated by Leica confocal microscopy.

Immunoprecipitation, Immunoblotting, and [^{3}H]Myristic Acid Uptake Assay—293T cell were transfected with FMNL1γ or G2T/A4T and 24 h later biosynthetically labeled with [^{3}H]myristic acid (0.2 mCi/ml) (PerkinElmer) followed by incubation for 16 h in Dulbecco's modified Eagle's medium supplemented with 5% heat-inactivated fetal bovine serum. Labeled cells were washed with phosphate-buffered saline and lysed in lysis buffer (20 mM Tris-HCl, 150 mM NaCl, pH 7.4, 150 mM Chaps, 1 mM phenylmethylsulfonyl fluoride, 1 mM Na$_3$VO$_4$, 1 mM NaF, 1× Complete). FMNL1γ and G2T/A4T proteins were immunoprecipitated with the FMNL1-specific antibody 8A8 and protein G-Sepharose 4 Fast Flow (Amersham Biosciences). Eluted proteins were split and forwarded for SDS-PAGE on two separated gels. One gel was used for immunoblotting to detect the presence of FMNL1 using the FMNL1-specific antibody 6F2. The other gel was treated with Amplify^{TM} fluorographic reagent (Amersham Biosciences) as indicated by the manufacturer and exposed for 12 days to Hyperfilm MP (Amersham Biosciences) at −80 °C using an intensifying screen.

RESULTS

Expression and Localization of Endogenous FMNL1 in Diverse Hematopoietic Lineage-derived Cells—We have previously demonstrated protein expression of endogenous human FMNL1 in different subtypes of PBMCs by Western blotting using the FMNL1-specific antibody 6F2 (3). Here, we investi-
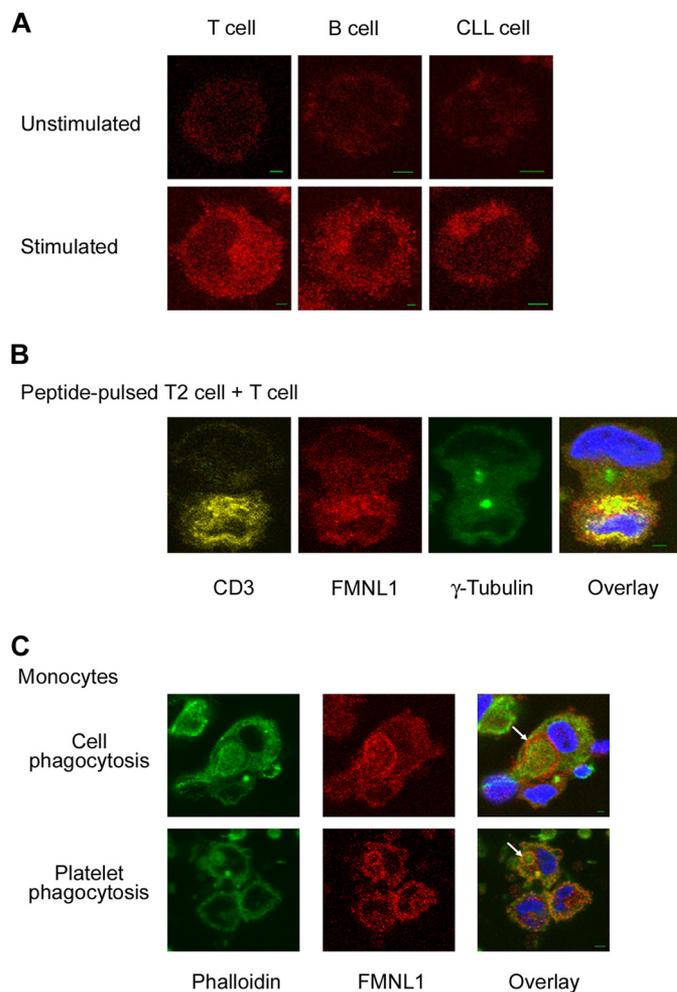
FIGURE 1. **FMNL1 is expressed in diverse hematopoietic lineage-derived cells and shows function-specific polarized localization.** *A*, FMNL1 was visualized in unstimulated and stimulated PBMC subtypes as T cells, B cells, and malignant B cells from patients with CLL by immunofluorescence staining with the rat FMNL1-specific antibody 6F2 followed by Cy3-labeled goat anti-rat antibody. T cells were stimulated with interleukin-2 and OKT3, and B cells as well as CLL cells were activated using soluble CD40-ligand. *Scale bars*, 2 μm. *B*, to investigate FMNL1 expression in polarized T cells, the FMNL2-PP2-specific T cell clone SK22 was incubated for 15 min with T2 cells pulsed with the peptide FMNL1-PP2 at 10 μmol. Cells were then fixed and stained with DAPI for nuclear staining (*blue*), rabbit anti-human CD3 antibody followed by Cy5-labeled goat anti-rabbit antibody (*yellow*) for T cell identification, and rat FMNL1-specific antibody 6F2 followed by Cy3-labeled goat anti-rat antibody (*red*). The microtubule-organizing center was stained with mouse anti-human γ-tubulin antibody followed by Alexa Fluor 488-labeled goat anti-mouse antibody (*green*). Enrichment of FMNL1 and CD3 was observed around the microtubule-organizing center. *Scale bar*, 2 μm. *C*, FMNL1 is localized at the phagocytic cup (*white arrows*) of monocytes during phagocytosis of cells and platelets. FMNL1 (*red*) was stained as above, F-actin was stained by Alexa 488-conjugated phalloidin (*green*), and nuclei were stained with DAPI (*blue*). *Scale bars*, 2 μm. Fluorescent images were visualized at room temperature through a LEICA TCS SP2/405 confocal microscope using the HCX PL APO objective (63 × 1.4-0.6 OIL λ_{BL}) and the LEICA DC 300F camera. The LEICA confocal software was used for acquisition and analysis (*A–C*).

gated the localization of FMNL1 in these cells by confocal microscopy. FMNL1 showed a dot-like expression pattern in the cytoplasma of unstimulated and unspecifically stimulated T cells, B cells, and CLL cells (Fig. 1*A*). In T cells, FMNL1 has been reported to be involved in reorientation of the microtubule-organizing center toward the immunological synapse (4). We similarly observed polarization of FMNL1 toward the immunological synapse after targeting of FMNL1-PP2-specific T cells

Regulation of FMNL1 by N-Myristoylation
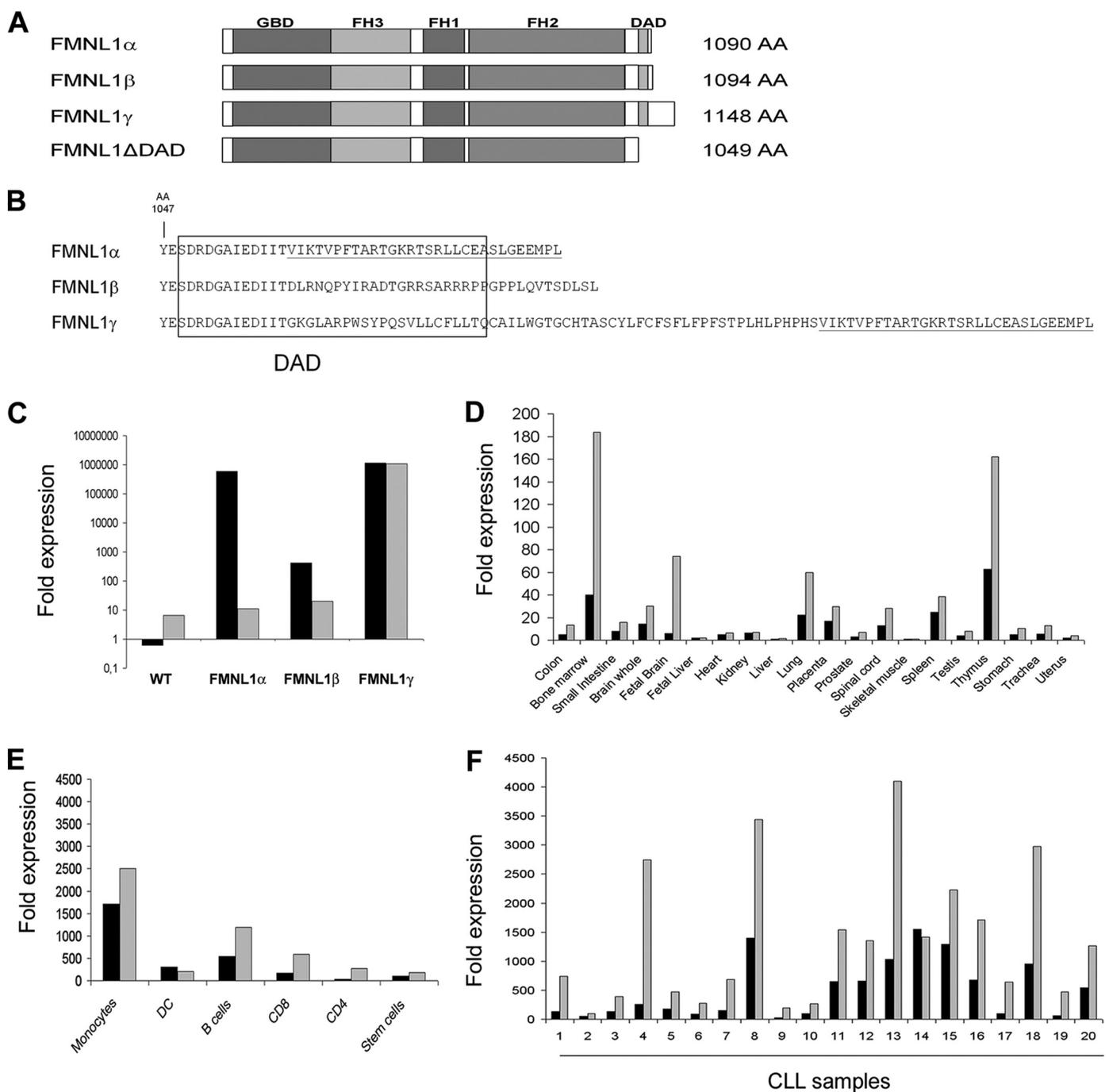
FIGURE 2. **Identification of a novel FMNL1 splice variant (FMNL1γ) containing an intron retention at the C terminus.** *A*, schematic diagrams of FMNL1α, FMNL1β, FMNL1γ, and FMNL1ΔDAD constructs used in this study. *B*, amino acid sequences of the C termini of FMNL1α and β, corresponding to murine FRLα and β, as well as of the novel isoform FMNL1γ containing a C-terminal intron retention but sharing the final C-terminal amino acids with FMNL1α. The DAD sequence responsible for autoinhibition in the murine homolog is *framed*, and the identical C-terminal amino acids in FMNL1α and FMNL1γ are *underlined*. *AA*, amino acids. *C*, quantitative mRNA expression of overall FMNL1 (*black bars*) and the isoform FMNL1γ (*gray bars*) with specific exon-overlapping primers in wild type (*WT*) 293T cells and 293T cells transduced with the different FMNL1 isoforms. The relative quantitative expression compared with skeletal muscle was calculated using the Δ-Δ cycle threshold method. *D–F*, quantitative mRNA expression of general FMNL1 (*black bars*) and isoform-specific FMNL1γ (*gray bars*) in healthy tissue (*D*) and in diverse cell populations isolated from peripheral blood of healthy donors (*E*) and 20 patients with CLL (*F*). PBMC subpopulations were isolated by negative (CD4, CD8, CD19, and CD14) and positive (CD34) selection. Dendritic cells (*DC*) were generated by adherence and cytokine maturation (*E*).

with peptide-pulsed T2 cells (Fig. 1*B*) (3). Function-associated localization of endogenous human FMNL1 was also observed at the phagocytic cup of monocytes during phagocytosis of cells and platelets (Fig. 1*C*) being in common with previous investigations of the function of murine FRL. Thus, our results confirm expression of human FMNL1 in different hematopoietic

lineage-derived cells as well as involvement in diverse polarized and membrane-associated processes.

Identification and Cloning of Different FMNL1 Splice Variants—DRFs including FRL have been previously described to be regulated by autoinhibition, which is dependent on the C-terminal DAD (5). Using exon-specific primers for the C
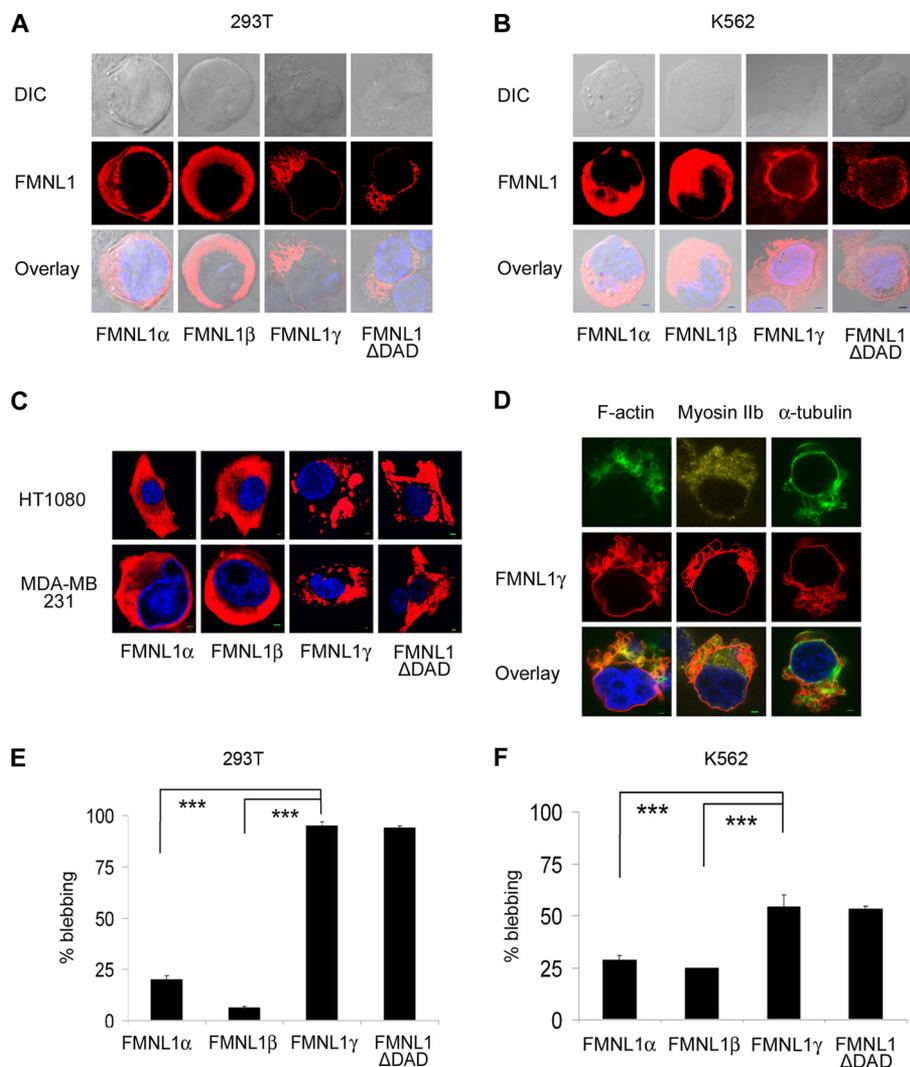
FIGURE 3. **FMNL1γ and FMNL1ΔDAD show membranous and cortical localization and induce bleb formation.** *A*, FMNL1γ and FMNL1ΔDAD induce extensive blebbing in 293T cells. 293T cells were transfected with the pcDNA3.1 vector containing three different isoforms of FMNL1 and analyzed by confocal microscopy after immunofluorescence staining with the rat FMNL1-specific antibody 6F2 followed by Cy3-labeled goat anti-rat antibody (*red*). Nuclei were stained with DAPI (*blue*). *Scale bars*, 2 μm. *DIC*, differential interference contrast. *B*, FMNL1γ and FMNL1ΔDAD induce blebbing in K562 cells. FMNL1 isoforms were adenovirally transduced into K562 cells and analyzed by confocal microscopy as described in *A*. *Scale bars*, 2 μm. *C*, FMNL1γ and FMNL1ΔDAD are enhanced in intracellular vesicles of HT1080 and MDA-MB 231 cells. FMNL1 isoforms were adenovirally transduced into HT1080 and MDA-MB 231 cells and analyzed by confocal microscopy as described above. *Scale bars*, 2 μm. *D*, F-actin, α-tubulin, and myosin IIb show polarized localization in FMNL1γ-induced blebs in 293T cells. 293T cells were transfected with the pcDNA3.1 vector containing FMNL1γ and stained with rat FMNL1-specific antibody 6F2 followed by Cy3-labeled goat anti-rat antibody (*red*). Myosin IIb was stained with a rabbit anti-myosin IIb antibody followed by Cy5-labeled goat anti-rabbit antibody (*yellow*). F-actin was stained with Alexa Fluor 488-conjugated phalloidin (*green*), and α-tubulin was stained with a mouse anti-α-tubulin antibody followed by Alexa Fluor 488-conjugated goat anti-mouse antibody (*green*). Nuclei were stained with DAPI (*blue*). *Scale bars*, 2 μm. *E* and *F*, cell blebbing was quantified by counting 100 FMNL1-transduced cells in 293T cells (*E*) and K562 cells (*F*) by independent counting experiments ($n \geq 3$), indicating a significant increase of blebbing in cells expressing FMNL1γ and FMNL1ΔDAD (***, $p < 0.001$). Fluorescent images (*A–D*) were investigated as described in Fig. 1.

and hematopoietic derived cells by quantitative reverse transcription-PCR. FMNL1γ shows a similar tissue-specific mRNA expression profile compared with the non-splice-specific expression of FMNL1 (Fig. 2, *D* and *E*), although some tissues such as bone marrow, fetal brain, and thymus show relatively higher expression of FMNL1γ compared with general FMNL1 (3). Of note, FMNL1γ is highly expressed in malignant cells of a subset of patients with CLL (Fig. 2*F*).

FMNL1γ and FMNL1 Lacking the C-terminal DAD Are Located at the Cell Membrane and Induce Membranous Bleb Formation—Because FMNL1γ differed in the DAD sequence representing an important region for FMNL1 regulation, we cloned all three different FMNL1 splice variants and investigated transfected 293T cells by confocal microscopy. 293T cells transfected with FMNL1α and FMNL1β showed mainly intracellular cytoplasmic distribution of FMNL1, whereas cells transfected with FMNL1γ showed a distinct membranous FMNL1 localization as well as extensive polarized membrane protrusions and blebs (Fig. 3*A*). Similar membrane protrusions were observed after adenoviral transduction of K562 cells with FMNL1γ but not with the other splice variants. However, in these cells the shape of the blebs was different, and a more prominent enrichment of FMNL1γ at the cell cortex has been observed (Fig. 3*B*). Similarly, 293T cells and K562 cells transfected or transduced with FMNL1 lacking the DAD domain (FMNL1ΔDAD, Fig. 2*A*) showed membranous and cortical localization of FMNL1 and extensive polarized membrane protrusions and blebs (Fig. 3, *A* and *B*), suggesting

that deregulation of autoinhibition is responsible for membrane localization and blebbing observed in cells overexpressing the splice variant FMNL1γ. Increase of blebbing was less obvious in HT1080 and MDA-MB 231 cells after adenoviral transduction of FMNL1γ. However, these cell lines also demonstrated FMNL1γ localization at the cell membrane and especially enrichment of FMNL1γ at intracellular vesicles, whereas cells transduced with the other two splice variants had a more dispersed distribution within the cytoplasm (Fig. 3*C*). Again,

cDNA of CLL cells and human lung carcinoma, resulting in varying C-terminal amino acid sequences (Fig. 2*A*). Two splice variants are corresponding to the previously described murine splice variants, FRLα and FRLβ (6, 19). We additionally identified another C-terminal splice variant, FMNL1γ, containing an intron retention but sharing the final C terminus with FMNL1α (Fig. 2*B*). We selected splice variant-specific exon-overlapping primers (Fig. 2*C*) to quantify the mRNA expression of the novel splice variant FMNL1γ in different tissues

Regulation of FMNL1 by N-Myristoylation

A

H₂O   Y-27632

DMSO   PP1   Latrunculin B   Blebbistatin   Nocodazole

B

FIGURE 4. **Blebbing induced by FMNL1γ is independent of ROCK and Src but depends on actin, myosin, and microtubules.** *A* and *B*, 293T cells were transfected with the pcDNA3.1 vector containing FMNL1γ and treated with different bleb inhibitors and solvent controls. Cells were stained after 2 days with the rat FMNL1-specific antibody 6F2 followed by Cy3-labeled goat anti-rat antibody (*red*). Nuclei were stained with DAPI (*blue*). *Scale bars*, 2 μm. Blebbing cells were analyzed by confocal microscopy as described in *A*. Cell blebbing was quantified by counting 100 FMNL1γ-transduced cells in three independent experiments (*B*), classifying them as cells exhibiting extended blebs (*white bars*), limited blebs (*black bars*), or none (*gray bars*). *DMSO*, dimethyl sulfoxide. The S.D. of independent counting experiments is shown ($n = 3$; ***, $p < 0.001$).

similar localization was observed in HT1080 and MDA-MB 231 cells after adenoviral transduction of FMNL1ΔDAD (Fig. 3*C*). We additionally noticed colocalization of FMNL1γ with F-actin in blebs of FMNL1γ-transfected 293T cells as shown by phalloidin staining pointing to an induction of actin assembly activity by FMNLγ (Fig. 3*D*). Myosin IIb and α-tubulin were also polarized to the FMNL1γ-induced blebs (Fig. 3*D*). A significant increase of membrane blebbing in 293T and K562 cells after transduction with FMNL1γ and FMNL1ΔDAD compared with the other splice variants was quantified by independent counting experiments (Fig. 3, *E* and *F*).

Blebbing Induced by FMNL1γ Is Independent of Src and ROCK but Depends on Actin, Myosin, and Tubulin Integrity—Plasma membrane blebbing has been previously shown to be induced by the formin FHOD1 when coexpressed with ROCK1 (24). Moreover, blebbing induced by FHOD1 requires Src activity (24). To investigate plasma membrane blebbing induced by FMNL1γ further, we transfected 293T cells with FMNL1γ and added different substances previously reported to inhibit membrane blebbing. Whereas the Src inhibitor PP1 and the ROCK inhibitor Y-27632 had only minimal effects on membrane blebbing, this was grossly reduced by addition of latrunculin B, blebbistatin, and nocodazole (Fig. 4, *A* and *B* and supplement Fig. S1), demonstrating that the mechanism of blebbing induced by

FMNL1γ is not mediated by Src and ROCK but depends on actin, myosin, and tubulin integrity. Similar data were obtained by FMNL1ΔDAD-transfected 293T cells (data not shown).

FMNL1 Is Myristoylated at the N Terminus—Membrane localization of FMNL1γ was a predominant feature in 293T cells transfected with the splice variant FMNL1γ and FMNL1ΔDAD. The mechanism of how FMNL1 is located to the cell membrane remains elusive. Investigation of the FMNL1 structure by prediction analyses revealed a potential N-terminal myristoylation site (see the Eukaryotic Linear Motif (ELM) resource on the Internet). This N-terminal myristoylation motif is highly specific for the leukocyte-specific formins FMNL1, 2, and 3 in man and mouse but is not present in other formin proteins. To prove whether FMNL1γ is myristoylated at the N terminus, we mutated glycine at position 2 and alanine at position 4 to threonine within FMNL1γ (G2T/A4T) (Fig. 5*A*). 293T cells were transfected with FMNL1γ or the G2T/A4T mutant form and then metabolically labeled with [³H]myristic acid. Total protein of transfected 293T cells was immunoprecipitated by the FMNL1-specific antibody 8A8 detecting an N-terminal epitope not including the N-terminal myristoylation site. Immunoprecipitated probes were investigated by immunoblotting using the FMNL1-specific antibody 6F2 (Fig. 5*B*) as well as autoradiography to analyze incorporation of [³H]myristic acid (Fig. 5*C*). Both proteins, FMNL1γ and G2T/A4T, were sufficiently immunoprecipitated by the FMNL1-specific antibody 8A8 (Fig. 5*B*). However, only FMNL1γ, but not G2T/A4T, was myristoylated after transfection in 293T cells.

Membrane Localization and Blebbing of FMNL1 Are Mediated by N-terminal Myristoylation—To investigate whether N-terminal myristoylation plays a role in FMNL1 function and membrane localization, cells were transfected with FMNL1γ or G2T/A4T. The mutant G2T/A4T, in fact, abolished membranous and cortical localization of FMNL1γ after transfection of the mutant splice variant in 293T cells as well as after genetic transfer of this mutant in other cell lines (Fig. 6*A*). Similarly, mutation of the *N*-myristoylation site in the FMNL1ΔDAD (G2T/A4TΔDAD) also abrogated membranous localization of FMNL1ΔDAD (Fig. 6*B*). Membrane localization of FMNL1γ and FMNL1ΔDAD could be also inhibited by adding 2-hydroxymyristate, a potent inhibitor of protein myristoylation (25), further confirming that plasma membrane localization of FMNL1 is dependent on N-terminal myristoylation (Fig. 6*C*). Blebbing was significantly reduced in 293T cells transfected with G2T/A4T or G2T/A4TΔDAD compared with FMNL1γ or FMNL1ΔDAD (Fig. 6*D*), indicating that membrane localization mediated by N-terminal myristoylation is important for bleb formation induced by FMNL1.

DISCUSSION

Formin proteins have been described to promote the formation of actin networks and to be involved in regulation of essential cellular functions such as cell division, migration, adhesion, and intracellular trafficking. So far, little is known about the hematopoietic lineage-specific formin FMNL1. Here, we show expression and polarized localization of native human FMNL1 in different hematopoietic lineage-derived cells, confirming
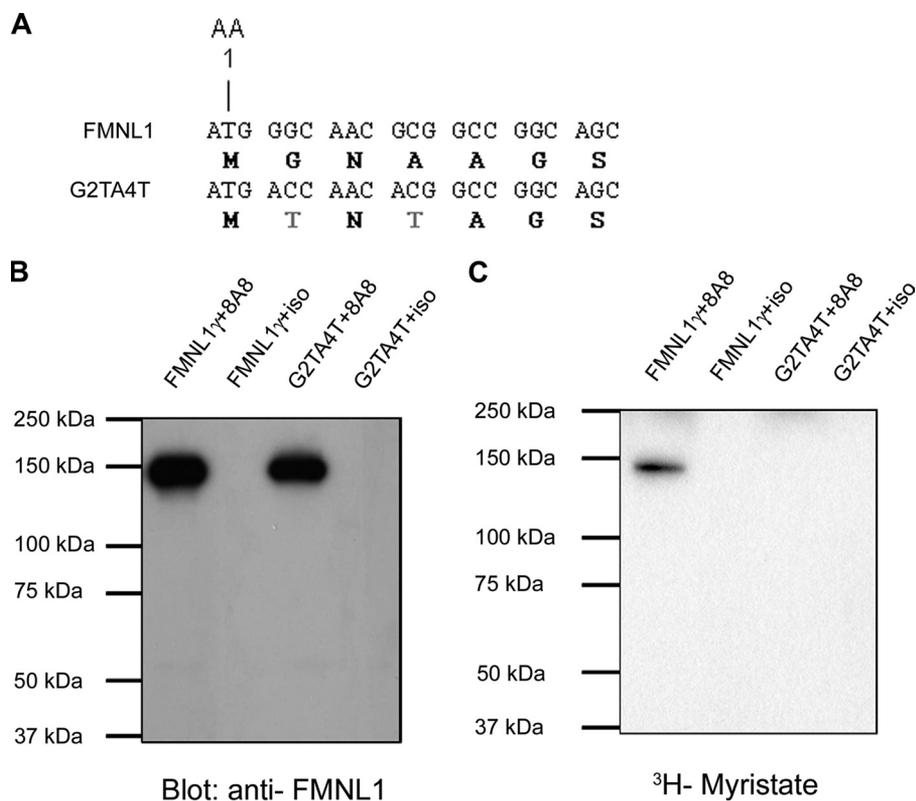
FIGURE 5. **FMNL1γ contains an N-terminal myristoylation site.** *A*, schematic view of the N terminus of FMNL1. The predicted N-terminal myristoylation site was mutated on positions 2 and 4, glycine and alanine to threonine (*gray*), respectively. *AA*, amino acid. *B* and *C*, immunoprecipitation and metabolic labeling of FMNL1γ with [³H]myristic acid. 293T cells transfected with FMNL1γ or G2T/A4T were cultured for 16 h with [³H]myristic acid. The indicated proteins were immunoprecipitated with the FMNL1-specific monoclonal antibody 8A8 as well as the isotype control (*iso*), separated by SDS-PAGE followed by immunoblotting with anti-FMNL1 monoclonal antibody 6F2 (*B*) or fluorography (*C*). Molecular mass sizes are indicated in kDa.

retention affects the DAD sequence and results in a positive charged polar amino acid lysine at position 1062 instead of the nonpolar amino acids leucine or isoleucine present in FMNL1α and FMNL1β. Because binding of the DAD peptide region to the DID armadillo repeat structure is mainly dependent on hydrophobic interactions as described for Dia1 (17, 26), this polar lysine may be responsible for release of autoinhibition of FMNL1γ, resulting in a constitutively activated form. In fact, the splice variant FMNL1γ was specifically located at the membrane and cortex and induced bleb formation. The shape and extent of blebs varied in different cell lines, indicating that cell type-specific interaction partners additionally play an important role in function and bleb shape. However, a similar effect on FMNL1 localization and function in diverse cell lines was observed in cells transfected with a FMNL1 mutant missing the DAD sequence, confirming that deregulation of autoinhibition is responsible for membrane localization and blebbing in FMNL1γ-transfected cells. FMNL1γ colocal-

previous reports about different functional aspects of human FMNL1 and murine FRL (4–6).

A complex regulation network seems to be responsible for activation and different functions of formin proteins. A central regulative tool for DRFs is autoregulation, which can be released by interaction with active Rho-GTPases and potentially additional factors (1). Splicing has been also shown to result in differential functionality of forming proteins (20). We isolated a novel FMNL1 splice variant (FMNL1γ) from malignant cells of patients with CLL. This splice variant showed increased mRNA expression in bone marrow, thymus, fetal brain, and diverse hematopoietic lineage-derived cells. Moreover, we observed a high expression in malignant cells of a subset of CLL patients. Detailed analyses of systematically isolated and processed patient samples need to be performed to clarify whether overexpression of FMNL1γ in CLL samples is associated with an activated malignant cell status and/or patient prognosis and will be a focus of further studies. However, although a role of FMNL1γ in malignant transformation could not be ascertained in this study, this splice variant showed distinct functional properties similar to cells expressing a mutant of FMNL1 with deregulated autoinhibition caused by the lack of the autoinhibitory DAD sequence (FMNL1ΔDAD). FMNL1γ contains an intron retention of 58 amino acids at the C terminus but shares the last 30 amino acids with the previously described FMNL1α. This intron

ized with F-actin in bleb protrusions, suggesting FMNL1γ induced actin assembly. Blebbing but not membrane localization of FMNL1γ was totally abrogated by latrunculin B, further confirming regulation of actin assembly and actin-mediated polarized bleb formation by FMNLγ. We additionally observed polarization of myosin IIb and α-tubulin to FMNL1γ-induced blebs in 293T cells. Moreover, bleb formation was significantly inhibited by blebbistatin and nocodazole, confirming a substantial role of myosin and microtubules in FMNL1γ-induced blebbing. These results are in common with previous reports demonstrating that bleb induction by the *Leishmania* parasite virulence factor HASPB depends on the integrity of F-actin and requires myosin II function as well as microtubule networks (27). Moreover, the formins FHOD1, mDia1, and mDia2 have been also previously associated with blebbing (24, 28, 29). However, in contrast to bleb formation induced by HASPB and FHOD1 (24, 27), blebbing induced by FMNL1γ is independent of Src and ROCK because the Src inhibitor PP1 and the ROCK inhibitor Y-27632 did not reduce blebbing in our experiments.

To evaluate the mechanism of membrane localization and bleb induction by FMNL1γ further, we analyzed the protein sequence motifs of FMNL1 and identified a myristoylation site at the N terminus of human FMNL1 and murine FRL with glycine at position 2 representing an essential requirement for myristoylation. In fact, N-terminal myristoylation of FMNL1γ but not the mutant G2T/A4T could be directly proved by

Regulation of FMNL1 by N-Myristoylation
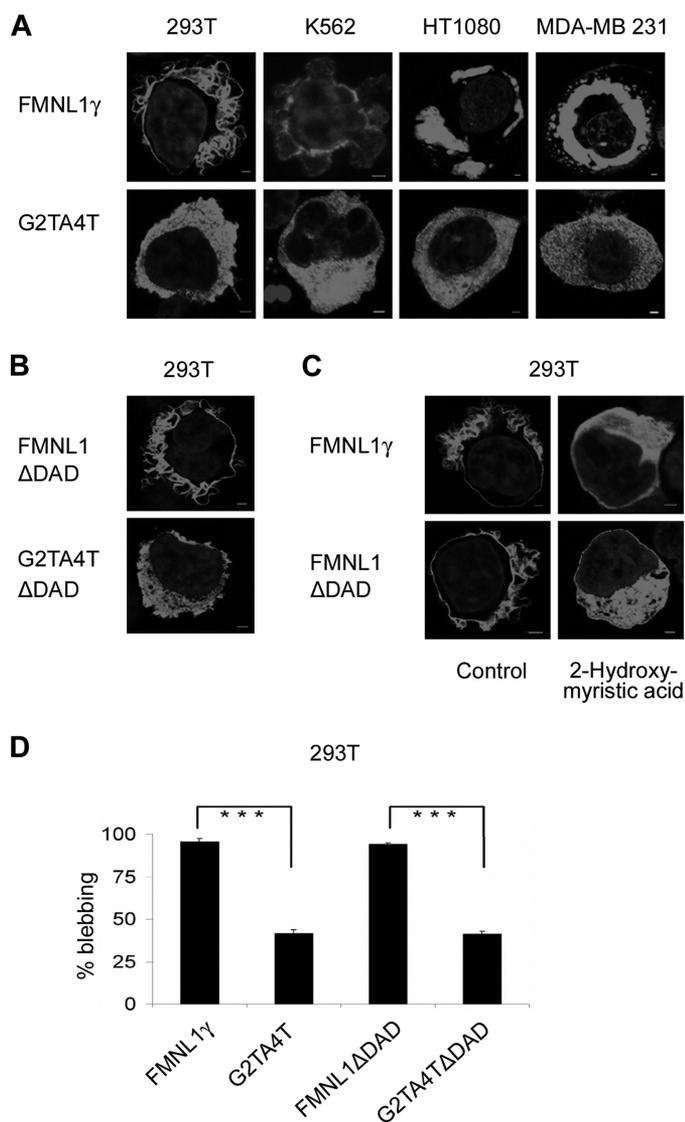
FIGURE 6. **Localization and function of FMNL1 are regulated by N-terminal myristoylation.** *A*, localization of FMNLγ at the membrane or intracellular vesicle is abrogated by mutation of the N-terminal myristoylation motif. Different cell lines were transfected or adenovirally transduced with either FMNL1γ or the mutant G2T/A4T followed by staining with the rat FMNL1-specific antibody 6F2 and Cy3-labeled goat anti-rat antibody (*red*). Nuclei were stained with DAPI (*blue*). *Scale bars*, 2 μm. *B*, localization of FMNL1ΔDAD at the membrane is abrogated by mutation of the N-terminal myristoylation motif. 293T cell lines were transfected with either FMNL1ΔDAD or the mutant G2T/A4TΔDAD followed by staining with the rat FMNL1-specific antibody 6F2 and Cy3-labeled goat anti-rat antibody (*red*). Nuclei were stained with DAPI (*blue*). *Scale bars*, 2 μm. *C*, 293T cells transfected with the isoform FMNL1γ and FMNL1ΔDAD were treated with the inhibitor 2-hydroxymyristic acid and stained as described above. *Scale bars*, 2 μm. *D*, mutation of the N-terminal myristoylation motif reduced membrane blebbing induced by FMNL1γ or FMNL1ΔDAD in 293T cells. For investigation of cell blebbing, 100 transduced cells were analyzed. The *bars* show the S.D. of independent counting experiments ($n = 3$; ***, $p < 0.001$). Fluorescent images (*A–C*) were investigated as described previously.

[³H]myristic acid uptake. Moreover, myristoylation could be inhibited by 2-hydroxymyristate, a potent inhibitor of myristoylation (25), resulting in loss of membrane localization and confirming the significance of N-terminal myristoylation for the specific membranous localization of FMNL1. Loss of myristoylation by mutation of glycine at position 2 additionally significantly reduced blebbing induced by FMNL1γ and

FMNL1ΔDAD, demonstrating that the induction of blebbing was dependent on N-terminal myristoylation of FMNL1. N-terminal myristoylation can facilitate anchoring of proteins to lipid membranes by hydrophobic interaction of myristate with the membrane bilayer. This motif is typically present in the SH4 domain of Src kinases, and myristoylation has been shown to be critical for malignant transformation of v-Src (30, 31). Moreover, it has been reported previously that expression of active SH4 domains is associated with cell blebbing (27). We therefore propose that activation of FMNL1 is regulated not only by binding of a Rho-GTPase but additionally by an increase of intracellular Ca^{2+} or a specific ligand binding. This may cause a myristoyl switch and therefore induces extrusion of the myristoyl group, enabling it to interact quickly and reversibly with lipid bilayer membranes as described previously for other myristoylated proteins (32, 33). Thus, by its N-terminal myristoylation site, FMNL1, in contrast to other formin proteins, may be able to perform expeditious cytoskeletal changes independent of Src and ROCK.

In conclusion, the newly identified splice variant FMNL1γ represents a constitutively active form of FMNL1 that localizes at the membrane and induces bleb formation. We identified N-terminal myristoylation as an important regulatory tool for FMNL1 necessary for bleb formation, enabling fast and reversible membrane localization compatible with diverse functions of hematopoietic lineage-derived cells. The identification of interaction partners of FMNL1 in diverse hematopoietic derived cells as well as the further characterization of splice variants will be highly interesting to identify key molecules regulating different FMNL1 functions, potentially revealing possibilities for specific therapeutic interaction in malignant and inflammatory diseases.

REFERENCES

1. Faix, J., and Grosse, R. (2006) *Dev. Cell* **10,** 693–706
2. Krackhardt, A. M., Witzens, M., Harig, S., Hodi, F. S., Zauls, A. J., Chessia, M., Barrett, P., and Gribben, J. G. (2002) *Blood* **100,** 2123–2131
3. Schuster, I. G., Busch, D. H., Eppinger, E., Kremmer, E., Milosevic, S., Hennard, C., Kuttler, C., Ellwart, J. W., Frankenberger, B., Nössner, E., Salat, C., Bogner, C., Borkhardt, A., Kolb, H. J., and Krackhardt, A. M. (2007) *Blood* **110,** 2931–2939
4. Gomez, T. S., Kumar, K., Medeiros, R. B., Shimizu, Y., Leibson, P. J., and Billadeau, D. D. (2007) *Immunity* **26,** 177–190
5. Seth, A., Otomo, C., and Rosen, M. K. (2006) *J. Cell Biol.* **174,** 701–713
6. Yayoshi-Yamamoto, S., Taniuchi, I., and Watanabe, T. (2000) *Mol. Cell. Biol.* **20,** 6872–6881
7. Wallar, B. J., and Alberts, A. S. (2003) *Trends Cell Biol.* **13,** 435–446
8. Watanabe, N., and Higashida, C. (2004) *Exp. Cell Res.* **301,** 16–22
9. Zigmond, S. H. (2004) *Curr. Opin. Cell Biol.* **16,** 99–105
10. Higgs, H. N., and Peterson, K. J. (2005) *Mol. Biol. Cell* **16,** 1–13
11. Higgs, H. N. (2005) *Trends Biochem. Sci.* **30,** 342–353
12. Evangelista, M., Blundell, K., Longtine, M. S., Chow, C. J., Adames, N., Pringle, J. R., Peter, M., and Boone, C. (1997) *Science* **276,** 118–122
13. Watanabe, N., Madaule, P., Reid, T., Ishizaki, T., Watanabe, G., Kakizuka, A., Saito, Y., Nakao, K., Jockusch, B. M., and Narumiya, S. (1997) *EMBO J.*

16, 3044–3056

14. Alberts, A. S. (2001) *J. Biol. Chem.* **276,** 2824–2830
15. Rose, R., Weyand, M., Lammers, M., Ishizaki, T., Ahmadian, M. R., and Wittinghofer, A. (2005) *Nature* **435,** 513–518
16. Otomo, T., Otomo, C., Tomchick, D. R., Machius, M., and Rosen, M. K. (2005) *Mol. Cell* **18,** 273–281
17. Nezami, A. G., Poy, F., and Eck, M. J. (2006) *Structure* **14,** 257–263
18. Li, F., and Higgs, H. N. (2003) *Curr. Biol.* **13,** 1335–1340
19. Harris, E. S., Li, F., and Higgs, H. N. (2004) *J. Biol. Chem.* **279,** 20076–20087
20. Gasman, S., Kalaidzidis, Y., and Zerial, M. (2003) *Nat. Cell Biol.* **5,** 195–204
21. Copeland, S. J., Green, B. J., Burchat, S., Papalia, G. A., Banner, D., and Copeland, J. W. (2007) *J. Biol. Chem.* **282,** 30120–30130
22. Chomczynski, P., and Sacchi, N. (1987) *Anal. Biochem.* **162,** 156–159
23. Livak, K. J., and Schmittgen, T. D. (2001) *Methods* **25,** 402–408
24. Hannemann, S., Madrid, R., Stastna, J., Kitzing, T., Gasteier, J., Schönichen, A., Bouchet, J., Jimenez, A., Geyer, M., Grosse, R., Benichou, S., and Fackler, O. T. (2008) *J. Biol. Chem.* **283,** 27891–27903
25. Paige, L. A., Zheng, G. Q., DeFrees, S. A., Cassady, J. M., and Geahlen, R. L. (1990) *Biochemistry* **29,** 10566–10573
26. Lammers, M., Meyer, S., Kühlmann, D., and Wittinghofer, A. (2008) *J. Biol. Chem.* **283,** 35236–35246
27. Tournaviti, S., Hannemann, S., Terjung, S., Kitzing, T. M., Stegmayer, C., Ritzerfeld, J., Walther, P., Grosse, R., Nickel, W., and Fackler, O. T. (2007) *J. Cell Sci.* **120,** 3820–3829
28. Kitzing, T. M., Sahadevan, A. S., Brandt, D. T., Knieling, H., Hannemann, S., Fackler, O. T., Grosshans, J., and Grosse, R. (2007) *Genes Dev.* **21,** 1478–1483
29. Eisenmann, K. M., Harris, E. S., Kitchen, S. M., Holman, H. A., Higgs, H. N., and Alberts, A. S. (2007) *Curr. Biol.* **17,** 579–591
30. Cross, F. R., Garber, E. A., Pellman, D., and Hanafusa, H. (1984) *Mol. Cell. Biol.* **4,** 1834–1842
31. Kamps, M. P., Buss, J. E., and Sefton, B. M. (1985) *Proc. Natl. Acad. Sci. U.S.A.* **82,** 4625–4628
32. Ames, J. B., Ishima, R., Tanaka, T., Gordon, J. I., Stryer, L., and Ikura, M. (1997) *Nature* **389,** 198–202
33. Seykora, J. T., Myat, M. M., Allen, L. A., Ravetch, J. V., and Aderem, A. (1996) *J. Biol. Chem.* **271,** 18797–18802